Approximate quantum error correction for generalized amplitude-damping errors

Carlo Cafaro[1,2] and Peter van Loock[2]
[1]*Max-Planck Institute for the Science of Light, 91058 Erlangen, Germany*
[2]*Institute of Physics, Johannes-Gutenberg University Mainz, 55128 Mainz, Germany*
(Received 26 August 2013; published 12 February 2014)

We present analytic estimates of the performances of various approximate quantum error-correction schemes for the generalized amplitude-damping (GAD) qubit channel. Specifically, we consider both stabilizer and nonadditive quantum codes. The performance of such error-correcting schemes is quantified by means of the entanglement fidelity as a function of the damping probability and the nonzero environmental temperature. The recovery scheme employed throughout our work applies, in principle, to arbitrary quantum codes and is the analog of the perfect Knill-Laflamme recovery scheme adapted to the approximate quantum error-correction framework for the GAD error model. We also analytically recover and/or clarify some previously known numerical results in the limiting case of vanishing temperature of the environment, the well-known traditional amplitude-damping channel. In addition, our study suggests that degenerate stabilizer codes and self-complementary nonadditive codes are especially suitable for the error correction of the GAD noise model. Finally, comparing the properly normalized entanglement fidelities of the best performant stabilizer and nonadditive codes characterized by the same length, we show that nonadditive codes outperform stabilizer codes not only in terms of encoded dimension but also in terms of entanglement fidelity.

DOI: 10.1103/PhysRevA.89.022316 PACS number(s): 03.67.Pp

I. INTRODUCTION

Quantum computers are especially sensitive to noise. Therefore, any technological implementation of such a machine requires the use of suitable error-mitigation techniques. Quantum error correction (QEC) represents one of the most efficient available techniques capable of giving us the realistic hope of building practical quantum computers [1]. For a detailed overview of the basic working principles of QEC, we refer to [2].

In general, it is a highly nontrivial task to design quantum codes for any given noise model. In the majority of cases, researchers have focused on the error correction of Pauli-type errors. This type of error model certainly constitutes the worst possible scenario to be considered and a quantum code that can correct all Pauli errors $\{I, X \equiv \sigma_x, Y \equiv \sigma_y, Z \equiv \sigma_z\}$,

$$I \stackrel{\text{def}}{=} \begin{pmatrix} 1 & 0 \\ 0 & 1 \end{pmatrix}, \quad \sigma_x \stackrel{\text{def}}{=} \begin{pmatrix} 0 & 1 \\ 1 & 0 \end{pmatrix}, \quad \sigma_y \stackrel{\text{def}}{=} \begin{pmatrix} 0 & -i \\ i & 0 \end{pmatrix}, \quad \sigma_z \stackrel{\text{def}}{=} \begin{pmatrix} 1 & 0 \\ 0 & -1 \end{pmatrix}, \tag{1}$$

can also provide protection against arbitrary qubit noise, since the Pauli operators form a basis of the 2×2 matrices. However, the worst possible scenario is not necessarily the most realistic one in actual experimental laboratories. Furthermore, aiming at designing quantum codes capable of error-correcting general noise errors may not be the most fruitful way to combat decoherence and noise in quantum computers.

A very common type of noise that appears in realistic settings is the so-called amplitude-damping (AD) noise model [3]. For instance, the AD noise model is employed to describe the photon loss in an optical fiber. The AD channel is the simplest channel whose Kraus operators cannot be described by unitary Pauli operations. The two nonunitary Kraus operators for the qubit AD channel are given by [3]

$$A_0 \stackrel{\text{def}}{=} \frac{1}{2}[(1+\sqrt{1-\gamma})I + (1-\sqrt{1-\gamma})\sigma_z] \quad \text{and}$$
$$A_1 \stackrel{\text{def}}{=} \frac{\sqrt{\gamma}}{2}(\sigma_x + i\sigma_y) = \sqrt{\gamma}|0\rangle\langle 1|, \tag{2}$$

where γ denotes the AD probability parameter. For the sake of completeness, we point out that AD channels acting on states characterized by higher photon numbers in combination with a finite number of modes can also be considered. For instance, qubits living in a two-dimensional Hilbert space can be replaced by bosonic states of higher photon numbers in a finite number of optical modes [4]. In general, the operator-sum decomposition of such higher-dimensional noise models is characterized by error operators A_k with $k = 1, \ldots, N$ and, in principle, N can approach infinity [3]. We observe that there is no simple way of reducing A_1 in Eq. (2) to one Pauli error operator, since $|0\rangle\langle 1|$ is not normal. The Pauli operators are remarkable in that they are unitary and Hermitian at the same time and, in addition, both unitary and Hermitian operators are normal. Although the five-qubit code [5,6] can be successfully used for the error correction of AD errors, since it is a universal 1-error-correcting quantum code, Leung *et al.* were capable of designing a four-qubit quantum code especially suitable for the error correction of arbitrary single-AD errors with a higher encoding rate equal to $1/4$ (greater than $1/5$) [7]. A quantum code with higher encoding rate is very welcome, since it would require fewer resources for its implementation. The two main points advocated in [7] were the following: First, when dealing with specific error models, better codes may be uncovered; second, the fulfillment of the approximate (relaxed) QEC conditions enlarges the realm of possible useful quantum error-correcting codes. Therefore, it can simplify the code construction process.

Both the five-qubit and the four-qubit codes are nondegenerate stabilizer (additive) quantum codes [3]. However,

the scientific literature accommodates a fairly wide variety of additional AD error-correction schemes where neither additive nor nondegenerate quantum codes are employed. For instance, one of the very first QEC schemes used to combat AD errors was quite unconventional, since it used bosonic states of higher photon numbers in a finite number of optical modes (the so-called bosonic quantum codes, [4]). More conventional and recent works are inspired by the seminal work presented in [7]. In [8], using the stabilizer formalism, generalizations of the Leung *et al.*'s four-qubit code for higher rates were constructed. Specifically, a class of $[[2(m+1),m]]$ channel-adapted quantum codes for integers $m \geqslant 1$ with encoding rate arbitrarily close to $1/2$ are generated. In [9], the performance of QEC schemes for the AD model has been investigated via semidefinite programs (that is, numerical convex optimization methods [10]). Specifically, the optimal recovery operation to maximize the entanglement fidelity [11] for a given encoding and noise process was uncovered. Unfortunately, numerically computed recovery maps are difficult to describe and understand analytically. Furthermore, recovery operations generated through convex optimization methods suffer two significant drawbacks. First, the dimensions of the optimization problem grow exponentially with the length of the code, limiting the technique to short codes. Second, the optimal recovery operation may be quite difficult to implement, despite being physically legitimate. However, this exponential growth can be mitigated in two manners. First, it is possible to reduce the high dimensionality of the convex optimization procedures for generating recovery operations in QEC by transforming the problem in a suitable manner. Consider a quantum noisy channel $\Lambda : \mathcal{H}_1 \to \mathcal{H}_2$ with $\dim \mathcal{H}_i = d_i$ for $i = 1,2$. By embedding the encoding into the noise process and redefining Λ as a quantum spreading channel with d_1 strictly less than d_2, the dimensionality of the convex optimization decreases from $d_1^2 d_2^2$ to d_1^4. For instance, for the $[[5,1,3]]$ five-qubit code, the dimensionality reduces from 2^{20} to 2^{12} in terms of the optimization variables. For more details, we refer to [9]. Second, if the focus is on near-optimal rather than on optimal recovery schemes, it turns out that it is possible to compute such recovery operations with less computationally intensive numerical algorithms that are more scalable than those involved in semidefinite programs. Briefly speaking, regarding the algorithm in terms of eigenanalysis, it is possible to significantly reduce the size of the eigenvector problem and this has a significant effect on the computational cost of these new algorithms. For illustrative purposes, consider the AD channel and an $[[n,k,d]]$ quantum code. In this case, the dimensionality of the full optimal semidefinite program grows as 4^n. Instead, if one considers the semidefinite programs for the first- and second-order subspaces, the dimensionality of the approximate programs only grows as n^2 and n^4, respectively. For instance, using the $[[7,1,3]]$ CSS seven-qubit code, the full optimal semidefinite program requires 65 536 optimization variables. However, the first-order semidefinite program requires 1024 variables and the second-order semidefinite program has 7056 optimization variables. For further details, we refer to [12]. In particular, in [12], to mitigate such drawbacks of the optimal recovery, a structured near-optimal channel-adapted recovery procedure was determined and applied to the AD noise model. In [13], an analytical approach to channel-adapted recovery based on the pretty-good measurement and the average entanglement fidelity appeared. Following [13], a simple analytical approach to approximate QEC based on the transpose channel was derived and used for the AD noise model in [14]. In particular, it was shown in [14] that the transpose channel is a recovery map that coincides with the perfect recovery map for codes satisfying the perfect Knill-Laflamme QEC conditions [15]. Very recently, it was also proved that the transpose channel works nearly as well as the optimal recovery channel, with optimality defined in terms of worst-case fidelity over all code states [16]. As a side remark, we underline that no definitive choice for the best figure of merit in quantum information processing tasks has been made yet [17] and this fact becomes especially relevant when quantifying the performance of quantum codes [18–22]. In [18], focusing on the AD noise model, it was shown that fidelity alone may be not be sufficient to compare the efficiency of different error-correction codes. In [23], a numerical search based upon a greedy algorithm [10] was employed to construct a family of high-rate nonadditive quantum codes adapted to the AD noise model that outperform (in terms of encoded dimension) the stabilizer codes presented in [8]. In [24], families of high-performance nonadditive quantum codes of the codeword-stabilized (CWS [25]) type for single AD errors that outperform, in terms of encoded dimension, the best possible additive codes were presented. These code families were built from nonlinear error-correcting codes for classical asymmetric channels or classical codes over $GF(3)$. Finally, for the sake of completeness, we also point out that a method for the construction of good multi-error-correcting AD codes that are both degenerate and additive can be found in [26].

Taking into account all these above-mentioned facts, we emphasize that there is

(i) no clear understanding of the role played by degeneracy in the analysis of the performance of stabilizer quantum codes for AD errors [12];

(ii) no explicit evidence of the relevance of the role played by self-complementarity in the analysis of the performance (quantified by means of the entanglement fidelity) of nonadditive quantum codes [24];

(iii) no explicit analytical computation of the entanglement fidelity of arbitrary quantum codes for AD errors for simple-to-construct recovery maps [16];

(iv) no explicit performance comparison in terms of the entanglement fidelity between additive and nonadditive quantum codes for AD errors [23].

In this article, following the working methodology advocated by one of the authors in [27,28], we seek to advance our quantitative understanding via simple analytical computations of the role played by degeneracy, self-complementarity, additivity, and nonadditivity of quantum codes for the GAD error model [3]. Specifically, we present the analysis of the performance of various approximate QEC schemes for the GAD channel. We consider both stabilizer and nonadditive quantum codes. The performance of such error-correcting schemes is quantified by means of the entanglement fidelity as a function of the damping probability and the nonzero environmental temperature. The recovery scheme employed throughout our work applies, in principle, to arbitrary quantum

codes and is the analog of the perfect Knill-Laflamme recovery scheme adapted to the approximate QEC framework for the GAD error model. We also analytically recover and/or clarify some previously known numerical results in the limiting case of vanishing temperature of the environment. In addition, our extended analytical investigation suggests that degenerate stabilizer codes and self-complementary nonadditive codes are especially suitable for the error correction of the GAD noise model. Finally, comparing the properly normalized entanglement fidelities of the best performant stabilizer and nonadditive codes characterized by the same length, we show that nonadditive codes outperform stabilizer codes not only in terms of encoded dimension but also in terms of fidelity.

This article is organized as follows. In Sec. II, we describe the GAD noise model. In Sec. III, we present some preliminary material concerning exact and approximate QEC conditions, recovery maps, and entanglement fidelity. In Sec. IV, we analyze the performances of various stabilizer codes, both degenerate and nondegenerate. In Sec. V, we quantify the performances of various nonadditive codes, both self-complementary and non-self-complementary. Finally, our conclusions are presented in Sec. VI. A number of appendixes with technical details of calculations are also provided.

II. THE GAD NOISE MODEL

The AD quantum operation can characterize the behavior of different types of dissipative open quantum systems [3]: The spontaneous emission of a single atom coupled to a single mode of the electromagnetic radiation, the gradual loss of energy from a principal system to the environment where both systems are modeled by simple harmonic oscillators, or the scattering of a photon via a beam splitter represent physical processes modeled by an AD channel.

It can be shown that the GAD qubit channel can be realized by considering the evolution of a two-level quantum system (that is, a qubit) in a dissipative interaction, in the Born-Markov rotating-wave approximation [29], with a bath of harmonic oscillators taken to be initially in a thermal state [30,31].

The Lindblad form of the master equation that describes the evolution that generates the GAD channel reads [31]

$$\frac{d\rho^S(t)}{dt} = \sum_{j=1}^{2}(2R_j\rho^S R_j^\dagger - R_j^\dagger R_j\rho^S - \rho^S R_j^\dagger R_j), \quad (3)$$

where the operators R_1, R_2, and R are given by

$$R_1 \stackrel{\text{def}}{=} \left[\frac{\gamma_0}{2}(N_{\text{th}}+1)\right]^{\frac{1}{2}} R, \quad R_2 \stackrel{\text{def}}{=} \left(\frac{\gamma_0 N_{\text{th}}}{2}\right)^{\frac{1}{2}} R^\dagger, \quad R \stackrel{\text{def}}{=} \sigma_-, \quad (4)$$

with γ_0, N_{th}, and σ_- defined as

$$\gamma_0 \stackrel{\text{def}}{=} \frac{4\omega^3|\mathbf{d}|^2}{3\hbar c^3}, \quad N_{\text{th}} \stackrel{\text{def}}{=} \frac{1}{e^{\frac{\hbar\omega}{k_B T}}-1}, \quad \sigma_- \stackrel{\text{def}}{=} \frac{\sigma_x - i\sigma_y}{2} = |1\rangle\langle 0|. \quad (5)$$

In Eq. (5), γ_0 denotes the spontaneous emission rate, ω is the photonic frequency, $\hbar$ is the Planck constant divided by 2π, c is the speed of light, $\mathbf{d}$ is the transition matrix of the atomic dipole operator describing the interaction between the two-level quantum system with the bath of harmonic oscillators, k_B is the Boltzmann constant, σ_- is the lowering operator, N_{th} is the Planck distribution that gives the number of thermal photons at frequency ω, and, finally, T denotes the temperature of the environment. The operator ρ^S denotes the reduced density matrix operator of the two-level quantum system interacting with a thermal bath in the weak Born-Markov rotating-wave approximation [31]. We remark that when $T = 0$, then $N_{\text{th}} = 0$ and $R_2 = 0$. Therefore, when the temperature of the environment is zero, a single Lindblad operator is sufficient to describe the master equation.

The evolution of the density operator ρ^S in Eq. (3) can be given a Kraus operator-sum decomposition. The Kraus representation is useful because it provides an intrinsic description of the principal system, without explicitly considering the detailed properties of the environment. The essential features of the problem are contained in the Kraus error operators A_k. This not only simplifies calculations, but often provides theoretical insight.

Following [31], it turns out that the Kraus decomposition of the GAD channel becomes

$$\Lambda_{\text{GAD}}(\rho) \stackrel{\text{def}}{=} \sum_{k=0}^{3} A_k \rho A_k^\dagger, \quad (6)$$

where the Kraus error operators A_k read

$$\begin{aligned}
A_0 &\stackrel{\text{def}}{=} \frac{\sqrt{p}}{2}[(1+\sqrt{1-\gamma})I + (1-\sqrt{1-\gamma})\sigma_z],\\
A_1 &\stackrel{\text{def}}{=} \frac{\sqrt{p}\sqrt{\gamma}}{2}(\sigma_x + i\sigma_y),\\
A_2 &\stackrel{\text{def}}{=} \frac{\sqrt{1-p}}{2}[(1+\sqrt{1-\gamma})I - (1-\sqrt{1-\gamma})\sigma_z],\\
A_3 &\stackrel{\text{def}}{=} \frac{\sqrt{1-p}\sqrt{\gamma}}{2}(\sigma_x - i\sigma_y),
\end{aligned} \quad (7)$$

where γ is the damping parameter and $0 \leqslant p \leqslant 1$ [3] . The (2×2)-matrix representation of the operators A_k in Eq. (7) is given by

$$\begin{aligned}
A_0 &= \sqrt{p}\begin{pmatrix}1 & 0\\ 0 & \sqrt{1-\gamma}\end{pmatrix}, \quad A_1 = \sqrt{p}\begin{pmatrix}0 & \sqrt{\gamma}\\ 0 & 0\end{pmatrix},\\
A_2 &= \sqrt{1-p}\begin{pmatrix}\sqrt{1-\gamma} & 0\\ 0 & 1\end{pmatrix}, \quad A_3 = \sqrt{1-p}\begin{pmatrix}0 & 0\\ \sqrt{\gamma} & 0\end{pmatrix},
\end{aligned} \quad (8)$$

and their action on the computational basis vectors $|0\rangle$ and $|1\rangle$ of the *complex* Hilbert space $\mathcal{H}_2^1$ (the Hilbert space of 1-qubit quantum states) reads

$$\begin{aligned}
&A_0|0\rangle = \sqrt{p}|0\rangle, \quad A_0|1\rangle = \sqrt{p}\sqrt{1-\gamma}|1\rangle,\\
&A_1|0\rangle \equiv 0, \quad A_1|1\rangle = \sqrt{p}\sqrt{\gamma}|0\rangle,\\
&A_2|0\rangle = \sqrt{1-p}\sqrt{1-\gamma}|0\rangle, \quad A_2|1\rangle = \sqrt{1-p}|1\rangle,\\
&A_3|0\rangle = \sqrt{1-p}\sqrt{\gamma}|1\rangle, \quad A_3|1\rangle \equiv 0.
\end{aligned} \quad (9)$$

Notice that for $p = 1$, the Kraus operator-sum decomposition of the AD channel can be recovered. The GAD channel generalizes the AD channel in that it allows transitions from

$|0\rangle \rightarrow |1\rangle$ as well as from $|1\rangle \rightarrow |0\rangle$. For an alternative and explicit derivation of the operator-sum decomposition of the GAD channel in the context of scattering of a photon via a beam splitter, we refer to Appendix A.

We emphasize that the GAD channel is particularly noisy and, unlike the AD channel, is characterized by a two-dimensional parametric region $(\gamma, p(\gamma))$ where it exhibits entanglement-breaking features (for details, see Appendix B). From [31], it also follows that the two GAD channel parameters γ and p are formally given by

$$\gamma(t) \stackrel{\text{def}}{=} 1 - e^{-\gamma_0(2N_{\text{th}}+1)t} \quad \text{and} \quad p \stackrel{\text{def}}{=} \frac{N_{\text{th}}+1}{2N_{\text{th}}+1}. \tag{10}$$

Observe that $p = 1$ when $T = 0$ and $p = \frac{1}{2}$ when T approaches infinity. For the sake of future convenience, we also introduce a new additional parameter ε defined as

$$\varepsilon(t) \stackrel{\text{def}}{=} 1 - p(t) = \frac{e^{-\frac{\hbar\omega}{k_B T}}}{1 + e^{-\frac{\hbar\omega}{k_B T}}} \stackrel{T \ll 1}{\approx} e^{-\frac{\hbar\omega}{k_B T}}. \tag{11}$$

Combining Eqs. (10) and (11), we get

$$\gamma(t) \equiv \gamma_\varepsilon(t) \stackrel{\text{def}}{=} 1 - \exp\left[-\left(\frac{1}{1-2\varepsilon}\right)\gamma_0 t\right] \stackrel{\varepsilon \ll 1}{\approx} 1 - e^{-\gamma_0(1+2\varepsilon)t}. \tag{12}$$

From Eq. (12), we conclude that γ_ε is a monotonic increasing function of ε for $\varepsilon \ll 1$ and fixed values of γ_0 and t.

III. QEC CONDITIONS, RECOVERY MAPS, AND ENTANGLEMENT FIDELITY

A. QEC conditions

1. Exact QEC

Sufficient conditions for approximate QEC were introduced by Leung *et al.* in [7]. They showed that quantum codes can be effective in the error-correction procedure even though they violate the traditional (exact) Knill-Laflamme QEC conditions [15]. However, these violations, characterized by small deviations from the standard error-correction conditions are allowed provided that they do not affect the desired fidelity order.

For the sake of reasoning, let us consider a binary quantum stabilizer code $\mathcal{C}$ with code parameters $[[n,k,d]]$ encoding k-logical qubits in the Hilbert space $\mathcal{H}_2^k$ into n-physical qubits in the Hilbert space $\mathcal{H}_2^n$ with distance d. Assume that the noise model after the encoding procedure is $\Lambda(\rho)$ and can be described by an operator-sum representation,

$$\Lambda(\rho) \stackrel{\text{def}}{=} \sum_{k \in \mathcal{K}} A_k \rho A_k^\dagger, \tag{13}$$

where $\mathcal{K}$ is the index set of all the enlarged Kraus operators A_k that appear in the sum. The noise channel Λ is a completely positive and trace-preserving (CPTP) map. The codespace of $\mathcal{C}$ is a 2^k-dimensional subspace of $\mathcal{H}_2^n$ where some error operators that characterize the error model Λ being considered can be reversed. Denote with $\mathcal{A}_{\text{reversible}} \subset \mathcal{A} \stackrel{\text{def}}{=} \{A_k\}$ with $k \in \mathcal{K}$ the set of reversible enlarged errors A_k on $\mathcal{C}$ such that $\mathcal{K}_{\text{reversible}} \stackrel{\text{def}}{=} \{k : A_k \in \mathcal{A}_{\text{reversible}}\}$ is the index set of $\mathcal{A}_{\text{reversible}}$. Therefore, the noise model $\Lambda'(\rho)$ given by

$$\Lambda'(\rho) \stackrel{\text{def}}{=} \sum_{k \in \mathcal{K}_{\text{reversible}}} A_k \rho A_k^\dagger \tag{14}$$

is reversible on $C \subset \mathcal{H}_2^n$. The noise channel Λ' denotes a CP but non-TP map. The enlarged error operators A_k in $\mathcal{A}_{\text{reversible}}$ satisfy the standard QEC conditions [3],

$$P_{\mathcal{C}} A_l^\dagger A_m P_{\mathcal{C}} = \alpha_{lm} P_{\mathcal{C}}, \tag{15}$$

or, equivalently,

$$\langle i_L | A_l^\dagger A_m | j_L \rangle = \alpha_{lm} \delta_{ij}, \tag{16}$$

for any l, $m \in \mathcal{K}_{\text{reversible}}$, $P_{\mathcal{C}}$ denotes the projector on the codespace, and α_{lm} are entries of a positive Hermitian matrix. It is helpful to regard the Knill-Laflamme condition in Eq. (16) as embodying two conditions [32]: the obvious off-diagonal condition saying that the matrix elements of $A_l^\dagger A_m$ must vanish when $i \neq j$ (orthogonality condition); and the diagonal condition which, since α_{lm} are entries of a positive Hermitian *complex* matrix, is nothing but the requirement that all diagonal elements of $A_l^\dagger A_m$ (inside the coding space) be identical (nondeformability condition). The fulfillment of Eq. (15) for some subset of enlarged error operators A_k that characterize the operator-sum representation of the noise model Λ implies that there exists a new operator-sum decomposition of Λ such that $\Lambda'(\rho)$ in Eq. (14) becomes

$$\Lambda'(\rho) \stackrel{\text{def}}{=} \sum_{k \in \mathcal{K}'_{\text{reversible}}} A'_k \rho A_k'^\dagger, \tag{17}$$

where Eq. (15) is replaced with

$$P_{\mathcal{C}} A_l'^\dagger A'_m P_{\mathcal{C}} = p_m \delta_{lm} P_{\mathcal{C}}, \tag{18}$$

for any l, $m \in \mathcal{K}'_{\text{reversible}}$ with the error detection probabilities p_m non-negative c numbers. We remark that Eq. (18) is equivalent to the traditional orthogonality and nondeformation conditions [see Eq. (16)] for a nondegenerate code,

$$\langle i_L | A_l^\dagger A_m | j_L \rangle = \delta_{ij} \delta_{lm} p_m, \tag{19}$$

for any i, j labeling the logical states and l, $m \in \mathcal{K}_{\text{reversible}}$. Observe that for any linear operator A'_k on a vector space V there exists a unitary U_k and a positive operator $J \stackrel{\text{def}}{=} \sqrt{A_k'^\dagger A'_k}$ such that [3]

$$A'_k = U_k J = U_k \sqrt{A_k'^\dagger A'_k}. \tag{20}$$

We stress that J is the unique positive operator that satisfies Eq. (20). As a matter of fact, multiplying $A'_k = U_k J$ on the left by the adjoint equation $A_k'^\dagger = J U_k^\dagger$ gives

$$A_k'^\dagger A'_k = J U_k^\dagger U_k J = J^2 \Rightarrow J = \sqrt{A_k'^\dagger A'_k}. \tag{21}$$

Furthermore, if A'_k is invertible (that is, $\det A'_k \neq 0$), U_k is unique and reads

$$U_k \stackrel{\text{def}}{=} A'_k J^{-1} = A'_k (\sqrt{A_k'^\dagger A'_k})^{-1}. \tag{22}$$

How do we choose the unitary U_k when A'_k is not invertible? The operator J is a positive operator and belongs to a special

subclass of Hermitian operators such that for any vector $|v\rangle \in V$, $(|v\rangle, J|v\rangle)$ is a *real* and non-negative number. Therefore, J has a spectral decomposition

$$J \stackrel{\text{def}}{=} \sqrt{A_k'^{\dagger} A_k'} = \sum_l \lambda_l \, |l\rangle \langle l|, \tag{23}$$

where $\lambda_l \geqslant 0$ and $\{|l\rangle\}$ denotes an orthonormal basis for the vector space V. Define the vectors $|\psi_l\rangle \stackrel{\text{def}}{=} A_k'|l\rangle$ and notice that

$$\langle \psi_l | \psi_l \rangle = \langle l | A_k'^{\dagger} A_k' | l \rangle = \langle l | J^2 | l \rangle = \lambda_l^2. \tag{24}$$

For the time being, consider only those l for which $\lambda_l \neq 0$. For those l, consider the vectors $|e_l\rangle$ defined as

$$|e_l\rangle \stackrel{\text{def}}{=} \frac{|\psi_l\rangle}{\lambda_l} = \frac{A_k' \, |l\rangle}{\lambda_l}, \tag{25}$$

with $\langle e_l | e_{l'} . \rangle = \delta_{ll'}$. For those l for which $\lambda_l = 0$, extend the orthonormal set $\{|e_l\rangle\}$ in such a manner that it forms an orthonormal basis $\{|E_l\rangle\}$. Then, a suitable choice for the unitary operator U_k such that

$$A_k' \, |l\rangle = U_k J |l\rangle, \tag{26}$$

with $\{|l\rangle\}$ an orthonormal basis for V, reads

$$U_k \stackrel{\text{def}}{=} \sum_l |E_l\rangle \, \langle l|. \tag{27}$$

In summary, the unitary U_k is uniquely determined by Eq. (22) when A_k' is invertible or Eq. (27) when A_k' is not necessarily invertible. We finally stress that the nonuniqueness of U_k when $\det A_k' = 0$ is due to the freedom in choosing the orthonormal basis $\{|l\rangle\}$ for the vector space V.

In the scenario being considered, when Eq. (18) is satisfied, the enlarged error operators A_m' admit polar decompositions,

$$A_m' P_{\mathcal{C}} = \sqrt{p_m} U_m P_{\mathcal{C}}, \tag{28}$$

with $m \in \mathcal{K}_{\text{reversible}}$. From Eqs. (18) and (28), we get

$$p_m \delta_{lm} P_{\mathcal{C}} = P_{\mathcal{C}} A_l'^{\dagger} A_m' P_{\mathcal{C}} = \sqrt{p_l p_m} P_{\mathcal{C}} U_l^{\dagger} U_m P_{\mathcal{C}}; \tag{29}$$

that is,

$$P_{\mathcal{C}} U_l^{\dagger} U_m P_{\mathcal{C}} = \delta_{lm} P_{\mathcal{C}}. \tag{30}$$

We stress that Eq. (30) is needed for an unambiguous syndrome detection, since, as a consequence of the orthogonality of different $R_m^{\dagger} \stackrel{\text{def}}{=} U_m P_{\mathcal{C}}$, the recovery operation $\mathcal{R}$ is trace preserving. This can be shown as follows.

Let $\mathcal{V}^{i_L}$ be the subspace of $\mathcal{H}_2^n$ spanned by the corrupted images $\{A_k'|i_L\rangle\}$ of the codewords $|i_L\rangle$. Let $\{|v_r^{i_L}\rangle\}$ be an orthonormal basis for $\mathcal{V}^{i_L}$. We define such a subspace $\mathcal{V}^{i_L}$ for each of the codewords. Because of the traditional Knill-Laflamme QEC conditions [15],

$$\begin{aligned} &\langle i_L | A_k^{\dagger} A_{k'} | i_L \rangle = \langle j_L | A_k^{\dagger} A_{k'} | j_L \rangle, \quad \forall \, i, j, \\ &\langle i_L | A_k^{\dagger} A_{k'} | j_L \rangle = 0, \quad \forall \, i \neq j, \end{aligned} \tag{31}$$

the subspaces $\mathcal{V}^{i_L}$ and $\mathcal{V}^{j_L}$ with $i \neq j$ are orthogonal subspaces. If $\mathcal{V}^{i_L} \oplus \mathcal{V}^{j_L}$ is a proper subset of $\mathcal{H}_2^n$ with $\mathcal{V}^{i_L} \oplus \mathcal{V}^{j_L} \neq \mathcal{H}_2^n$, we denote its orthogonal complement by O,

$$\mathcal{H}_2^n \stackrel{\text{def}}{=} (\mathcal{V}^{i_L} \oplus \mathcal{V}^{j_L}) \oplus O, \tag{32}$$

where

$$O \stackrel{\text{def}}{=} (\mathcal{V}^{i_L} \oplus \mathcal{V}^{j_L})^{\perp}. \tag{33}$$

Let $\{|o_k\rangle\}$ be an orthonormal basis for O. Then, the set of states $\{|v_r^{i_L}\rangle, |o_k\rangle\}$ constitutes an orthonormal basis for $\mathcal{H}_2^n$. Notice that, since $|v_r^{i_L}\rangle$ are mutually orthogonal, there exist unitary V_r such that $V_r |v_r^{i_L}\rangle = |i_L\rangle$ (V_r is an isometry which returns $|v_r^{i_L}\rangle$ to the corresponding $|i_L\rangle$). We introduce the quantum recovery operation $\mathcal{R}$ with operation elements

$$\mathcal{R} \stackrel{\text{def}}{=} \{R_1, \ldots, R_r, \ldots, \hat{O}\}, \tag{34}$$

with

$$\mathcal{R}(\rho) = \sum_{k \in \mathcal{K}'_{\text{reversible}}} R_k \rho R_k^{\dagger} + \hat{O} \rho \hat{O}^{\dagger}, \tag{35}$$

where [15]

$$R_r \stackrel{\text{def}}{=} V_r \sum_i |v_r^{i_L}\rangle\langle v_r^{i_L}| = \sum_i |i_L\rangle\langle v_r^{i_L}|, \tag{36}$$

and $\hat{O}$ (with $\hat{O} = \hat{O}^{\dagger} = \hat{O}^{\dagger}\hat{O}$) is a projector onto the subspace O in Eq. (33),

$$\hat{O} \stackrel{\text{def}}{=} \sum_k |o_k\rangle\langle o_k|. \tag{37}$$

We remark that the recovery operation $\mathcal{R}$ is a trace-preserving quantum operation since

$$\begin{aligned} &\sum_r R_r^{\dagger} R_r + \hat{O}^{\dagger} \hat{O} \\ &= \sum_r \left[\left(\sum_i |i_L\rangle\langle v_r^{i_L}| \right)^{\dagger} \left(\sum_j |j_L\rangle\langle v_r^{j_L}| \right) \right] \\ &\quad + \left(\sum_k |o_k\rangle\langle o_k| \right)^{\dagger} \left(\sum_{k'} |o_{k'}\rangle\langle o_{k'}| \right) \\ &= \sum_{r,i,j} |v_r^{i_L}\rangle\langle i_L | j_L\rangle\langle v_r^{j_L}| + \sum_{k,k'} |o_k\rangle\langle o_k | o_{k'}\rangle\langle o_{k'}| \\ &= \sum_{r,i,j} |v_r^{i_L}\rangle\langle v_r^{j_L}| \delta_{ij} + \sum_{k,k'} |o_k\rangle\langle o_{k'}| \delta_{kk'} \\ &= \sum_{r,i} |v_r^{i_L}\rangle\langle v_r^{i_L}| + \sum_k |o_k\rangle\langle o_k| = \mathcal{I}_{2^n \times 2^n}, \end{aligned} \tag{38}$$

because $\mathcal{B}_{\mathcal{H}_2^n} \stackrel{\text{def}}{=} \{|v_r^{j_L}\rangle, |o_k\rangle\}$ is an orthonormal basis for $\mathcal{H}_2^n$. We emphasize that $\mathcal{R}$ is indeed a CPTP superoperator (whose recovery operators R_k can be regarded as projective measurements followed by unitary rotations), since it is a sum of orthogonal projections followed by unitary operators where the projections span the Hilbert space $\mathcal{H}_2^n$. Furthermore, we point out that the recovery scheme $\mathcal{R}$ in Eq. (34) applies, in principle, to any quantum code satisfying the QEC conditions independent of the stabilizer formalism [15]. For more technical details, we refer to [15] and [33].

2. *Approximate QEC*

In general, approximate QEC becomes useful when the operator-sum representation of the noise model is defined by errors parametrized by a certain number of small parameters such as the coupling strength between the environment and the quantum system. For the sake of simplicity, suppose the error model is characterized by a single small parameter δ and assume the goal is to uncover a quantum code for the noise model Λ' with fidelity,

$$\mathcal{F} \geqslant 1 - O(\delta^{\beta+1}). \tag{39}$$

How strong can be the violation of the traditional perfect Knill-Laflamme QEC conditions in order to preserve the desired fidelity order in Eq. (39)? In other words, how relaxed can the approximate error-correction conditions be so that the inequality in Eq. (39) is satisfied? The answer to this important question was provided by Leung *et al.* in [7].

It turns out that for both exact and approximate QEC conditions, it is necessary that

$$P_{\text{detection}} \stackrel{\text{def}}{=} \sum_{k \in \mathcal{K}'_{\text{reversible}}} p_k \geqslant \mathcal{F}, \tag{40}$$

where $P_{\text{detection}}$ denotes the total error detection probability. Equation (40) requires that all the enlarged error operators A'_l with maximum detection probability must be included in $\mathcal{A}'_{\text{reversible}}$,

$$\max_{|\psi_{\text{in}}\rangle \in \mathcal{C}} \text{Tr}(|\psi_{\text{in}}\rangle\langle\psi_{\text{in}}| A_l'^{\dagger} A'_l) \approx O(\delta^{\alpha}) \quad \text{with} \quad \alpha \leqslant \beta. \tag{41}$$

The important point is that a good overlap between the input and output states is needed while it is not necessary to recover the exact input state $|\psi_{\text{in}}\rangle\langle\psi_{\text{in}}|$, since we do not require $\mathcal{F} = 1$. In terms of the enlarged error operators restricted to the codespace, this means that such errors need to be only approximately unitary and mutually orthogonal. These considerations lead to the relaxed sufficient QEC conditions.

In analogy to Eq. (28), assume that the polar decomposition for A'_l is given by

$$A'_l P_{\mathcal{C}} = U_l \sqrt{P_{\mathcal{C}} A_l'^{\dagger} A'_l P_{\mathcal{C}}}. \tag{42}$$

Since $P_{\mathcal{C}} A_l'^{\dagger} A'_l P_{\mathcal{C}}$ restricted to the codespace $\mathcal{C}$ have different eigenvalues, the exact error-correction conditions are not fulfilled. Let us say that $\lambda_l^{(\max)} \stackrel{\text{def}}{=} p_l$ and $\lambda_l^{(\min)} \stackrel{\text{def}}{=} \lambda_l p_l$ are the largest and the smallest eigenvalues, respectively, where both p_l and λ_l are c numbers. Furthermore, let us define the so-called residue operator π_l as [7]

$$\pi_l \stackrel{\text{def}}{=} \sqrt{P_{\mathcal{C}} A_l'^{\dagger} A'_l P_{\mathcal{C}}} - \sqrt{\lambda_l p_l} P_{\mathcal{C}}, \tag{43}$$

where

$$0 \leqslant |\pi_l| \stackrel{\text{def}}{=} (\pi_l^{\dagger} \pi_l)^{\frac{1}{2}} \leqslant \sqrt{p_l} - \sqrt{\lambda_l p_l}. \tag{44}$$

Substituting Eq. (43) into Eq. (42), we obtain

$$A'_l P_{\mathcal{C}} = U_l (\sqrt{\lambda_l p_l} I + \pi_l) P_{\mathcal{C}}. \tag{45}$$

From Eq. (45) and imposing that $P_{\mathcal{C}} U_l^{\dagger} U_m P_{\mathcal{C}} = \delta_{lm} P_{\mathcal{C}}$, the analog of Eq. (18) becomes

$$P_{\mathcal{C}} A_l'^{\dagger} A'_m P_{\mathcal{C}} = (\sqrt{\lambda_l p_l} I + \pi_l^{\dagger})(\sqrt{\lambda_m p_m} I + \pi_m) P_{\mathcal{C}} \delta_{lm}, \tag{46}$$

where

$$\lambda_l^{(\max)} - \lambda_l^{(\min)} \equiv p_l (1 - \lambda_l) \leqslant O(\delta^{\beta+1}), \quad \forall\, l \in \mathcal{K}'_{\text{reversible}}. \tag{47}$$

We point out that when the exact QEC conditions are satisfied, $\lambda_l = 1$ and $\pi_l = 0$, thus, Eqs. (18) and (46) coincide. Finally, we point out that an approximate recovery operation $\mathcal{R} \stackrel{\text{def}}{=} \{R_1, \ldots, R_r, \ldots, \hat{O}\}$ with R_k defined in Eq. (36) and $\hat{O}$ formally defined just as in the exact case can be employed in this new scenario as well. However, extra care in the explicit computation of the unitary operators U_k is needed in view of the fact that the polar decomposition in Eq. (28) is replaced by the one in Eq. (42). More details can be found in [7].

B. Recovery maps

In general, numerically constructed recovery maps do not exhibit any practical implementation structure while the perfect Knill-Laflamme recovery map can be implemented simply using syndrome measurements and conditional unitary gates [15]. For these reasons, our intention here is to pursue an analytical approach to the recovery scheme that reduces to the perfect Knill-Laflamme recovery scheme in the limiting case of small deviations from the exact QEC conditions.

We stress that one of the main points advocated in [15] includes treating a code solely in terms of its subspace in a larger Hilbert space and defining decoding operations in terms of general recovery superoperator. Basically, the focus is on the construction of the recovery superoperator rather than on the encoding and decoding operators. This allows studying the codes and their properties for arbitrary interaction superoperator and avoids explicitly dealing with decoding and encoding issues when studying the fidelity of a code given its recovery operator. We also emphasize that the approximate QEC conditions, like the perfect QEC conditions, provide a way to check if a code is approximately correctable, without requiring knowledge of the optimal recovery. Once again, we emphasize here that the perfect Knill-Laflamme recovery scheme $\mathcal{R}$ in Eq. (34) applies, in principle, to any quantum code satisfying the QEC conditions and no mention to the stabilizer formalism appeared in [15]. Furthermore, for the sake of completeness, we also remark that the traditional recovery operation for stabilizer codes can be summarized as follows. First, measure all the eigenvalues of the stabilizer generators; this is the so-called syndrome measurement. Second, given the measured syndrome, compute the minimum Hamming weight error (that is, the most probable error) that could have caused the syndrome. Third, apply the Pauli matrices that correct this error. For the sake of completeness, we point out that for various codes and error models, the minimum Hamming weight error cannot be efficiently determined. More generally, rather than the most likely single error, the most likely equivalence class of errors is determined.

One of the first important theoretical approaches to near-optimal recovery schemes was presented in [13], where reversal recovery operations that are near optimal for the average entanglement fidelity $\bar{\mathcal{F}}(E, \Lambda)$,

$$\bar{\mathcal{F}}(E, \Lambda) \stackrel{\text{def}}{=} \sum_i p_i \mathcal{F}(\rho_i, \Lambda), \tag{48}$$

with $E \stackrel{\text{def}}{=} \{p_i, \rho_i\}$ denoting an ensemble with states ρ_i that occur with probability p_i [where $\mathcal{F}$ denotes the entanglement fidelity, see Eq. (58)] were constructed analytically. The near-optimal reversal operation reads [13],

$$\mathcal{R}_{\Lambda,\rho}^{(\text{Barnum-Knill})} \sim \{\rho^{\frac{1}{2}} A_k^\dagger \Lambda(\rho)^{-\frac{1}{2}}\}, \tag{49}$$

where $\Lambda \sim \{A_k\}$. In [34,35], generalizing the traditional Knill-Laflamme QEC conditions [15], necessary and sufficient conditions for approximate correctability of a quantum code were derived. In particular, a class of near-optimal recovery channels for the worst-case entanglement fidelity (that is, entanglement fidelity minimized over all input states) was also provided. Following [13] and assuming $\rho = P_{\mathcal{C}}/d$, where d is the dimension of the codespace and $P_{\mathcal{C}}$ the projector on the codespace, a special case of the near-optimal reversal operation in Eq. (49) was introduced in [14,16]. Such reversal operation is the so-called transpose channel recovery map,

$$\mathcal{R}_{\text{TC}} \stackrel{\text{def}}{=} \mathcal{R}_{\Lambda, P_{\mathcal{C}}/d}^{(\text{Barnum-Knill})} \sim \{P_{\mathcal{C}} A_k^\dagger \Lambda(P_{\mathcal{C}})^{-\frac{1}{2}}\}. \tag{50}$$

The transpose channel recovery map $\mathcal{R}_{\text{TC}}$ is a simple-to-construct recovery map built from the noise channel Λ and the code $\mathcal{C}$. In particular it works nearly as well as the optimal recovery channel, with optimality defined in terms of worst-case fidelity over all input states [the fidelity between any two states ρ and σ is given by $f(\rho,\sigma) \stackrel{\text{def}}{=} \text{Tr}\sqrt{\rho^{\frac{1}{2}}\sigma\rho^{\frac{1}{2}}}$]. We point out, as mentioned in [13] and explicitly shown in [14], that the transpose channel $\mathcal{R}_{\text{TC}}$ in Eq. (50) reduces to the perfect Knill-Laflamme recovery operation $\mathcal{R}_{\text{perfect}}^{(\text{Knill-Laflamme})}$ when the traditional exact QEC conditions are satisfied.

The recovery scheme that we choose to use in this work is formally defined in terms of recovery operators that are just like the operators R_k in Eq. (36),

$$\begin{aligned} R_k \stackrel{\text{def}}{=} V_k P_k \equiv V_k \sum_i |v_k^{i_L}\rangle\langle v_k^{i_L}| &= \sum_i |i_L\rangle\langle v_k^{i_L}| \\ &= \frac{|0_L\rangle\langle 0_L| A_k^\dagger}{\sqrt{\langle 0_L| A_k^\dagger A_k |0_L\rangle}} + \frac{|1_L\rangle\langle 1_L| A_k^\dagger}{\sqrt{\langle 1_L| A_k^\dagger A_k |1_L\rangle}}, \end{aligned} \tag{51}$$

where, however, we must now take into account that $\langle 0_L| A_k^\dagger A_k |0_L\rangle$ may only be approximately equal to $\langle 1_L| A_k^\dagger A_k |1_L\rangle$ in the approximate QEC framework. Thus, the set of errors $\{A_k\}$ that appear in Eq. (51) has to be considered correctable in the approximate sense specified in the previous section. For this reason, the recovery operators R_k in Eq. (51) cannot assume the simple expression they exhibit in the case of exact fulfillment of the QEC conditions. In the optimal (exact) case, the superoperator $\mathcal{R}$ with elements R_k in Eq. (51) becomes

$$\mathcal{R}_{\text{perfect}}^{(\text{Knill-Laflamme})} \sim \left\{ \frac{P_{\mathcal{C}} A_k^\dagger}{\sqrt{p_k}} \right\}, \tag{52}$$

with $p_k \stackrel{\text{def}}{=} \langle 0_L| A_k^\dagger A_k |0_L\rangle \equiv \langle 1_L| A_k^\dagger A_k |1_L\rangle$. Explicit analytical investigations in the framework of exact QEC where the superoperator in Eq. (52) was employed can be found in [19,27,28].

Before describing the concept of entanglement fidelity, we wish to hint at what happens with our recovery scheme in the traditional AD noise model when error correction is performed via the Leung *et al*. four-qubit code [7]. For the sake of clarity, we only consider the recovery operator for the enlarged error $A_{0000} \stackrel{\text{def}}{=} A_0 \otimes A_0 \otimes A_0 \otimes A_0$ with A_0 defined as in Eq. (2). In this case, we have

$$\begin{aligned} R_{A_{0000}} A_{0000} |\psi\rangle &= \alpha\sqrt{1-2\gamma}\sqrt{1 + \frac{3\gamma^2 - 2\gamma^3 + \frac{1}{2}\gamma^4}{1-2\gamma}}|0_L\rangle \\ &\quad + \beta\sqrt{1-2\gamma}\sqrt{1 + \frac{\gamma^2}{1-2\gamma}}|1_L\rangle \\ &= \sqrt{1-2\gamma}|\psi\rangle + O(\gamma^2), \end{aligned} \tag{53}$$

with $|\psi\rangle \stackrel{\text{def}}{=} \alpha|0_L\rangle + \beta|1_L\rangle$, where $\alpha, \beta \in \mathbb{C}$ and $|\alpha|^2 + |\beta|^2 = 1$ and $\{|0_L\rangle, |1_L\rangle\}$ span the codespace of the four-qubit code. The approximate nature of Eq. (53) is in agreement with the modified version of the Knill-Laflamme QEC conditions in Eq. (15),

$$P_{\mathcal{C}} A_{0000}^\dagger A_{0000} P_{\mathcal{C}} = \lambda_{00}(\gamma) P_{\mathcal{C}} + P_{\mathcal{C}} \hat{B}_{00}(\gamma) P_{\mathcal{C}}, \tag{54}$$

with

$$\begin{aligned} &\lambda_{00}(\gamma) \stackrel{\text{def}}{=} 1 - 2\gamma \quad \text{and,} \\ &\hat{B}_{00}(\gamma) \stackrel{\text{def}}{=} \left(3\gamma^2 - 2\gamma^3 + \tfrac{1}{2}\gamma^4\right)|0_L\rangle\langle 0_L| + \gamma^2 |1_L\rangle\langle 1_L|, \end{aligned} \tag{55}$$

while $P_{\mathcal{C}}$ is the projector on the codespace of the code $\mathcal{C}$. For more details on this point, we refer to [35].

C. Entanglement fidelity

Entanglement fidelity is a useful performance measure of the efficiency of quantum error-correcting codes. It is a quantity that keeps track of how well the state and entanglement of a subsystem of a larger system are stored, without requiring the knowledge of the complete state or dynamics of the larger system. More precisely, the entanglement fidelity is defined for a mixed state,

$$\rho \stackrel{\text{def}}{=} \sum_i p_i \rho_i = \text{Tr}_{\mathcal{H}_R} |\psi\rangle\langle\psi|, \tag{56}$$

in terms of a purification $|\psi\rangle \in \mathcal{H} \otimes \mathcal{H}_R$ to a reference system $\mathcal{H}_R$. The purification $|\psi\rangle$ encodes all of the information in ρ. Entanglement fidelity is a measure of how well the channel Λ preserves the entanglement of the state $\mathcal{H}$ with its reference system $\mathcal{H}_R$. The entanglement fidelity is defined as [11]

$$\mathcal{F}(\rho,\Lambda) \stackrel{\text{def}}{=} \langle\psi|(\Lambda \otimes I_{\mathcal{H}_R})(|\psi\rangle\langle\psi|)|\psi\rangle, \tag{57}$$

where $|\psi\rangle$ is any purification of ρ, $I_{\mathcal{H}_R}$ is the identity map on $\mathcal{M}(\mathcal{H}_R)$ (the space of all linear operators on the Hilbert space $\mathcal{H}_R$), and $\Lambda \otimes I_{\mathcal{H}_R}$ is the evolution operator extended to the space $\mathcal{H} \otimes \mathcal{H}_R$, the space on which ρ has been purified. If the quantum operation Λ is written in terms of its Kraus error operators $\{A_k\}$ as $\Lambda(\rho) \stackrel{\text{def}}{=} \sum_k A_k \rho A_k^\dagger$, then it can be shown that [36]

$$\mathcal{F}(\rho,\Lambda) = \sum_k \text{Tr}(A_k\rho)\text{Tr}(A_k^\dagger\rho) = \sum_k |\text{Tr}(\rho A_k)|^2. \tag{58}$$

This expression for the entanglement fidelity is very useful for explicit calculations. Finally, assuming that

$$\Lambda : \mathcal{M}(\mathcal{H}) \ni \rho \mapsto \Lambda(\rho) = \sum_k A_k \rho A_k^\dagger \in \mathcal{M}(\mathcal{H}),$$
$$\dim_{\mathbb{C}} \mathcal{H} = N, \tag{59}$$

and choosing a purification described by a maximally entangled unit vector for the mixed state $\rho = I_{\mathcal{H}}/\dim_{\mathbb{C}}\mathcal{H}$, we obtain

$$\mathcal{F}\left(\frac{1}{N} I_{\mathcal{H}}, \Lambda\right) = \frac{1}{N^2} \sum_k |\mathrm{Tr} A_k|^2. \tag{60}$$

The expression in Eq. (60) represents the entanglement fidelity when no error correction is performed on the noisy channel Λ defined in Eq. (59).

Finally, for the sake of completeness, we point out that there exists a relation between the fidelity of a recovery operation $\mathcal{R}$ and the worst-case error probability parameter p [37],

$$p \stackrel{\text{def}}{=} 1 - \mathcal{F}(\mathcal{R},\mathcal{C},\mathcal{E}), \tag{61}$$

where $\mathcal{C}$ and $\mathcal{E}$ denote the code and the noise channel, respectively. The meaning of the above relation can be described as follows. Consider a quantum state $|\psi\rangle$ encoded into the state $U_{\text{enc}}|\psi\rangle|00\cdots0\rangle$, then subjected to some noise (corresponding to the $\mathcal{E}_i$ operators), then subjected to a recovery operation (corresponding to the R_j operators). Finally, the ancilla work space is discarded, giving back some state ρ_ψ on the original Hilbert space,

$$\rho_\psi = \mathrm{Tr}_{\text{ancilla}}\left[\sum_j R_j U_{\text{enc}}^\dagger \left(\sum_i \mathcal{E}_i U_{\text{enc}}|\psi\rangle|00\cdots0\rangle \times \langle 0\cdots00|\langle\psi|U_{\text{enc}}^\dagger \mathcal{E}_i^\dagger\right) U_{\text{enc}} R_j^\dagger\right]. \tag{62}$$

We are interested in how close ρ_ψ is to the original state $|\psi\rangle\langle\psi|$. The probability $p_\psi = \langle\psi|\rho_\psi|\psi\rangle$ can be regarded as the probability of no error on the encoded state and the fidelity of a recovery operation $\mathcal{R}$ is defined as

$$\mathcal{F}(\mathcal{R},\mathcal{C},\mathcal{E}) \stackrel{\text{def}}{=} \min_{|\psi\rangle} p_\psi, \tag{63}$$

the minimum of all such probabilities p_ψ over all encoded states $|\psi\rangle$. Thus, the probability parameter p gives an upper bound on the probability with which a generic encoded state will end up in the wrong state.

IV. ADDITIVE CODES

We denote by $[[n,k,d]]$ a stabilizer (or additive) code that encodes k logical qubits into n physical qubits correcting $\lfloor\frac{d-1}{2}\rfloor$-qubit errors, where d is the distance of the code and $\lfloor x\rfloor$ denotes the largest integer less than x. Additive quantum codes are characterized by a codespace, the space spanned by the so-called codewords, which is a simultaneous eigenspace of an Abelian subgroup of the Pauli group. For more details on the stabilizer formalism, we refer to [38].

A. Nondegenerate codes

Formally speaking, quantum codes for which the positive Hermitian matrix α in Eq. (15) is nonsingular are called nondegenerate codes. Instead, codes for which α is singular are called degenerate. For nondegenerate codes, each error is individually identifiable and, for a given choice of error operators, the quantum code is transformed into a set of distinct orthogonal subspaces by applying the errors. In short, for nondegenerate codes, all the errors acting on the codewords produce linearly independent quantum states.

1. The five-qubit code

The $[[5,1,3]]$ code is the smallest single-error-correcting quantum code [5,6]. Of all QECCs that encode one qubit of data and correct all single-qubit errors, the $[[5,1,3]]$ is the most efficient, saturating the quantum Hamming bound. It encodes $k = 1$ qubit in $n = 5$ qubits. The cardinality of its stabilizer group $\mathcal{S}$ is $|\mathcal{S}| = 2^{n-k} = 16$ and the set $\mathcal{B}_{\mathcal{S}}^{[[5,1,3]]}$ of $n-k=4$ stabilizer group generators is given by [33]

$$\mathcal{B}_{\mathcal{S}}^{[[5,1,3]]} \stackrel{\text{def}}{=} \{X^1Z^2Z^3X^4, X^2Z^3Z^4X^5, X^1X^3Z^4Z^5, Z^1X^2X^4Z^5\}, \tag{64}$$

with $X \stackrel{\text{def}}{=} \sigma_x$, $Y \stackrel{\text{def}}{=} \sigma_y$, and $Z \stackrel{\text{def}}{=} \sigma_z$ and $\{\sigma_x,\sigma_y,\sigma_z\}$ as given in Eq. (1). For the sake of notational clarity, we emphasize that when describing stabilizer generators as tensor products of Pauli operators, we may omit to use the symbol $\otimes$. In addition, the superscripts on the right-hand side of Eq. (64) label the qubits $1,\ldots,5$. The distance of the code is $d = 3$ and therefore the weight of the smallest enlarged error operators of the form $A_l^\dagger A_k$ that cannot be detected by the code is 3. Finally, we recall that it is a nondegenerate code, since the smallest weight for elements of $\mathcal{S}$ (other than identity) is 4 and therefore it is greater than the distance $d = 3$. The encoding for the $[[5,1,3]]$ code is given by [5]

$$\begin{aligned}|0_L\rangle &\stackrel{\text{def}}{=} \frac{1}{\sqrt{8}}[-|00000\rangle + |01111\rangle - |10011\rangle + |11100\rangle \\ &\quad + |00110\rangle + |01001\rangle + |10101\rangle + |11010\rangle], \\ |1_L\rangle &\stackrel{\text{def}}{=} \frac{1}{\sqrt{8}}[-|11111\rangle + |10000\rangle + |01100\rangle - |00011\rangle \\ &\quad + |11001\rangle + |10110\rangle - |01010\rangle - |00101\rangle].\end{aligned} \tag{65}$$

The enlarged GAD quantum channel after performing the encoding defined by means of Eq. (65) reads

$$\Lambda_{\text{GAD}}^{[[5,1,3]]}(\rho) \stackrel{\text{def}}{=} \sum_{r=0}^{2^{10}-1} A_r' \rho A_r'^\dagger = \sum_{i,j,k,l,m=0}^{3} A_{ijklm} \rho A_{ijklm}^\dagger, \tag{66}$$

where to any of the 2^{10} values of r we can associate a set of indices (i,j,k,l,m) (and vice versa) such that

$$A_r' \leftrightarrow A_{ijklm} \stackrel{\text{def}}{=} A_i \otimes A_j \otimes A_k \otimes A_l \otimes A_m \equiv A_i A_j A_k A_l A_m. \tag{67}$$

The errors A_i with $i \in \{0,1,2,3\}$ are defined in Eq. (8) and $\rho \in \mathcal{M}(\mathcal{C})$ with $\mathcal{C} \subset \mathcal{H}_2^5$. In particular, the number of weight-q

enlarged error operators A'_r is given by $3^q\binom{5}{q}$ and

$$2^{10} = \sum_{q=0}^{5} 3^q \binom{5}{q}. \tag{68}$$

We point out that consistency requires that the sum of the probabilities $P(A_{ijklm})$ that an $A'_r = A_{ijklm}$ error occurs must sum up to unity. For clarity of exposition, consider the limiting case with $\varepsilon = 0$, where only $2^5 = 32$ enlarged errors A'_r are present. In this case, we have

$$\begin{aligned}
&\sum_{i,j,k,l,m=0}^{1} P(A_{ijklm}) \\
&= \sum_{r=0}^{2^5-1} P(A'_r) = \frac{1}{2}\sum_{a=0}^{2^5-1} \mathrm{Tr}(A'_a P_{\mathcal{C}} A'^{\dagger}_a) \\
&= \frac{1}{2}\sum_{a=0}^{2^5-1} [\langle 0_L|A'^{\dagger}_a A'_a|0_L\rangle + \langle 1_L|A'^{\dagger}_a A'_a|1_L\rangle] = 1;
\end{aligned} \tag{69}$$

that is,

$$\begin{aligned}
\sum_{i,j,k,l,m=0}^{1} P(A_{ijklm}) &= P_{\text{weight-0}} + P_{\text{weight-1}} + P_{\text{weight-2}} \\
&\quad + P_{\text{weight-3}} + P_{\text{weight-4}} + P_{\text{weight-5}} = 1,
\end{aligned} \tag{70}$$

where

$$\begin{aligned}
P_{\text{weight-0}} &= 1 - \tfrac{5}{2}\gamma + \tfrac{5}{2}\gamma^2 - \tfrac{5}{4}\gamma^3 + \tfrac{3}{8}\gamma^4 - \tfrac{1}{16}\gamma^5, \\
P_{\text{weight-1}} &= \tfrac{5}{2}\gamma - 5\gamma^2 + \tfrac{15}{4}\gamma^3 - \tfrac{3}{2}\gamma^4 + \tfrac{5}{16}\gamma^5, \\
P_{\text{weight-2}} &= \tfrac{5}{2}\gamma^2 - \tfrac{15}{4}\gamma^3 + \tfrac{9}{4}\gamma^4 - \tfrac{5}{8}\gamma^5, \\
P_{\text{weight-3}} &= \tfrac{5}{4}\gamma^3 - \tfrac{3}{2}\gamma^4 + \tfrac{5}{8}\gamma^5, \\
P_{\text{weight-4}} &= \tfrac{3}{8}\gamma^4 - \tfrac{5}{16}\gamma^5, \quad P_{\text{weight-5}} = \tfrac{1}{16}\gamma^5.
\end{aligned} \tag{71}$$

Using the brute-force approach, it would be fairly straightforward, though very tedious, to check the approximate QEC conditions for all the 2^{10} enlarged errors. Fortunately, this is not necessary. Indeed, we aim at finding an analytical estimate of the entanglement fidelity of the code such that

$$\mathcal{F}^{[[5,1,3]]}(\gamma,\varepsilon) \geqslant 1 - O(2), \tag{72}$$

where $O(2) \sim O(\gamma^{n_1}\varepsilon^{n_2})$; that is, the pair (n_1,n_2) is such that,

$$\lim_{\gamma,\varepsilon\to 0} \frac{O(2)}{O(\gamma^{n_1}\varepsilon^{n_2})} = \text{constant}. \tag{73}$$

For instance, we may have $\{(n_1,n_2)\} = \{(2,0),(0,2),(1,1)\}$. Observe that the codewords that span the code belong to the $2^5 = 32$-dimensional *complex* Hilbert space $\mathcal{H}_2^5$. Thus, a basis of orthonormal vectors for $\mathcal{H}_2^5$ requires 32 elements. For $\varepsilon = 0$, it turns out that none of the $\binom{5}{2} = 10$ weight-2 errors is correctable. Specifically, errors A_{01100}, A_{00011}, A_{01010}, and A_{00101} are not compatible with A_{00000}; A_{00110} and A_{01001} are not compatible with A_{10000}; A_{11000} is not compatible with A_{01000}; A_{10100} is not compatible with A_{00100}; A_{10010} is not compatible with A_{00010}; and, finally, A_{10001} is not compatible with A_{00001}. For the general case, it can be shown that all weight-0 (1 error) and weight-1 (15 errors) enlarged error operators satisfy the approximate QEC conditions up to the sought order. However, the action on the codewords of five weight-1 enlarged errors (specifically, A_{20000}, A_{02000}, A_{00200}, A_{00020}, and A_{00002}) leads to vectors that are not orthogonal to those obtained from the action of the weight-0 error A_{00000} on the codewords. Thus, we omit them from the construction of our recovery scheme. In view of these considerations, we construct our recovery operation $\mathcal{R}$ as

$$\mathcal{R} \stackrel{\text{def}}{=} \{R_0, R_1, R_2, R_3, R_4, R_5\ R_6, R_7, R_8, R_9, R_{10}, \hat{O}\}, \tag{74}$$

where

$$R_r \stackrel{\text{def}}{=} |0_L\rangle\langle v_r^{0_L}| + |1_L\rangle\langle v_r^{1_L}|, \quad \text{with} \quad |v_r^{i_L}\rangle \stackrel{\text{def}}{=} \frac{A'_k|i_L\rangle}{\sqrt{\langle i_L|A'^{\dagger}_k A_k|i_L\rangle}}, \tag{75}$$

for $i \in \{0,1\}$ and $\langle v_r^{i_L}|v_{r'}^{j_L}\rangle = \delta_{rr'}\delta_{ij}$. To be clear, R_0 is associated with the weight-0 error A_{00000}; R_k with $k = 1,\ldots,5$ are associated with the five weight-1 errors where single-qubit errors of type A_1 occur; finally, R_k with $k = 6,\ldots,10$ are associated with the five weight-1 errors where single-qubit errors of type A_3 occur. The construction of these 11 recovery operators R_k is described in terms of 22 orthonormal vectors in $\mathcal{H}_2^5$. The missing 10 orthonormal vectors can be uncovered using the rank-nullity (dimension) theorem together with the Gram-Schmidt orthonormalization procedure (for more details, see Appendix C). They define the operator $\hat{O}$ in Eq. (74),

$$\hat{O} = \sum_{j=1}^{10} |o_j\rangle\langle o_j|. \tag{76}$$

For the sake of convenience, we put $R_{11} \stackrel{\text{def}}{=} \hat{O}$. Finally, the estimate of the entanglement fidelity of the five-qubit code, when the recovery operation $\mathcal{R}$ in Eq. (74) is employed, becomes (for more details, see Appendix D)

$$\begin{aligned}
\mathcal{F}^{[[5,1,3]]}(\gamma,\varepsilon) &\stackrel{\text{def}}{=} \frac{1}{(\dim_{\mathbb{C}}\mathcal{C})^2}\sum_{k=0}^{2^{10}-1}\sum_{l=0}^{11} |\mathrm{Tr}(R_l A'_k)_{|\mathcal{C}}|^2 \\
&\approx 1 - \frac{5}{2}\gamma^2 - 10\varepsilon^2\left(1 + \frac{\gamma}{\varepsilon}\right) + O(3).
\end{aligned} \tag{77}$$

We point out that in the limiting case of $\varepsilon = 0$, the AD noise model is recovered and our analytical estimate in Eq. (77) reduces to the numerically obtained truncated series expansion appeared in [9] and [39] (specifically, see page 48 in [39]). The effect of the nonzero environmental temperature on the five-qubit code is illustrated in Fig. 1.

2. *The CSS seven-qubit code*

The Calderbank-Shor-Steane (CSS) codes are constructed from two classical binary codes $\mathcal{C}$ and $\mathcal{C}'$ that have the following properties [40,41]: (1) $\mathcal{C}$ and $\mathcal{C}'$ are $[n,k,d]$ and $[n,k',d']$ codes,

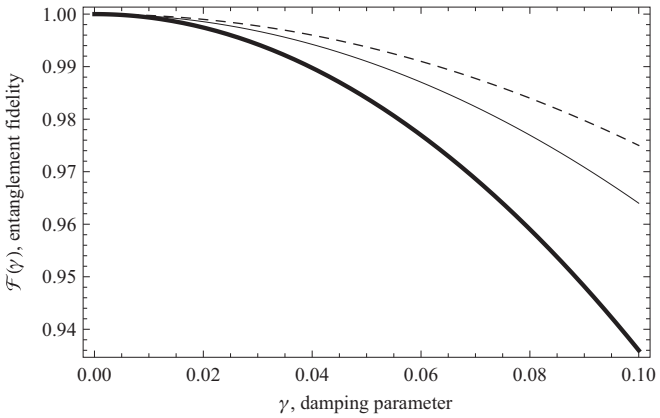

FIG. 1. Effect of the nonzero environmental temperature on quantum coding. The truncated series expansion of the entanglement fidelity $\mathcal{F}(\gamma)$ vs the AD parameter γ with $0 \leqslant \gamma \leqslant 10^{-1}$ for the five-qubit code: $\varepsilon(t) = 0$ (dashed line); $\varepsilon(t) = 10^{-1}\gamma$ (thin solid line); $\varepsilon(t) = 3 \times 10^{-1}\gamma$ (thick solid line).

respectively; (2) $\mathcal{C}' \subset \mathcal{C}$; (3) $\mathcal{C}$ and $\mathcal{C}'_{\perp}$ (the dual code of $\mathcal{C}'$) are both t-error-correcting codes. For instance, in case of the seven-qubit code, the two classical codes are the [7,4,3] binary Hamming code ($\mathcal{C}$) and the [7,3,4] binary simplex code ($\mathcal{C}'$). The dual code $\mathcal{C}'_{\perp}$ is the [7,4,3] binary Hamming code. Thus, $\mathcal{C}$ and $\mathcal{C}'_{\perp}$ are both 1-error-correcting codes. In this case, $n = 7$, $k = 4$, $k' = 3$, $k - k' = 1$ so that one qubit is mapped into seven qubits. The seven-qubit code is the simplest example of a CSS code. Although the seven-qubit code is ostensibly more complicated that the five-qubit code, it is actually more useful in certain situations by virtue of being a CSS code. The CSS codes are a particularly interesting class of codes for two reasons. First, they are built using classical codes which have been more heavily studied than quantum codes, so it is fairly easy to construct useful quantum codes simply by looking at lists of classical codes. Second, because of the form of generators, the CSS codes are precisely those for which a CNOT applied between every pair of corresponding qubits in two blocks performs a valid fault-tolerant operation. This makes them particularly good candidates in fault-tolerant computation.

The CSS seven-qubit code encodes $k = 1$ qubit in $n = 7$ qubits. The cardinality of its stabilizer group $\mathcal{S}$ is $|\mathcal{S}| = 2^{n-k} = 64$ and the set $\mathcal{B}_{\mathcal{S}}^{[[7,1,3]]}$ of $n - k = 6$ stabilizer group generators reads [33]

$$\mathcal{B}_{\mathcal{S}}^{[[7,1,3]]} \stackrel{\text{def}}{=} \{X^4X^5X^6X^7, X^2X^3X^6X^7, X^1X^3X^5X^7, Z^4Z^5Z^6Z^7, Z^2Z^3Z^6Z^7, Z^1Z^3Z^5Z^7\}. \tag{78}$$

The distance of the code is $d = 3$ and therefore the weight of the smallest error $A_l'^{\dagger}A'_k$ that cannot be detected by the code is 3. Finally, we recall that it is a nondegenerate code, since the smallest weight for elements of $\mathcal{S}$ (other than identity) is 4 and therefore it is greater than the distance $d = 3$. The encoding for the [[7,1,3]] code is given by [33]

$$|0\rangle \to |0_L\rangle \stackrel{\text{def}}{=} \frac{1}{(\sqrt{2})^3}[|0000000\rangle + |0110011\rangle + |1010101\rangle + |1100110\rangle + |0001111\rangle + |0111100\rangle + |1011010\rangle + |1101001\rangle], \tag{79}$$

and

$$|1\rangle \to |1_L\rangle \stackrel{\text{def}}{=} \frac{1}{(\sqrt{2})^3}[|1111111\rangle + |1001100\rangle + |0101010\rangle + |0011001\rangle + |1110000\rangle + |1000011\rangle + |0100101\rangle + |0010110\rangle]. \tag{80}$$

The enlarged GAD quantum channel after performing the encoding defined by means of Eqs. (79) and (80) reads

$$\Lambda_{\text{GAD}}^{[[7,1,3]]}(\rho) \stackrel{\text{def}}{=} \sum_{r=0}^{2^{14}-1} A'_r \rho A_r'^{\dagger} = \sum_{i,j,k,l,m,n,s=0}^{3} A_{ijklmns} \rho A_{ijklmns}^{\dagger}, \tag{81}$$

where to any of the 2^{14} values of r we can associate a set of indices (i,j,k,l,m,n,s) (and vice versa) such that

$$A'_r \leftrightarrow A_{ijklmns} \stackrel{\text{def}}{=} A_i \otimes A_j \otimes A_k \otimes A_l \otimes A_m \otimes A_n \otimes A_s \equiv A_i A_j A_k A_l A_m A_n A_s. \tag{82}$$

The errors A_i with $i \in \{0,1,2,3\}$ are defined in Eq. (8) and $\rho \in \mathcal{M}(\mathcal{C})$ with $\mathcal{C} \subset \mathcal{H}_2^7$. In particular, the number of weight-q enlarged error operators A'_r is given by $3^q\binom{7}{q}$ and

$$2^{14} = \sum_{q=0}^{7} 3^q \binom{7}{q}. \tag{83}$$

For $\varepsilon = 0$, it can be shown that for any of the $\binom{7}{2} = 21$ weight-2 errors, there exists at least one of the seven weight-1 errors for which the correctability conditions are not satisfied. For the general case, it can be shown that all weight-0 (1 error) and weight-1 (21 errors) enlarged error operators satisfy the approximate QEC conditions up to the sought order. In this case, the recovery scheme $\mathcal{R}$ that we use can be described as follows: R_0 is associated with the weight-0 error $A_{0000000}$; R_k with $k = 1,\ldots,7$ are associated with the seven weight-1 errors where single-qubit errors of type A_1 occur; finally, R_k with $k = 8,\ldots,14$ are associated with the five weight-1 errors where single-qubit errors of type A_3

occur. The construction of these 15 recovery operators R_k is described in terms of 30 orthonormal vectors in $\mathcal{H}_2^7$. In analogy to the case of the five-qubit code, the action on the codewords of seven weight-1 enlarged errors (specifically, $A_{2000000}$, $A_{0200000}$, $A_{0020000}$, $A_{0002000}$, $A_{0000200}$, $A_{0000020}$, and $A_{0000002}$) leads to vectors that are not orthogonal to those obtained from the action of the weight-0 error $A_{0000000}$ on the codewords. Thus, we omit them from the construction of our recovery scheme. The missing 98 orthonormal vectors (needed to obtain an orthonormal basis of $\mathcal{H}_2^7$ and to construct $R_{15} \stackrel{\text{def}}{=} \hat{O}$) can be formally computed by using the rank-nullity theorem together with the Gram-Schmidt orthonormalization procedure. Omitting further technical details (for more details, see Appendix D) but using the very same line of reasoning presented for the five-qubit code, our analytical estimate of the entanglement fidelity of the CSS seven-qubit code reads

$$\mathcal{F}^{[[7,1,3]]}(\gamma,\varepsilon) \stackrel{\text{def}}{=} \frac{1}{(\dim_{\mathbb{C}} \mathcal{C})^2} \sum_{k=0}^{2^{14}-1} \sum_{l=0}^{15} |\text{Tr}(R_l A'_k)_{|\mathcal{C}}|^2$$
$$\approx 1 - \frac{21}{4}\gamma^2 - 21\varepsilon^2\left(1+\frac{\gamma}{\varepsilon}\right) + O(3). \quad (84)$$

To the best of our knowledge and unlike the case of the five-qubit code, no truncated series expansion of $\mathcal{F}^{[[7,1,3]]}(\gamma,\varepsilon)$ with $\varepsilon = 0$ is available in the literature. However, we emphasize that in the special case of $\varepsilon = 0$, our analytical estimate in Eq. (84) appears to exhibit a fairly good agreement with the numerical plot presented in [12] (specifically, see Fig. 9 in [12]). For $\varepsilon = 0$, we compared our nontruncated analytical estimate in Eq. (84) to the single-qubit baseline performance (entanglement fidelity when no QEC is performed) given by

$$\mathcal{F}^{\text{1-qubit}}_{\text{baseline}}(\gamma) \stackrel{\text{def}}{=} 2^{-2}(1+\sqrt{1-\gamma})^2. \quad (85)$$

Then, we checked the good overlap between our results (nontruncated fidelity expressions with and without error correction) and those plotted in [12]. For some more details, see Appendix E. The robustness against nonzero environmental temperature of the CSS seven-qubit code is compared to that of the Shor nine-qubit code in Fig. 2.

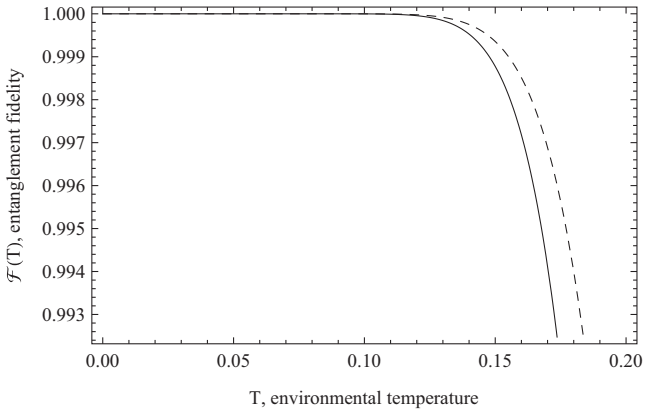

FIG. 2. Robustness against nonzero environmental temperature of degenerate and nondegenerate codes. The truncated series expansions of the entanglement fidelity $\mathcal{F}(t)$ vs the environmental temperature T for $\hbar = \omega = k_B = 1$ and $\gamma = 10\varepsilon$: the Shor nine-qubit code (dashed line) and the CSS seven-qubit code (thin solid line).

3. *The eight-qubit concatenated code*

The notion of correctability depends on all the errors in the error set that one is considering and, unlike detectability, cannot be applied to individual errors. However, for a given code $\mathcal{C}$, both sets of detectable and correctable errors are closed under linear combinations. Within the stabilizer formalism, the error-correction conditions can be described as follows [3,38]: An $[[n,k,d]]$ quantum code with stabilizer $\mathcal{S}$ and generators g_j where $j = 1,\ldots,n-k$, corrects an error set $\mathcal{A}$ if every error pair $A_l^\dagger A_m \in \mathcal{A}$ either anticommutes with at least one stabilizer generator,

$$\exists\, g_j \in \mathcal{S} : \{g_j, A_l^\dagger A_m\} = 0,$$

or is in the stabilizer, $A_l^\dagger A_m \in \mathcal{S}$.

The two Kraus operators for the AD noise model are given by $A_0 = I - O(\gamma)$ and $A_1 \propto \sigma_x + i\sigma_y$. In the GAD noise model, the error $A_3 \propto \sigma_x - i\sigma_y$ appears as well. The linear span of A_1 and A_3 equals the linear span of σ_x and σ_y. Thus, if a code is capable of correcting $t\,\sigma_x$ and $t\ \sigma_y$ errors, it can also correct $t\ A_1$ and $t\ A_3$ errors. The stabilizer of the Leung *et al.* four-qubit code,

$$|0_L\rangle \stackrel{\text{def}}{=} \frac{|0000\rangle + |1111\rangle}{\sqrt{2}}, \quad |1_L\rangle \stackrel{\text{def}}{=} \frac{|0011\rangle + |1100\rangle}{\sqrt{2}}, \quad (86)$$

is given by $\mathcal{S} \stackrel{\text{def}}{=} \langle \sigma_x^1\sigma_x^2\sigma_x^3\sigma_x^4, \sigma_z^1\sigma_z^2, \sigma_z^3\sigma_z^4\rangle$. According to the above-mentioned considerations, it follows that the error set $\{I,\sigma_x^i,\sigma_y^i\}$ with $i = 1, 2, 3, 4$ is not correctable. For instance, the set $\{\sigma_x^1,\sigma_x^2\}$ is not correctable because $\sigma_x^1\sigma_x^2$ commutes with all the stabilizer generators.

To construct a quantum code capable of error correcting the set $\{I,\sigma_x^i,\sigma_y^i\}$ with $i = 1,2,3,4$, we concatenate the quantum dual rail code $\mathcal{C}_{\text{QDR}}$ (inner code) with the perfect 1-erasure correcting code $\mathcal{C}_{\text{erasure}}$ (outer code) given by

$$|0_L\rangle \stackrel{\text{def}}{=} |01\rangle, \quad |1_L\rangle \stackrel{\text{def}}{=} |10\rangle, \quad (87)$$

and [42]

$$|0_L\rangle \stackrel{\text{def}}{=} \frac{|0000\rangle + |1111\rangle}{\sqrt{2}}, \quad |1_L\rangle \stackrel{\text{def}}{=} \frac{|0110\rangle + |1001\rangle}{\sqrt{2}}, \quad (88)$$

respectively. Both $\mathcal{C}_{\text{QDR}}$ and $\mathcal{C}_{\text{erasure}}$ are stabilizer codes with stabilizer groups given by

$$\mathcal{S} \stackrel{\text{def}}{=} \langle -\sigma_z^1\sigma_z^2\rangle, \quad (89)$$

and

$$\mathcal{S} \stackrel{\text{def}}{=} \langle \sigma_x^1\sigma_x^2\sigma_x^3\sigma_x^4, \sigma_z^1\sigma_z^4, \sigma_z^2\sigma_z^3\rangle, \quad (90)$$

respectively. We recall that, as pointed out in [43], minus signs do not really matter when the stabilizers are specified. Erasures are errors at known positions and a t-error-correcting code is a $2t$-erasure correcting code. It can be shown that the perfect 1-erasure correcting code is also a single AD-error-correcting codes and is local permutation equivalent to the Leung *et al.* four-qubit code. Using Eqs. (87) and (88), the concatenated code $\mathcal{C}_{\text{conc.}} \stackrel{\text{def}}{=} \mathcal{C}_{\text{QDR}} \circ \mathcal{C}_{\text{erasure}}$ is spanned by the following

codewords:

$$|0_L\rangle \stackrel{\text{def}}{=} \frac{|00000110\rangle + |00001001\rangle + |11110110\rangle + |11111001\rangle}{\sqrt{4}},$$
$$|1_L\rangle \stackrel{\text{def}}{=} \frac{|01100000\rangle + |01101111\rangle + |10010000\rangle + |10011111\rangle}{\sqrt{4}}. \tag{91}$$

The stabilizer generators of the concatenated code can be obtained as follows. The concatenated code uses eight qubits that parse two blocks, each containing four qubits. Qubits 1–4 belong to block 1; qubits 5–8 belong to block 2. To each block we associate a copy of the generators of $\mathcal{C}_{\text{erasure}}$. This gives the following six generators,

$$g_1 \stackrel{\text{def}}{=} \sigma_x^1\sigma_x^2\sigma_x^3\sigma_x^4, \quad g_2 \stackrel{\text{def}}{=} \sigma_x^5\sigma_x^6\sigma_x^7\sigma_x^8, \quad g_3 \stackrel{\text{def}}{=} \sigma_z^1\sigma_z^4,$$
$$g_4 \stackrel{\text{def}}{=} \sigma_z^5\sigma_z^8, \quad g_5 \stackrel{\text{def}}{=} \sigma_z^2\sigma_z^3, \quad g_6 \stackrel{\text{def}}{=} \sigma_z^6\sigma_z^7. \tag{92}$$

The remaining generator g_7 is the encoded version of $-\sigma_z^1\sigma_z^2$, that is $g_7 \stackrel{\text{def}}{=} -\sigma_z^1\sigma_z^2\sigma_z^5\sigma_z^6$. Summing up, the stabilizer group for the concatenated code reads

$$\mathcal{S}_{\mathcal{C}_{\text{conc.}}} \stackrel{\text{def}}{=} \langle \sigma_x^1\sigma_x^2\sigma_x^3\sigma_x^4, \sigma_x^5\sigma_x^6\sigma_x^7\sigma_x^8, \sigma_z^1\sigma_z^4, \sigma_z^5\sigma_z^8, \sigma_z^2\sigma_z^3, \sigma_z^6\sigma_z^7, -\sigma_z^1\sigma_z^2\sigma_z^5\sigma_z^6 \rangle. \tag{93}$$

It turns out that the concatenated code with stabilizer structure defined in Eq. (93) is a nondegenerate code of distance 2. Furthermore, it can be explicitly checked that the error set $\{I, \sigma_x^i, \sigma_y^i\}$ with $i = 1, \ldots, 8$ is a set of linearly independent errors with unequal error syndromes, a property of correctable errors by means of nondegenerate codes [33]. We recall that the syndrome $s(E)$ for an error E in the Pauli group $\mathcal{P}_{\mathcal{H}_2^n}$ is the bit string $l = l_1, \ldots, l_{n-k}$, where the component bits l_i are given by

$$l_i \stackrel{\text{def}}{=} \begin{cases} 0, & \text{if} \quad [E, g_i] = 0, \\ 1, & \text{if} \quad \{E, g_i\} = 0, \end{cases} \tag{94}$$

with $i = 1, \ldots, n-k$ and $\mathcal{S} \stackrel{\text{def}}{=} \langle g_i \rangle$ the stabilizer group of the quantum code.

Before discussing the computation of the entanglement fidelity, recall that the quantum Hamming bound places an upper bound on the number of errors t that an $[[n,k,d]]$ nondegenerate code can correct for given n and k,

$$2^k \sum_{j=0}^{t} 3^j \binom{n}{j} \leqslant 2^n. \tag{95}$$

Since the code distance d equals $2t + 1$, it also places an upper bound on the code distance. At present it is unknown whether a degenerate code might allow a violation of the Hamming bound [44]. For the sake of completeness, we also point out that the Hamming bound for q-dimensional systems reads

$$K \sum_{j=0}^{t} (q^2 - 1)^j \binom{n}{j} \leqslant q^n, \tag{96}$$

where $k = \log_q K$ and $\dim_{\mathbb{C}} \mathcal{H} = q^n$ with $\mathcal{H} = (\mathbb{C}^q)^{\otimes n}$.

The enlarged GAD quantum channel after performing the encoding defined by means of Eq. (91) reads

$$\Lambda_{\text{GAD}}^{[[8,1]]}(\rho) \stackrel{\text{def}}{=} \sum_{r=0}^{2^{16}-1} A_r' \rho A_r'^{\dagger} = \sum_{i,j,k,l,m,n,s,t=0}^{3} A_{ijklmnst} \rho A_{ijklmnst}^{\dagger}, \tag{97}$$

where to any of the 2^{16} values of r we can associate a set of indices (i,j,k,l,m,n,s,t) (and vice versa) such that

$$A_r' \leftrightarrow A_{ijklmnst} \stackrel{\text{def}}{=} A_i \otimes A_j \otimes A_k \otimes A_l \otimes A_m \otimes A_n \otimes A_s \otimes A_t \equiv A_i A_j A_k A_l A_m A_n A_s A_t. \tag{98}$$

The errors A_i with $i \in \{0,1,2,3\}$ are defined in Eq. (8) and $\rho \in \mathcal{M}(\mathcal{C})$, with $\mathcal{C} \subset \mathcal{H}_2^8$. In particular, the number of weight-q enlarged error operators A_r' is given by $3^q \binom{8}{q}$ and

$$2^{16} = \sum_{q=0}^{8} 3^q \binom{8}{q}. \tag{99}$$

In this case, the recovery scheme $\mathcal{R}$ that we use can be described as follows: R_0 is associated with the weight-0 error $A_{00000000}$; R_k with $k = 1, \ldots, 8$ are associated with the eight weight-1 errors where single-qubit errors of type A_1 occur; R_k with $k = 9, \ldots, 16$ are associated with the eight weight-1 errors where single-qubit errors of type A_3 occur. In analogy to the case of the CSS seven-qubit code, the action on the codewords of seven weight-1 enlarged errors (specifically, $A_{20000000}$, $A_{02000000}$, $A_{00200000}$, $A_{00020000}$, $A_{00002000}$, $A_{00000200}$, $A_{00000020}$, and $A_{00000002}$) leads to vectors that are not orthogonal to those obtained from the action of the weight-0 error $A_{00000000}$ on the codewords. Thus, we omit them from the construction of our recovery scheme. We also choose to recover the weight-2 errors that are more likely to occur where the likelihood can be expressed in terms of the perturbation parameters γ and ϵ. For instance, in the limiting case of $\varepsilon = 0$, it can be shown that the sum of all the probabilities for errors of weight-k to occur reads

$$P_{\text{weight-}k} \stackrel{\text{def}}{=} \frac{1}{2}\left[\binom{2}{k}\gamma^k(1-\gamma)^{2-k} + \binom{6}{k}\gamma^k(1-\gamma)^{6-k}\right], \tag{100}$$

with the normalization constraint

$$\sum_{k=0}^{8} P_{\text{weight-}k} = 1. \tag{101}$$

Therefore, to the 17 recovery operators R_k constructed so far, we add the additional 20 of the possible $28 = \binom{8}{2}$ recovery operators constructed by means of weight-2 errors where errors of type A_1 occur. We point out that we only consider 20

recovery operators, since the following eight errors are not correctable:

$$A_{11000000},\quad A_{10100000},\quad A_{01010000},\quad A_{00110000},\quad A_{00001100},$$
$$A_{00001010},\quad A_{00000101},\quad A_{00000011}. \tag{102}$$

We finally arrive at the construction of 37 recovery operators R_k with $k = 0,\ldots,36$ described in terms of 74 orthonormal vectors in $\mathcal{H}_2^8$. The missing 182 orthonormal vectors (needed to obtain an orthonormal basis of $\mathcal{H}_2^8$ and to construct $R_{37} \stackrel{\text{def}}{=} \hat{O}$) can be formally computed using the rank-nullity theorem together with the Gram-Schmidt orthonormalization. Omitting further technical details but using the very same line of reasoning presented for the CSS seven-qubit code, our analytical estimate of the entanglement fidelity of the eight-qubit concatenated code reads

$$\mathcal{F}^{[[8,1]]}(\gamma,\varepsilon) \stackrel{\text{def}}{=} \frac{1}{(\dim_{\mathbb{C}} \mathcal{C})^2} \sum_{k=0}^{2^{16}-1} \sum_{l=0}^{37} |\mathrm{Tr}(R_l A'_k)_{|\mathcal{C}}|^2$$
$$\approx 1 - 2\gamma^2 - 28\varepsilon^2\left(1 + \frac{\gamma}{\varepsilon}\right) + O(3). \tag{103}$$

We remark that in the limiting case of $\varepsilon = 0$, the GAD noise model reduces to the traditional AD model and the concatenated code $\mathcal{C}_{\text{conc.}}$ applied to AD errors works as follows: The inner code $\mathcal{C}_{\text{QDR}}$ transforms AD errors into erasures which are then corrected by the outer code $\mathcal{C}_{\text{erasure}}$ [26]. We also point out that in the limit of $\varepsilon = 0$ our estimated series expansion of the entanglement fidelity of the eight-qubit concatenated code coincides with that obtained by means of the traditional Leung *et al.* four-qubit code applied to AD errors,

$$\mathcal{F}^{[[8,1]]}(\gamma,\varepsilon = 0) \approx 1 - 2\gamma^2 + O(3) \approx \mathcal{F}^{[[4,1]]}_{\text{Leung}}(\gamma), \tag{104}$$

where we assume to use recovery schemes with the same structure as in Eq. (36). This finding is not unexpected and is in agreement with the fact that, as pointed out earlier, $\mathcal{C}_{\text{erasure}}$ and $\mathcal{C}_{\text{Leung}}$ are local permutation equivalent quantum codes.

Finally, we compare the performances of the additive codes employed in our error-correction schemes in Fig. 3.

B. Degenerate codes

Degeneracy is a property of quantum codes which has no analog for classical error-correcting codes and it arises from the fact that two different error patterns can have indistinguishable effects on a coded quantum state [45]. A degenerate code has linearly independent matrices that act in a linearly dependent way on the codewords, while in a nondegenerate code, all the errors acting on the codewords produce linearly independent quantum states. For instance, the Shor nine-qubit code is a degenerate code, since phase errors within a group of three qubits act the same way. A striking feature of degenerate quantum codes is that they can be used to correct more errors than they can uniquely identify [46]. Also, strictly speaking, degeneracy is not a property of a code, but a property of a code together with a family of errors it is designed to correct [33,46].

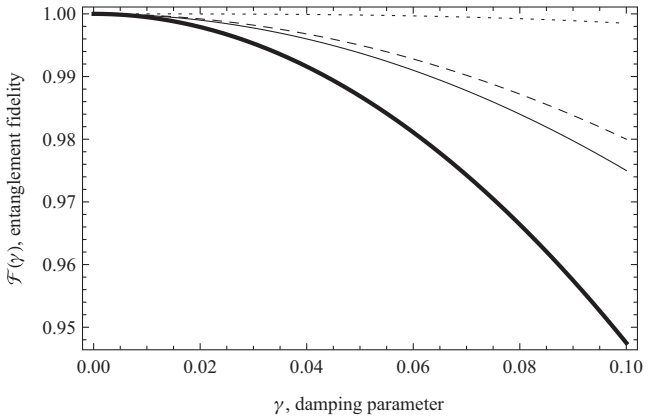

FIG. 3. Ranking additive codes. The truncated series expansions of the entanglement fidelity $\mathcal{F}(\gamma)$ vs the AD parameter γ for $\varepsilon = 0$ and $0 \leqslant \gamma \leqslant 10^{-1}$: the Shor nine-qubit code (dotted line), the degenerate six-qubit code (dashed line), the five-qubit code (thin solid line), and the CSS seven-qubit code (thick solid line).

1. The six-qubit code

Calderbank *et al.* discovered two distinct six-qubit degenerate quantum codes encoding one logical qubit into six physical qubits [47]. The first of these codes was discovered by trivially extending the five-qubit code while the other one was discovered through an exhaustive search of the encoding space. In particular, in [47] it was argued that this second example is unique up to equivalence. The example that we consider here was originally introduced by Bilal *et al.* in [48]. They argue that, since their example is not reducible to the trivial six-qubit code because every one of its qubits is entangled with the others, their code is equivalent to the second nontrivial six-qubit code according to the arguments of Calderbank *et al.* The codespace of this nontrivial [[6,1,3]] six-qubit code is spanned by the codewords $|0_L\rangle$ and $|1_L\rangle$ defined as [48],

$$|0_L\rangle \stackrel{\text{def}}{=} \frac{1}{\sqrt{8}}[|000000\rangle - |100111\rangle + |001111\rangle - |101000\rangle$$
$$- |010010\rangle + |110101\rangle + |011101\rangle - |111010\rangle], \tag{105}$$

and

$$|1_L\rangle \stackrel{\text{def}}{=} \frac{1}{\sqrt{8}}[|001010\rangle + |101101\rangle + |000101\rangle + |1000010\rangle$$
$$- |011000\rangle - |111111\rangle + |010111\rangle + |110000\rangle], \tag{106}$$

respectively. The five stabilizer generators for this code can be written as

$$g_1 \stackrel{\text{def}}{=} Y^1 Z^3 X^4 X^5 Y^6, \quad g_2 \stackrel{\text{def}}{=} Z^1 X^2 X^5 Z^6,$$
$$g_3 \stackrel{\text{def}}{=} Z^2 X^3 X^4 X^5 X^6, \quad g_4 \stackrel{\text{def}}{=} Z^4 Z^6, \quad g_5 \stackrel{\text{def}}{=} Z^1 Z^2 Z^3 Z^5. \tag{107}$$

Within the quantum stabilizer formalism, an $[[n,k,d]]$ code is degenerate if the stabilizer group contains elements of weight less than d (other than the identity) [33]. Thus, it

appears evident from Eq. (107) that this distance $d = 3$ code is degenerate.

The enlarged GAD quantum channel after performing the encoding defined by means of Eqs. (105) and (106) reads

$$\Lambda_{\mathrm{GAD}}^{[[6,1,3]]}(\rho) \stackrel{\mathrm{def}}{=} \sum_{r=0}^{2^{12}-1} A'_r \rho A_r'^{\dagger} = \sum_{i,j,k,l,m,n=0}^{3} A_{ijklmn} \rho A_{ijklmn}^{\dagger}, \tag{108}$$

where to any of the 2^{12} values of r we can associate a set of indices (i,j,k,l,m,n) (and vice versa) such that

$$\begin{aligned} A'_r \leftrightarrow A_{ijklmn} &\stackrel{\mathrm{def}}{=} A_i \otimes A_j \otimes A_k \otimes A_l \otimes A_m \otimes A_n \\ &\equiv A_i A_j A_k A_l A_m A_n. \end{aligned} \tag{109}$$

The errors A_i with $i \in \{0,1,2,3\}$ are defined in Eq. (8) and $\rho \in \mathcal{M}(\mathcal{C})$ with $\mathcal{C} \subset \mathcal{H}_2^6$. In particular, the number of weight-q enlarged error operators A'_r is given by $3^q\binom{6}{q}$ and

$$2^{12} = \sum_{q=0}^{6} 3^q \binom{6}{q}. \tag{110}$$

For $\varepsilon = 0$, it can be shown that among the $\binom{6}{2} = 15$ weight-2 errors, the set of five weight-2 errors given by $\{A_{110000}, A_{100010}, A_{011000}, A_{001010}, A_{000101}\}$ is not correctable, since they are not compatible with A_{000000}. In addition, the action of the two weight-2 errors A_{101000} and A_{010010} on the codewords leads to state vectors that are not orthogonal to $A_{000000}|i_L\rangle$ with $i \in \{0,1\}$. All weight-1 errors are correctable, of course. In view of these considerations, we construct the recovery scheme $\mathcal{R}$ for the general case as follows: R_0 is associated with the weight-0 error A_{000000}; R_k with $k = 1,\ldots,6$ are associated with the six weight-1 errors where single-qubit errors of type A_1 occur; R_k with $k = 7,\ldots,12$ are associated with the six weight-1 errors where single-qubit errors of type A_3 occur; finally, R_k with $k = 13,\ldots,20$ are associated with the eight correctable weight-2 errors where errors of type A_1 occur. The construction of these 21 recovery operators R_k is described in terms of 42 orthonormal vectors in $\mathcal{H}_2^6$. As pointed out earlier, the missing 22 orthonormal vectors (needed to obtain an orthonormal basis of $\mathcal{H}_2^6$ and to construct $R_{21} \stackrel{\mathrm{def}}{=} \hat{O}$) can be formally computed by using the rank-nullity theorem together with the Gram-Schmidt orthonormalization procedure. Our analytical estimate of the entanglement fidelity of the nontrivial six-qubit degenerate code reads

$$\begin{aligned} \mathcal{F}^{[[6,1,3]]}(\gamma,\varepsilon) &\stackrel{\mathrm{def}}{=} \frac{1}{(\dim_{\mathbb{C}} \mathcal{C})^2} \sum_{k=0}^{2^{12}-1} \sum_{l=0}^{21} |\mathrm{Tr}(R_l A'_k)_{|\mathcal{C}}|^2 \\ &\approx 1 - 2\gamma^2 - 15\varepsilon^2\left(1 + \frac{\gamma}{\varepsilon}\right) + O(3). \end{aligned} \tag{111}$$

Comparing Eqs. (77), (84), and (103) to Eq. (111), we observe that the six-qubit degenerate code outperforms the five-, CSS seven-, and eight-qubit concatenated nondegenerate codes. Our findings show that despite the fact that the CSS seven- and eight-qubit concatenated codes have larger Hilbert spaces for encoding than that allowed for the six-qubit code, their error-correcting capability is smaller, given the noise model considered and the recovery schemes employed. Our finding in Eq. (111) strengthens the *suspect* advanced in [12] where it was conjectured that, thanks to their degenerate structure, such codes can outperform nondegenerate codes despite their shorter length.

2. The Shor nine-qubit code

We consider here the [[9,1,3]] Shor nine-qubit code [1], the code that gave birth to the subject of quantum error correcting codes. The codespace of such a code is spanned by the following two codewords [33]:

$$|0_L\rangle \stackrel{\mathrm{def}}{=} \frac{1}{\sqrt{8}}[|000\rangle + |111\rangle][|000\rangle + |111\rangle][|000\rangle + |111\rangle] \tag{112}$$

and

$$|1_L\rangle \stackrel{\mathrm{def}}{=} \frac{1}{\sqrt{8}}[|000\rangle - |111\rangle][|000\rangle - |111\rangle][|000\rangle - |111\rangle]. \tag{113}$$

This degenerate code can be constructed by concatenating two nondegenerate [[3,1,1]] codes and its eight stabilizer generators can be written as

$$\begin{aligned} &g_1 \stackrel{\mathrm{def}}{=} Z^1Z^2, \quad g_2 \stackrel{\mathrm{def}}{=} Z^1Z^3, \quad g_3 \stackrel{\mathrm{def}}{=} Z^4Z^5, \quad g_4 \stackrel{\mathrm{def}}{=} Z^4Z^6, \\ &g_5 \stackrel{\mathrm{def}}{=} Z^7Z^8, \quad g_6 \stackrel{\mathrm{def}}{=} Z^7Z^9, \quad g_7 \stackrel{\mathrm{def}}{=} X^1X^2X^3X^4X^5X^6, \\ &g_8 \stackrel{\mathrm{def}}{=} X^1X^2X^3X^7X^8X^9. \end{aligned} \tag{114}$$

The enlarged GAD quantum channel after performing the encoding defined by means of Eqs. (112) and (113) reads

$$\begin{aligned} \Lambda_{\mathrm{GAD}}^{[[9,1,3]]}(\rho) &\stackrel{\mathrm{def}}{=} \sum_{r=0}^{2^{18}-1} A'_r \rho A_r'^{\dagger} \\ &= \sum_{i,j,k,l,m,n,s,t,u=0}^{3} A_{ijklmnstu} \rho A_{ijklmnstu}^{\dagger}, \end{aligned} \tag{115}$$

where to any of the 2^{18} values of r we can associate a set of indices (i,j,k,l,m,n,s,t,u) (and vice versa) such that

$$\begin{aligned} A'_r \leftrightarrow A_{ijklmnstu} &\stackrel{\mathrm{def}}{=} A_i \otimes A_j \otimes A_k \otimes A_l \otimes A_m \otimes A_n \otimes A_s \otimes A_t \otimes A_u \\ &\equiv A_i A_j A_k A_l A_m A_n A_s A_t A_u. \end{aligned} \tag{116}$$

The errors A_i with $i \in \{0,1,2,3\}$ are defined in Eq. (8) and $\rho \in \mathcal{M}(\mathcal{C})$ with $\mathcal{C} \subset \mathcal{H}_2^9$. In particular, the number of weight-q enlarged error operators A'_r is given by $3^q\binom{9}{q}$ and

$$2^{18} = \sum_{q=0}^{9} 3^q \binom{9}{q}. \tag{117}$$

As a side remark, we recall that a quantum code has distance d if all errors of weight less than d satisfy the QEC conditions $\langle i_L|A_l^{\dagger}A_m|j_L\rangle = \alpha_{lm}\delta_{ij}$ and at least one error of weight d exists that violates it. Otherwise stated, the distance of a code is the

weight of the smallest error $A_l^\dagger A_m$ that cannot be detected by the code. For instance, using the three-qubit bit-flip repetition code [[3,1,1]] to correct bit-flip errors, it turns out that the weight-1 error σ_z^1 cannot be detected. However, this code of distance $d=1$ also detects errors of weight-2 such as, for instance, $\sigma_x^1\sigma_x^2$.

For $\varepsilon=0$, it turns out that all the 9 weight-1 and 36 weight-2 errors are correctable. In addition, all weight-3 errors can be recovered as well, except for $A_{111000000}$, $A_{000111000}$, and $A_{000000111}$. These three errors could be potentially recovered by means of the recovery operator constructed with the weight-0 error $A_{000000000}$. However, it can be checked that their contribution is null. For the general case, the recovery scheme $\mathcal{R}$ that we use can be described as follows: R_0 is associated with the weight-0 error $A_{000000000}$; R_k with $k=1,\ldots,9$ are associated with the 9 weight-1 errors where single-qubit errors of type A_1 occur; R_k with $k=10,\ldots,18$ are associated with the 9 weight-1 errors where single-qubit errors of type A_3 occur; R_k with $k=19,\ldots,54$ are associated with the 36 weight-2 errors where errors of type A_1 occur; finally, R_k with $k=55,\ldots,135$ are associated with the 81 weight-3 errors where errors of type A_1 occur. The construction of these 136 recovery operators R_k is described in terms of 272 orthonormal vectors in $\mathcal{H}_2^9$. The missing 240 orthonormal vectors, needed to obtain an orthonormal basis of $\mathcal{H}_2^9$ and to construct $R_{136}\overset{\text{def}}{=}\hat{O}$, can be formally computed by using the rank-nullity theorem together with the Gram-Schmidt orthonormalization procedure. Our analytical estimate of the entanglement fidelity of the Shor nine-qubit code reads

$$\mathcal{F}^{[[9,1,3]]}(\gamma,\varepsilon)\overset{\text{def}}{=}\frac{1}{(\dim_{\mathbb{C}}\mathcal{C})^2}\sum_{k=0}^{2^{18}-1}\sum_{l=0}^{136}|\mathrm{Tr}(R_lA'_k)_{|\mathcal{C}}|^2$$
$$\approx 1-\frac{3}{2}\gamma^3-36\varepsilon^2\left(1+\frac{\gamma}{\varepsilon}\right)+O(3). \quad (118)$$

To the best of our knowledge, and unlike the case of the five-qubit code, no truncated series expansion of $\mathcal{F}^{[[9,1,3]]}(\gamma,\varepsilon)$ with $\varepsilon=0$ is available in the literature. However, we emphasize that in the special case of $\varepsilon=0$, our analytical estimate in Eq. (118) appears to exhibit a fairly good agreement with the numerical plot presented in [8] (specifically, see Fig. 12 in [8]). For $\varepsilon=0$, we compared our nontruncated analytical estimate in Eq. (118) to the baseline performance of a single qubit given by Eq. (85). Then we checked the good overlap between our results (nontruncated fidelity expressions with and without error correction) and the ones plotted in [8]. For some more details, see Appendix F.

V. NONADDITIVE CODES

There are codes that do not exhibit stabilizer structures. Such codes are known as nonadditive quantum codes. A quantum code is nonadditive if it is not additive, that is, if it cannot be constructed within the stabilizer framework.

Examples of nonstabilizer codes can be found when one of the two following requirements are satisfied [32].

(i) A state $|\psi\rangle\notin\mathcal{C}$ exists such that $g|\psi\rangle=|\psi\rangle$ for any operator g that belongs to the group stabilizer $\mathcal{S}_\mathcal{C}$ of the code $\mathcal{C}$. This happens when $\mathcal{C}$ is not maximal.

(ii) A state $g\notin\mathcal{S}_\mathcal{C}$ exists such that $g|\psi\rangle=|\psi\rangle$ for any state in the codespace of $\mathcal{C}$. This happens when $\mathcal{S}_\mathcal{C}$ is not maximal.

We point out it can also occur that the code $\mathcal{C}$ does not allow any stabilizer group $\mathcal{S}_\mathcal{C}$ at all, neither maximal nor minimal. For instance, consider the code $\mathcal{C}$ defined as

$$\mathcal{C}\overset{\text{def}}{=}\text{Span}\left\{|0_L\rangle\overset{\text{def}}{=}\frac{|01\rangle+|10\rangle}{\sqrt{2}},|1_L\rangle\overset{\text{def}}{=}|11\rangle\right\}. \quad (119)$$

The code $\mathcal{C}$ in Eq. (119) is not the joint $+1$ eigenspace of any operator in the Pauli group $\mathcal{P}_{\mathcal{H}_1^2}$. Therefore, this code is not a stabilizer code, since it does not have the standard stabilizer structure.

A nonadditive $((n,K,d))$ code is a K-dimensional subspace of a n-qubit Hilbert space correcting $\lfloor\frac{d-1}{2}\rfloor$-qubit errors and d is the distance of the code. The first example of nonadditive code was a ((5,6,2)) code presented in [49]. This code was constructed numerically by building a projector operator with a given weight distribution. It encodes six logical qubits into five physical qubits and can correct single-qubit erasure. This code outperforms any known stabilizer code in terms of encoded dimension ($\log_2 6/5$). In [50], a family of nonadditive codes of distance $d=2$ capable of detecting any single-qubit error (or, equivalently, correct any single-qubit erasure) with high encoded dimensions was introduced. The simplest example of a nonadditive code in such a family is represented by a self-complementary ((5,5,2)) nonadditive quantum code that is not a subcode of the ((5,6,2)) code in [49]. Necessary and sufficient conditions for the error correction of AD errors with self-complementary nonadditive quantum codes were presented in [23,24]. In particular, in [23] a numerical investigation of a ((8,12)) self-complementary nonadditive quantum code with a high encoding rate ($\log_2 12/8$) was presented for the correction of AD errors. The performance of this code was quantified by means of the entanglement fidelity and evaluated numerically for a maximum likelihood recovery scheme that corrects all the first-order AD errors. We stress that for nonadditive codes, the decoding procedure does not have the syndrome diagnosis and the recovery structure of the stabilizer codes. However, like the additive case, recovery schemes for nonadditive codes may exhibit a projection nature as well. Furthermore, thanks to the graph-state formalism [51], many nonadditive codes can be characterized by a stabilizerlike structure [25]. The stabilizerlike structure of some classes of nonadditive codes simplify significantly the encoding and decoding procedures for these codes [52]. Nonadditive codes of distance $d=2$ can detect but cannot correct arbitrary single-qubit errors. To achieve this task, codes of distance $d=3$ are needed. In [53], sufficient general conditions for the existence of nonadditive codes were given. In particular, an example of a strongly nonadditive ((11,2,3)) quantum code was presented. However, the question of whether the nonadditive codes correcting errors beyond erasures are more efficient (in terms of the encoded dimension) than the corresponding stabilizer codes remained open. The very first example of a 1-error-correcting nonadditive code capable of outperforming the optimal stabilizer code (the [[9,3,3]] code) of the same length was the nondegenerate ((9,12,3)) code in [54].

A. Non-self-complementary codes

1. *The* ((11,2,3)) *code*

According to [53], two quantum codes $\mathcal{C}_1$ and $\mathcal{C}_2$ in $\mathbb{C}^{2^n}$ are *locally equivalent* if there is a transversal operator $U \stackrel{\text{def}}{=} u_1 \otimes \cdots \otimes u_n$ with $u_j \in SU(2,\mathbb{C})$, mapping $\mathcal{C}_1$ into $\mathcal{C}_2$. Instead, two codes are *globally equivalent*, or simply equivalent, if $\mathcal{C}_1$ is locally equivalent to a code obtained from $\mathcal{C}_2$ by a permutation on qubits. A quantum code $\mathcal{C} \subset \mathbb{C}^{2^n}$ is called nonadditive if it is not equivalent to any additive code; moreover, $\mathcal{C}$ is strongly nonadditive if the only additive code that contains any code equivalent to $\mathcal{C}$ is the trivial code $\mathbb{C}^{2^n}$ (in other words, if $\pm X_\alpha Z_\beta$ with $\alpha, \beta \in \{0,1\}^n$ is in the stabilizer of any code equivalent to a supercode of $\mathcal{C}$, then $\alpha = \beta = \mathbf{0}$). Also, the generalized stabilizer $\mathcal{GS}_\mathcal{C}$ of a code $\mathcal{C} \subset \mathbb{C}^{2^n}$ is the set of all unitary operators V on $\mathbb{C}^{2^n}$ such that $V|c\rangle = |c\rangle$ for every $|c\rangle \in \mathcal{C}$. Then, the stabilizer $\mathcal{S}_\mathcal{C}$ of a code $\mathcal{C}$ is $\mathcal{S}_\mathcal{C} = \mathcal{P}_{\mathbb{C}^{2^n}} \cap \mathcal{GS}_\mathcal{C}$, where $\mathcal{P}_{\mathbb{C}^{2^n}}$ is the n-qubit Pauli group.

The strong nonadditivity is guaranteed by the fulfillment of two conditions [53]: (i) the identity operator is the only operator in the stabilizer of the code; (ii) there is no element in $\mathcal{GS}_\mathcal{C}$ of the form $X_\alpha T$ with $\{0,1\}^n \ni \alpha \neq \mathbf{0}$, where T is a Z-type unitary operator of the form

$$T \stackrel{\text{def}}{=} \bigotimes_{j=1}^{n} \begin{pmatrix} e^{i\theta_j} & 0 \\ 0 & \pm e^{-i\theta_j} \end{pmatrix}, \tag{120}$$

where i is the *complex* imaginary unit.

The first example of a 1-error-correcting strongly nonadditive code was a ((11,2,3)) code with codespace spanned by the following two codewords [53]:

$$|0_L\rangle \stackrel{\text{def}}{=} \frac{1}{\sqrt{12}} \sum_{i=1}^{12} |r_i\rangle \tag{121}$$

and

$$|1_L\rangle \stackrel{\text{def}}{=} \frac{1}{\sqrt{12}} \sum_{i=1}^{12} |\mathbf{1} + r_i\rangle. \tag{122}$$

The quantity $\mathbf{1}$ is the all-1 vector of length 11 and r_i denotes the ith row of the following (12×11)-matrix H defined as

$$H \stackrel{\text{def}}{=} \begin{pmatrix} 0&0&0&0&0&0&0&0&0&0&0 \\ 1&0&1&0&0&0&1&1&1&0&1 \\ 1&1&0&1&0&0&0&1&1&1&0 \\ 0&1&1&0&1&0&0&0&1&1&1 \\ 1&0&1&1&0&1&0&0&0&1&1 \\ 1&1&0&1&1&0&1&0&0&0&1 \\ 1&1&1&0&1&1&0&1&0&0&0 \\ 0&1&1&1&0&1&1&0&1&0&0 \\ 0&0&1&1&1&0&1&1&0&1&0 \\ 0&0&0&1&1&1&0&1&1&0&1 \\ 1&0&0&0&1&1&1&0&1&1&0 \\ 0&1&0&0&0&1&1&1&0&1&1 \end{pmatrix}. \tag{123}$$

The enlarged GAD quantum channel after performing the encoding defined by means of Eqs. (121) and (122) reads

$$\Lambda_{\text{GAD}}^{((11,2,3))}(\rho) \stackrel{\text{def}}{=} \sum_{r=0}^{2^{22}-1} A'_r \rho A'^{\dagger}_r = \sum_{a_1,\ldots,a_{11}=0}^{3} A_{a_1 a_2 \cdots a_{10} a_{11}} \rho A^{\dagger}_{a_1 a_2 \cdots a_{10} a_{11}}, \tag{124}$$

where to any of the 2^{22} values of r we can associate a set of indices $(a_1, \ldots, a_{11})$ (and vice versa) such that

$$A'_r \leftrightarrow A_{a_1 a_2 \cdots a_{10} a_{11}} \stackrel{\text{def}}{=} A_{a_1} \otimes A_{a_2} \otimes \cdots \otimes A_{a_{10}} \otimes A_{a_{11}} \equiv A_{a_1} A_{a_2} \cdots A_{a_{10}} A_{a_{11}}. \tag{125}$$

The errors A_i with $i \in \{0,1,2,3\}$ are defined in Eq. (8) and $\rho \in \mathcal{M}(\mathcal{C})$ with $\mathcal{C} \subset \mathcal{H}_2^{11}$. In particular, the number of weight-q enlarged error operators A'_r is given by $3^q \binom{11}{q}$ and,

$$2^{22} = \sum_{q=0}^{11} 3^q \binom{11}{q}. \tag{126}$$

We assume to focus on the recovery of weight-1 errors only and pay no attention to the possible recovery of higher-order enlarged errors. For instance, this working hypothesis is especially plausible for values of the perturbation parameters γ and ε with $0 \leqslant \varepsilon \ll \gamma \ll 1$. In this case, the recovery scheme $\mathcal{R}$ that we use can be described as follows: R_0 is associated with the weight-0 error; R_k with $k = 1, \ldots, 11$ are associated with the 11 weight-1 errors where single-qubit errors of type A_1 occur; finally, R_k with $k = 12, \ldots, 22$ are associated with the 11 weight-1 errors where single-qubit errors of type A_3 occur. The construction of these 23 recovery operators R_k is described in terms of 46 orthonormal vectors in $\mathcal{H}_2^{11}$. The missing orthonormal vectors needed to obtain an orthonormal basis of $\mathcal{H}_2^{11}$ and to construct $R_{23} \stackrel{\text{def}}{=} \hat{O}$ can be formally computed by using the rank-nullity theorem together with the Gram-Schmidt orthonormalization procedure. Finally, our analytical estimate of the entanglement fidelity of the ((11,2,3)) code reads

$$\mathcal{F}_{\text{first-order}}^{((11,2,3))}(\gamma,\varepsilon) \stackrel{\text{def}}{=} \frac{1}{(\dim_{\mathbb{C}} \mathcal{C})^2} \sum_{k=0}^{2^{14}-1} \sum_{l=0}^{22} |\text{Tr}(R_l A'_k)_{|\mathcal{C}}|^2 \approx 1 - \frac{55}{4}\gamma^2 - 55\varepsilon^2\left(1 + \frac{\gamma}{\varepsilon}\right) + O(3), \tag{127}$$

with

$$\mathcal{F}^{((11,2,3))}(\gamma,\varepsilon) \stackrel{\text{def}}{=} \frac{1}{(\dim_{\mathbb{C}} \mathcal{C})^2} \sum_{k=0}^{2^{14}-1} \sum_{l=0}^{23} |\text{Tr}(R_l A'_k)_{|\mathcal{C}}|^2. \tag{128}$$

From Eq. (127), we conclude that the performance of this strongly nonadditive code whose encoding rate equals 1/11 is not especially good for GAD errors. After all, this code was originally introduced in [53] for conceptual reasons without any claim about its error-correcting capabilities against any specific noise model. This code lacks two essential features: high encoding rate and self-complementarity [50].

The nonadditive code we consider next, although not self-complementary, has a very high encoding rate.

2. *The* ((9,12,3)) *code*

We consider next the nondegenerate ((9,12,3)) code [54], the first example of a 1-error-correcting nonadditive code capable of outperforming (in terms of encoded dimension) the optimal stabilizer code with the same length, namely, the [[9,3,3]] code. This is trivially a nonadditive code, since it encodes a fractional number of qubits, $k = \log_2 12 \approx 3.6$. This code was constructed by means of the graph-state formalism [51]. Therefore, in order to justify the structure of the codewords spanning this $K = 12$-dimensional codespace of this code, a subspace of the 2^9-dimensional *complex* Hilbert space $\mathcal{H}_2^9$, we introduce first the basic ingredients of the graph-state formalism and we refer to [51] and [55] for more details on this specific point.

The starting point in the graph-state formalism is the notion of graph. A unidirected simple graph $G \stackrel{\text{def}}{=} G(V,\Gamma)$ with $n = |V|$ vertices is characterized by the so-called adjacency matrix Γ. This is a $n \times n$ symmetric matrix with vanishing diagonal elements such that $\Gamma_{ij} = 1$ if vertices i and j are connected and $\Gamma_{ij} = 0$ otherwise. The graph state $|G\rangle$ associated with the graph G reads

$$|G\rangle \stackrel{\text{def}}{=} \frac{1}{\sqrt{2^n}} \sum_{\vec{\mu}=\mathbf{0}}^{\mathbf{1}} (-1)^{\frac{1}{2}\vec{\mu}\cdot\Gamma\cdot\vec{\mu}} |\vec{\mu}\rangle_z, \tag{129}$$

where $|\vec{\mu}\rangle_z$ are the simultaneous eigenstates of $\{Z_j\}_{j\in V}$ with $(-1)^{\mu_j}$ as eigenvalues and Z_j the Pauli operator acting on qubit $j \in V$.

The ((9,12,3)) code is associated with the so-called loop graph L_9 whose 9×9 adjacency matrix reads

$$\Gamma_{L_9} \stackrel{\text{def}}{=} \begin{pmatrix} 0&1&0&0&0&0&0&0&1\\ 1&0&1&0&0&0&0&0&0\\ 0&1&0&1&0&0&0&0&0\\ 0&0&1&0&1&0&0&0&0\\ 0&0&0&1&0&1&0&0&0\\ 0&0&0&0&1&0&1&0&0\\ 0&0&0&0&0&1&0&1&0\\ 0&0&0&0&0&0&1&0&1\\ 1&0&0&0&0&0&0&1&0 \end{pmatrix}, \tag{130}$$

and its corresponding graph state is denoted as $|L_9\rangle$. In terms of $|L_9\rangle$, the codespace of the code is spanned by the states

$$|i_L\rangle \stackrel{\text{def}}{=} Z_{V_i}|L_9\rangle, \tag{131}$$

where $i = 1,\ldots,12$ and

$$Z_{V_i} \stackrel{\text{def}}{=} \prod_{a\in V_i} Z_a, \tag{132}$$

with the set of vertices V_i defined as

$$\begin{aligned} &V_1 \stackrel{\text{def}}{=} \{\varnothing\}, \quad V_2 \stackrel{\text{def}}{=} \{2,6,7\}, \quad V_3 \stackrel{\text{def}}{=} \{4,5,9\}, \quad V_4 \stackrel{\text{def}}{=} \{2,3,6,8\}, \quad V_5 \stackrel{\text{def}}{=} \{3,5,8,9\}, \quad V_6 \stackrel{\text{def}}{=} \{2,3,4,5,6,7,8,9\},\\ &V_7 \stackrel{\text{def}}{=} \{1,4,7\}, \quad V_8 \stackrel{\text{def}}{=} \{1,2,4,6\}, \quad V_9 \stackrel{\text{def}}{=} \{1,5,7,9\}, \quad V_{10} \stackrel{\text{def}}{=} \{1,2,3,4,6,7,8\}, \quad V_{11} \stackrel{\text{def}}{=} \{1,3,4,5,7,8,9\},\\ &V_{12} \stackrel{\text{def}}{=} \{1,2,3,5,6,8,9\}. \end{aligned} \tag{133}$$

To be explicit, the 12 codewords are given by

$$\begin{aligned} &|1_L\rangle \stackrel{\text{def}}{=} |L_9\rangle, \quad |2_L\rangle \stackrel{\text{def}}{=} Z^2Z^6Z^7|L_9\rangle, \quad |3_L\rangle \stackrel{\text{def}}{=} Z^4Z^5Z^9|L_9\rangle, \quad |4_L\rangle \stackrel{\text{def}}{=} Z^2Z^3Z^6Z^8|L_9\rangle, \quad |5_L\rangle \stackrel{\text{def}}{=} Z^3Z^5Z^8Z^9|L_9\rangle,\\ &|6_L\rangle \stackrel{\text{def}}{=} Z^2Z^3Z^4Z^5Z^6Z^7Z^8Z^9|L_9\rangle, \quad |7_L\rangle \stackrel{\text{def}}{=} Z^1Z^4Z^7|L_9\rangle, \quad |8_L\rangle \stackrel{\text{def}}{=} Z^1Z^2Z^4Z^6|L_9\rangle, \quad |9_L\rangle \stackrel{\text{def}}{=} Z^1Z^5Z^7Z^9|L_9\rangle,\\ &|10_L\rangle \stackrel{\text{def}}{=} Z^1Z^2Z^3Z^4Z^6Z^7Z^8|L_9\rangle, \quad |11_L\rangle \stackrel{\text{def}}{=} Z^1Z^3Z^4Z^5Z^7Z^8Z^9|L_9\rangle, \quad |12_L\rangle \stackrel{\text{def}}{=} Z^1Z^2Z^3Z^5Z^6Z^8Z^9|L_9\rangle. \end{aligned} \tag{134}$$

We stress that each codeword is the sum of 512 state vectors,

$$\sum_{k=0}^{9} \binom{9}{k} = 2^9 = 512,$$

where $\binom{9}{k}$ denotes the number of state vectors of length 9 in this sum with k-1s in their definition. For each codeword, the sign distribution of these 512 state vectors changes according to the action of Z_{V_k} with $k \in \{1,\ldots,12\}$.

The enlarged GAD quantum channel after performing the encoding defined by means of Eq. (131) reads

$$\Lambda_{\text{GAD}}^{((9,12,3))}(\rho) \stackrel{\text{def}}{=} \sum_{r=0}^{2^{18}-1} A'_r \rho A'^{\dagger}_r = \sum_{a_1,\ldots,a_9=0}^{3} A_{a_1a_2\cdots a_8a_9} \rho A^{\dagger}_{a_1a_2\cdots a_8a_9}, \tag{135}$$

where to any of the 2^{18} values of r we can associate a set of indices $(a_1,\ldots,a_9)$ (and vice versa) such that

$$\begin{aligned} A'_r \leftrightarrow A_{a_1a_2\cdots a_8a_9} &\stackrel{\text{def}}{=} A_{a_1} \otimes A_{a_2} \otimes \cdots \otimes A_{a_8} \otimes A_{a_9}\\ &\equiv A_{a_1}A_{a_2}\cdots A_{a_8}A_{a_9}. \end{aligned} \tag{136}$$

The errors A_i with $i \in \{0,1,2,3\}$ are defined in Eq. (8) and $\rho \in \mathcal{M}(\mathcal{C})$ with $\mathcal{C} \subset \mathcal{H}_2^9$. In particular, the number of weight-q enlarged error operators A'_r is given by $3^q\binom{9}{q}$ and

$$\sum_{q=0}^{9} 3^q \binom{9}{q} = 2^{18}. \tag{137}$$

Before describing our recovery scheme, let us make two remarks. First, the codespace of this nonadditive code is a 12-dimensional subspace of $\mathcal{H}_2^9$ spanned by 12 codewords. Each codeword is the sum-decomposition of 512

vector states in $\mathcal{H}_2^9$. The number of vector states in such decomposition with m nonzero components is given by $\binom{9}{m}$. This binomial factor can be regarded as the cardinality of vector states of Hamming weight m that appear in the sum-decomposition of the codewords. The normalization condition requires

$$2^9 = \sum_{q=0}^{9} \binom{9}{q} = 2^9 = 512. \tag{138}$$

Second, after some thinking, it can be shown that the action of any weight-1 enlarged error operator (where single-qubit errors of type A_1 or A_3 may occur) on each of these codewords with the above-mentioned structure leads to quantum states in $\mathcal{H}_2^9$ described in terms of a sum-decomposition of 162 vector states which give rise to the following Hamming weight distribution: 1 vector with Hamming weight $m = 1$, 8 vectors with $m = 2$, 28 vectors with $m = 3$, 56 vectors with $m = 4$, 35 vectors with $m = 5$, 20 vectors with $m = 6$, 10 vectors with $m = 7$, 3 vectors with $m = 8$ and, finally, 1 vector with $m = 9$.

As stated earlier, we assume to focus on the recovery of weight-1 errors only and pay no attention to the possible recovery of higher-order enlarged errors. In this case, the recovery scheme $\mathcal{R}$ that we use can be described as follows: R_0 is associated with the weight-0 error; R_k with $k = 1, \ldots, 9$ are associated with the 11 weight-1 errors where single-qubit errors of type A_1 occur; finally, R_k with $k = 10, \ldots, 18$ are associated with the 11 weight-1 errors where single-qubit errors of type A_3 occur. The construction of these 19 recovery operators R_k is described in terms of $19 \times 12 = 228$ orthonormal vectors in $\mathcal{H}_2^9$. The missing orthonormal vectors needed to obtain an orthonormal basis of $\mathcal{H}_2^9$ and to construct $R_{19} \stackrel{\text{def}}{=} \hat{O}$ can be formally computed by using the rank-nullity theorem together with the Gram-Schmidt orthonormalization procedure. Finally, our analytical estimate of the entanglement fidelity of the ((9,12,3)) code reads

$$\begin{aligned} \mathcal{F}_{\text{first-order}}^{((9,12,3))}(\gamma,\varepsilon) &\stackrel{\text{def}}{=} \frac{1}{(\dim_{\mathbb{C}} \mathcal{C})^2} \sum_{k=0}^{2^{18}-1} \sum_{l=0}^{18} |\text{Tr}(R_l A'_k)_{|\mathcal{C}}|^2 \\ &\approx 1 - 9\gamma^2 - 36\varepsilon^2\left(1 + \frac{\gamma}{\varepsilon}\right) + O(3), \end{aligned} \tag{139}$$

with

$$\mathcal{F}^{((9,12,3))}(\gamma,\varepsilon) \stackrel{\text{def}}{=} \frac{1}{(\dim_{\mathbb{C}} \mathcal{C})^2} \sum_{k=0}^{2^{18}-1} \sum_{l=0}^{19} |\text{Tr}(R_l A'_k)_{|\mathcal{C}}|^2. \tag{140}$$

From Eqs. (127) and (139), we conclude that the nondegenerate ((9,12,3)) code not only outperforms the ((11,2,3)) in terms of encoded dimension but also in terms of entanglement fidelity with recovery schemes limited to first-order recovery. Furthermore, from Eq. (118), it can be shown that

$$\begin{aligned} &\mathcal{F}_{\text{first-order}}^{[[9,1,3]]}(\gamma,\varepsilon = 0) \\ &\quad\approx 1 - \frac{45}{4}\gamma^2 + O(\gamma^3) \lesssim 1 - \frac{9}{\log_2 12}\gamma^2 + O(\gamma^3) \\ &\quad\approx \tilde{\mathcal{F}}_{\text{first-order}}^{((9,12,3))}(\gamma,\varepsilon = 0), \end{aligned} \tag{141}$$

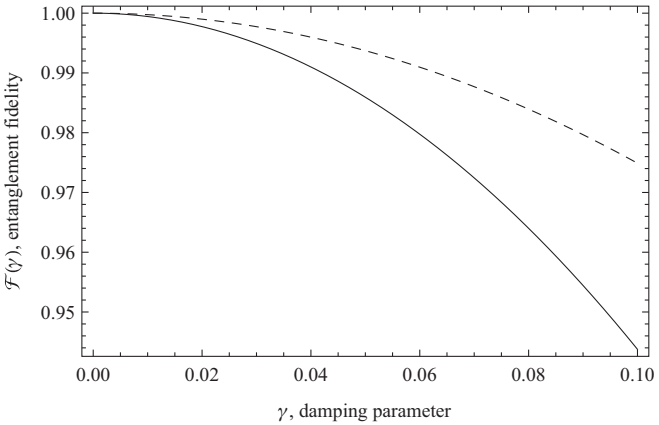

FIG. 4. Additive vs nonadditive codes of length nine. The truncated series expansions of the normalized entanglement fidelity $\mathcal{F}(\gamma)$ vs the AD parameter γ for $\varepsilon = 0$ and $0 \leqslant \gamma \leqslant 10^{-1}$: the Shor nine-qubit code (thin solid line) and the ((9,12,3)) code (dashed line).

where $\tilde{\mathcal{F}}$ denotes the entanglement fidelity normalized with exponentiation by $1/k$, where $k \stackrel{\text{def}}{=} \log_2 K$ is the number of encoded logical qubits ($k = 1$ for the Shor nine-qubit code) [8]. From the comparison of the first-order entanglement-based performances of these two codes in Eq. (141), we are lead to the conclusion that the nondegenerate and nonadditive code ((9,12,3)) outperforms the degenerate and additive code [[9,1,3]] not only in terms of encoded dimension. The comparison between these two codes is shown in Fig. 4.

B. Self-complementary codes

In what follows, we consider single-AD error-correcting codes. For this reason, we set $\varepsilon = 0$ and limit our considerations to the approximate QEC of AD errors by means of self-complementary nonadditive quantum codes. An $((n,K,d))$ code is called self-complementary if its codespace is spanned by codewords $\{|c_a\rangle\}$ defined as [50],

$$|c_a\rangle \stackrel{\text{def}}{=} \frac{|a\rangle + |\bar{a}\rangle}{\sqrt{2}}, \tag{142}$$

where a is a binary string of length n and $\bar{a} \stackrel{\text{def}}{=} \mathbf{1} \oplus a$ is the complement of a. The suitability of self-complemetary nonadditive codes for the error correction of AD errors was first proposed in [23,24]. However, no explicit comparison of the performances quantified by means of analytical estimates of the entanglement fidelity of self-complementary and non-self-complementary nonadditive codes for AD errors was presented. Furthermore, no similar comparison between nonadditive self-complementary and stabilizer codes for AD errors exists as well. In view of these considerations, we seek to provide some useful insights into these unexplored issues.

1. The ((6,5)) code

The first self-complementary single-AD error-correcting code that we consider is the ((6,5)) code whose codespace

is spanned by the following five codewords in $\mathcal{H}_2^6$:

$$\begin{aligned}
|0_L\rangle &\stackrel{\text{def}}{=} \frac{|000000\rangle + |111111\rangle}{\sqrt{2}},\\
|1_L\rangle &\stackrel{\text{def}}{=} \frac{|110000\rangle + |001111\rangle}{\sqrt{2}},\\
|2_L\rangle &\stackrel{\text{def}}{=} \frac{|001100\rangle + |110011\rangle}{\sqrt{2}},\\
|3_L\rangle &\stackrel{\text{def}}{=} \frac{|000011\rangle + |111100\rangle}{\sqrt{2}},\\
|4_L\rangle &\stackrel{\text{def}}{=} \frac{|010101\rangle + |101010\rangle}{\sqrt{2}}.
\end{aligned} \tag{143}$$

We point out that the existence of such a code was originally proposed in [23], although it was neither explicitly shown nor used for error correction of single-AD errors.

The enlarged AD quantum channel after performing the encoding defined by means of Eq. (143) reads

$$\Lambda_{\text{AD}}^{((6,5))}(\rho) \stackrel{\text{def}}{=} \sum_{r=0}^{2^6-1} A'_r \rho A'^{\dagger}_r = \sum_{a_1,\ldots,a_6=0}^{1} A_{a_1a_2\cdots a_5a_6} \rho A^{\dagger}_{a_1a_2\cdots a_5a_6}, \tag{144}$$

where to any of the 2^6 values of r we can associate a set of indices $(a_1,\ldots,a_6)$ (and vice versa) such that

$$\begin{aligned}
A'_r \leftrightarrow A_{a_1a_2\cdots a_5a_6} &\stackrel{\text{def}}{=} A_{a_1} \otimes A_{a_2} \otimes \cdots \otimes A_{a_5} \otimes A_{a_6}\\
&\equiv A_{a_1} A_{a_2} \cdots A_{a_5} A_{a_6}.
\end{aligned} \tag{145}$$

The errors A_i with $i \in \{0,1\}$ are defined in Eq. (8) and $\rho \in \mathcal{M}(\mathcal{C})$ with $\mathcal{C} \subset \mathcal{H}_2^6$. In particular, the number of weight-q enlarged error operators A'_r is given by $\binom{6}{q}$ and

$$\sum_{q=0}^{6} \binom{6}{q} = 2^6. \tag{146}$$

The recovery scheme $\mathcal{R}$ that we use can be described as follows: R_0 is associated with the weight-0 error; R_k with $k = 1,\ldots,6$ are associated with the six weight-1 errors where single-qubit errors of type A_1 occur. The construction of these seven recovery operators R_k is described in terms of $7 \times 5 = 35$ orthonormal vectors in $\mathcal{H}_2^6$. The missing orthonormal vectors needed to obtain an orthonormal basis of $\mathcal{H}_2^6$ and to construct $R_7 \stackrel{\text{def}}{=} \hat{O}$ can be formally computed by using the rank-nullity theorem together with the Gram-Schmidt orthonormalization procedure. Finally, our analytical estimate of the entanglement fidelity of the ((6,5)) code reads

$$\begin{aligned}
\mathcal{F}_{\text{first-order}}^{((6,5))}(\gamma) &\stackrel{\text{def}}{=} \frac{1}{(\dim_{\mathbb{C}} \mathcal{C})^2} \sum_{k=0}^{2^6-1} \sum_{l=0}^{6} |\text{Tr}(R_l A'_k)_{|\mathcal{C}.}|^2\\
&\approx 1 - \frac{21}{5}\gamma^2 + O(\gamma^3),
\end{aligned} \tag{147}$$

with

$$\mathcal{F}^{((6,5))}(\gamma) \stackrel{\text{def}}{=} \frac{1}{(\dim_{\mathbb{C}} \mathcal{C})^2} \sum_{k=0}^{2^6-1} \sum_{l=0}^{7} |\text{Tr}(R_l A'_k)_{|\mathcal{C}}|^2. \tag{148}$$

From Eqs. (111) and (147), it follows that

$$\begin{aligned}
\tilde{\mathcal{F}}_{\text{first-order}}^{((6,5))}(\gamma) &\approx 1 - \frac{21}{5\log_2 5}\gamma^2 + O(\gamma^3) \geqslant 1 - 2\gamma^2 + O(\gamma^3)\\
&\approx \mathcal{F}^{[[6,1,3]]}(\gamma, \varepsilon = 0) \geqslant \mathcal{F}_{\text{first-order}}^{[[6,1,3]]}(\gamma, \varepsilon = 0).
\end{aligned} \tag{149}$$

Equation (149) is an explicit manifestation of the superiority, in terms of both encoded dimension and entanglement fidelity, of nonadditive over additive codes.

2. *The* ((8,12)) *code*

The second self-complementary single-AD error-correcting code that we consider is the ((8,12)) code whose codespace is spanned by the following 12 codewords in $\mathcal{H}_2^8$ [23]:

$$\begin{aligned}
|0_L\rangle &\stackrel{\text{def}}{=} \frac{|00000000\rangle + |11111111\rangle}{\sqrt{2}}, \quad |1_L\rangle \stackrel{\text{def}}{=} \frac{|00000011\rangle + |11111100\rangle}{\sqrt{2}}, \quad |2_L\rangle \stackrel{\text{def}}{=} \frac{|00001100\rangle + |11110011\rangle}{\sqrt{2}},\\
|3_L\rangle &\stackrel{\text{def}}{=} \frac{|00110000\rangle + |11001111\rangle}{\sqrt{2}}, \quad |4_L\rangle \stackrel{\text{def}}{=} \frac{|11000000\rangle + |00111111\rangle}{\sqrt{2}}, \quad |5_L\rangle \stackrel{\text{def}}{=} \frac{|10101000\rangle + |01010111\rangle}{\sqrt{2}},\\
|6_L\rangle &\stackrel{\text{def}}{=} \frac{|01011000\rangle + |10100111\rangle}{\sqrt{2}}, \quad |7_L\rangle \stackrel{\text{def}}{=} \frac{|01100100\rangle + |10011011\rangle}{\sqrt{2}}, \quad |8_L\rangle \stackrel{\text{def}}{=} \frac{|10010100\rangle + |01101011\rangle}{\sqrt{2}},\\
|9_L\rangle &\stackrel{\text{def}}{=} \frac{|11110000\rangle + |00001111\rangle}{\sqrt{2}}, \quad |10_L\rangle \stackrel{\text{def}}{=} \frac{|11001100\rangle + |00110011\rangle}{\sqrt{2}}, \quad |11_L\rangle \stackrel{\text{def}}{=} \frac{|00111100\rangle + |11000011\rangle}{\sqrt{2}}.
\end{aligned} \tag{150}$$

The enlarged AD quantum channel after performing the encoding defined by means of Eq. (150) reads

$$\Lambda_{\text{AD}}^{((8,12))}(\rho) \stackrel{\text{def}}{=} \sum_{r=0}^{2^8-1} A'_r \rho A'^{\dagger}_r = \sum_{a_1,\ldots,a_8=0}^{1} A_{a_1a_2\cdots a_7a_8} \rho A^{\dagger}_{a_1a_2\cdots a_7a_8}, \tag{151}$$

where to any of the 2^8 values of r we can associate a set of indices $(a_1,\ldots,a_8)$ (and vice versa) such that

$$\begin{aligned}
A'_r \leftrightarrow A_{a_1a_2\cdots a_7a_8} &\stackrel{\text{def}}{=} A_{a_1} \otimes A_{a_2} \otimes \cdots \otimes A_{a_7} \otimes A_{a_8}\\
&\equiv A_{a_1} A_{a_2} \cdots A_{a_7} A_{a_8}.
\end{aligned} \tag{152}$$

The errors A_i with $i \in \{0,1\}$ are defined in Eq. (8) and $\rho \in \mathcal{M}(\mathcal{C})$ with $\mathcal{C} \subset \mathcal{H}_2^8$. In particular, the number of weight-q enlarged error operators A'_r is given by $\binom{8}{q}$ and

$$\sum_{q=0}^{8} \binom{8}{q} = 2^8. \tag{153}$$

The recovery scheme $\mathcal{R}$ that we use can be described as follows: R_0 is associated with the weight-0 error; R_k with $k = 1, \ldots, 8$ are associated with the eight weight-1 errors where single-qubit errors of type A_1 occur. The construction of these nine recovery operators R_k is described in terms of $9 \times 12 = 108$ orthonormal vectors in $\mathcal{H}_2^8$. The missing orthonormal vectors needed to obtain an orthonormal basis of $\mathcal{H}_2^8$ and to construct $R_9 \stackrel{\text{def}}{=} \hat{O}$ can be formally computed by using the rank-nullity theorem together with the Gram-Schmidt orthonormalization procedure. Finally, our analytical estimate of the entanglement fidelity of the ((8,12)) code reads

$$\begin{aligned}\mathcal{F}^{((8,12))}_{\text{first-order}}(\gamma) &\stackrel{\text{def}}{=} \frac{1}{(\dim_{\mathbb{C}} \mathcal{C})^2} \sum_{k=0}^{2^8-1} \sum_{l=0}^{8} |\text{Tr}(R_l A'_k)_{|\mathcal{C}.}|^2 \\ &\approx 1 - \frac{15}{2}\gamma^2 + O(\gamma^3),\end{aligned} \tag{154}$$

with

$$\mathcal{F}^{((8,12))}(\gamma) \stackrel{\text{def}}{=} \frac{1}{(\dim_{\mathbb{C}} \mathcal{C})^2} \sum_{k=0}^{2^8-1} \sum_{l=0}^{9} |\text{Tr}(R_l A'_k)_{|\mathcal{C}}|^2. \tag{155}$$

It is convenient to compare the performance of this code with that of a multiqubit encoding stabilizer code with the same length. For instance, the [[8,3,3]] code is a special case of a class of $[[2^j, 2^j - j - 2, 3]]$ codes [56]. It encodes three logical qubits into eight physical qubits and corrects all single-qubit errors. The five stabilizer generators are given by [33]

$$\begin{aligned}&g_1 \stackrel{\text{def}}{=} X^1X^2X^3X^4X^5X^6X^7X^8, \quad g_2 \stackrel{\text{def}}{=} Z^1Z^2Z^3Z^4Z^5Z^6Z^7Z^8, \\ &g_3 \stackrel{\text{def}}{=} X^2X^4Y^5Z^6Y^7Z^8, \quad g_4 \stackrel{\text{def}}{=} X^2Z^3Y^4X^6Z^7Y^8, \\ &g_5 \stackrel{\text{def}}{=} Y^2X^3Z^4X^5Z^6Y^8,\end{aligned} \tag{156}$$

and a suitable choice for the logical operations $\bar{X}_i$ and $\bar{Z}_i$ with $i \in \{1,2,3\}$ reads

$$\begin{aligned}&\bar{X}_1 \stackrel{\text{def}}{=} X^1X^2Z^6Z^8, \quad \bar{X}_2 \stackrel{\text{def}}{=} X^1X^3Z^4Z^7, \quad \bar{X}_3 \stackrel{\text{def}}{=} X^1Z^4X^5Z^6, \\ &\bar{Z}_1 \stackrel{\text{def}}{=} Z^2Z^4Z^6Z^8, \quad \bar{Z}_2 \stackrel{\text{def}}{=} Z^3Z^4Z^7Z^8, \quad \bar{Z}_3 \stackrel{\text{def}}{=} Z^5Z^6Z^7Z^8.\end{aligned} \tag{157}$$

A convenient choice for the basis codewords reads

$$|\overline{ijk}\rangle \stackrel{\text{def}}{=} (\bar{X}_1)^i(\bar{X}_2)^j(\bar{X}_3)^k \sum_{g \in \mathcal{S}} g|00000000\rangle. \tag{158}$$

For an explicit representation of the codewords of the [[8,3,3]] code, we refer to [56] (specifically, see Table III in [56]). Following our line of reasoning presented for the error correction of AD errors by means of stabilizer codes and omitting technical details, it turns out that the entanglement fidelity of the [[8,3,3]] with our recovery up to first-order errors becomes

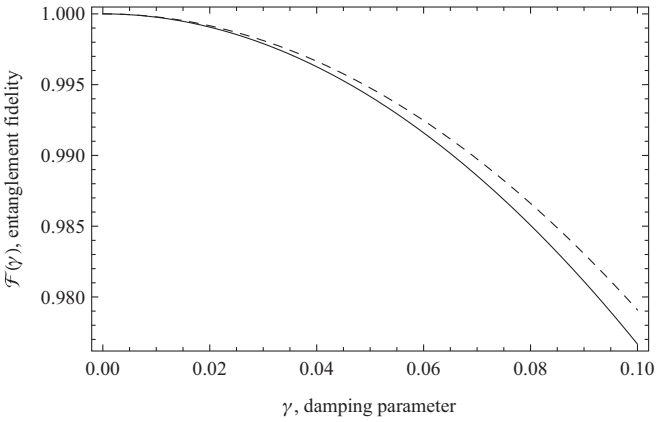

FIG. 5. Additive vs nonadditive codes of length eight. The truncated series expansions of the normalized entanglement fidelity $\mathcal{F}(\gamma)$ vs the AD parameter γ for $\varepsilon = 0$ and $0 \leqslant \gamma \leqslant 10^{-1}$: Gottesman's [[8,3,3]] code (thin solid line) and the ((8,12)) code (dashed line).

$$\mathcal{F}^{[[8,3,3]]}_{\text{first-order}}(\gamma) \approx 1 - 7\gamma^2 + O(\gamma^3). \tag{159}$$

Unlike the case of single-qubit encoding, in this case the entanglement fidelity when no QEC is performed is represented by the three-qubit baseline performance given by

$$\mathcal{F}^{\text{3-qubit}}_{\text{baseline}}(\gamma) \stackrel{\text{def}}{=} 8^{-2}[1 + 3\sqrt{1-\gamma} + 3(1-\gamma) + (1-\gamma)^{\frac{3}{2}}]^2. \tag{160}$$

In addition, from Eqs. (154) and (159), we get

$$\begin{aligned}\tilde{\mathcal{F}}^{((8,12))}_{\text{first-order}}(\gamma) &\approx 1 - \frac{15}{2\log_2 12}\gamma^2 + O(\gamma^3) \geqslant 1 - \frac{7}{3}\gamma^2 + O(\gamma^3) \\ &\approx \tilde{\mathcal{F}}^{[[8,3,3]]}_{\text{first-order}}(\gamma).\end{aligned} \tag{161}$$

Equation (161) is yet another clear fingerprint of the superiority, in terms of both encoded dimension and entanglement fidelity, of nonadditive over additive codes. The comparison

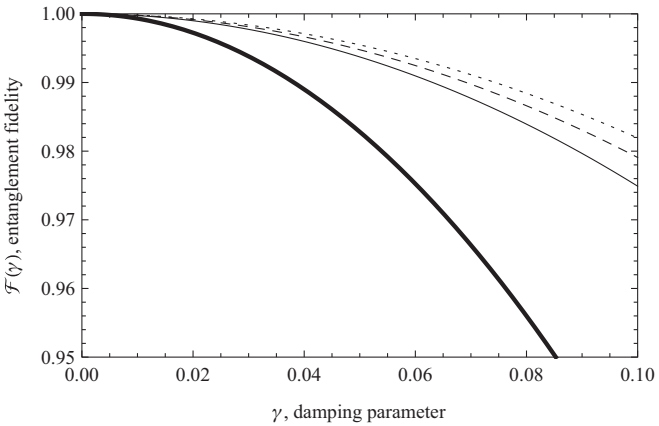

FIG. 6. Ranking nonadditive codes. The truncated series expansions of the normalized entanglement fidelity $\mathcal{F}(\gamma)$ vs the AD parameter γ for $\varepsilon = 0$ and $0 \leqslant \gamma \leqslant 10^{-1}$: the ((6,5))-code (dotted line), the ((8,12)) code (dashed line), the ((9,12,3)) code (thin solid line), and the ((11,2,3)) code (thick solid line).

between these two codes is shown in Fig. 5. Finally, we compare the performances of the nonadditive codes employed in our error-correction schemes in Fig. 6.

VI. FINAL REMARKS

In this article, we presented an analytic analysis of the performance of various approximate QEC codes for GAD errors. Specifically, we considered both stabilizer and nonadditive quantum codes. The performance of such codes was quantified by means of the entanglement fidelity as a function of the damping probability and the nonzero environmental temperature. We analytically recovered and clarified some previously known numerical results in the limiting case of the AD channel (zero environmental temperature). In addition, our extended investigation suggested that degenerate stabilizer codes and self-complementary nonadditive codes are especially suitable for the error correction of GAD errors. Finally, comparing the properly normalized entanglement fidelities of the best performant stabilizer and nonadditive codes characterized by the same length, we showed that, in general, nonadditive codes outperform stabilizer codes not only in terms of encoded dimension but also in terms of entanglement fidelity.

Our main findings may be summarized as follows.

(1) We have explicitly shown that in the presence of nonzero environmental temperature, the performance of both additive and nonadditive quantum codes decreases (with respect to zero environmental temperature case). In particular, degenerate stabilizer codes seem to be more robust than the nondegenerate ones against this effect, as evident from Eqs. (111) and (118).

(2) In the limiting case of $\varepsilon = 0$ and considering the $[[5,1,3]]$ code, our analytic estimate in Eq. (77) reduces to the numeric ones in [9] and [39]; in the same limiting case, considering the CSS $[[7,1,3]]$ code, our estimate in Eq. (84) reduces to the numeric one in [12]; finally, considering the Shor $[[9,1,3]]$ code, our estimate in Eq. (118) reduces to that numerically obtained in [8].

(3) We have constructed a nondegenerate eight-qubit concatenated stabilizer code [see Eq. (91)], a natural generalization of the Leung *et al*. four-qubit code, suitable for the QEC of GAD errors. We have also checked that in the limit of $\varepsilon = 0$, our estimated performance for such a code reduces to that of the four-qubit code applied to AD errors [see Eq. (104)].

(4) We have provided further evidence (see Eq. (111) for the $[[6,1,3]]$ code) in support of the *suspect* advanced in [12], where it was conjectured that, thanks to their degenerate structure, such codes can outperform nondegenerate codes despite their shorter length.

(5) From Eqs. (127) and (139), we have explicitly shown that the nonadditive $((9,12,3))$ code not only outperforms the $((11,2,3))$ code in terms of encoded dimension but also in terms of entanglement fidelity with recovery schemes limited to first-order recovery.

(6) We have shown that, to first-order recovery, self-complementary nonadditive codes can outperform non-self-complementary nonadditive codes despite exhibiting smaller encoded dimension [see Eqs. (139) and (147) for the $((6,5))$ and $((9,12,3))$ codes, respectively].

(7) From the comparison of the first-order entanglement-based performances between additive and nonadditive quantum codes with identical lengths [see Eqs. (141), (149), and (161)], we concluded that nonadditive codes outperform, in general, additive codes not only in terms of encoded dimension. In particular, nonadditivity seems to matter more than degeneracy in the approximate QEC of both GAD and AD errors [see Eq. (141)].

We wish to emphasize three aspects of our analysis.

(i) First, despite the great variety of quantum codes employed in this work, we have limited our attention to qubit channels only. The AD and GAD channels can, of course, be extended to quantum systems of dimension greater than two, leading to the so-called qudit channels. For instance, a qutrit is a three-state quantum system. In such higher-dimensional cases, the physical processes that we may consider are described by the modeling of atoms as having more than two states (multilevel atoms) interacting with environments modeled by a bath of harmonic oscillators which can be initially in the vacuum state or, more generally, in a thermal state with temperature greater than zero. The study of the effectiveness of QEC schemes suitable for such additional realistic scenarios will be the object of our attention in future efforts.

(ii) Second, the QEC strategy that we have employed for our analytic estimates may be considered mildly conservative, since we might have slightly underestimated the quantum codes performances to avoid false overestimations. However, we have tried to maintain the same degree of conservativeness in all our estimates in order to preserve the fairness of the comparisons between pairs of different quantum codes. After all, exact analytical calculations of the entanglement fidelities can be quite intimidating. They are conceptually straightforward but computationally extremely tedious if performed by hands to avoid the drawbacks of numerical results [12,14]. We also emphasize that conservative estimates are not uncommon in QEC since, after all, we are led to deal with approximations. For instance, conservativeness appears in analytic estimates of error thresholds in topological QEC when crude combinatorics arguments are employed [57] as well as in the numerical estimation of the error threshold to depolarization of toric codes by means of Monte Carlo simulations [58].

(iii) Third, despite the variety of quantum codes employed in the approximate QEC of GAD errors presented in this work, we emphasize that we cannot state without a doubt that for any given arbitrary noise model, nonadditive and degenerate codes are more efficient, in general, than additive and nondegenerate codes. In all honesty, we feel uncomfortable in extrapolating a general statement from a large, but yet limited, number of special cases. Perhaps this is the reason why QEC is an art: General statements cannot be made *a priori*; each scenario has to be taken into consideration separately. It is a matter of finding a good matching between the noise model and the quantum code. Furthermore, we are not able to quantify exactly the effect on the code performances provided by fractional encoding, a feature of nonadditive codes, or by the possibility of correcting a number of errors greater than the one that is uniquely identified, a feature of degenerate codes. Also, we cannot rule out the possibility that the mathematical structure behind the sign pattern that characterizes the various

codewords spanning the codespaces may play a relevant role in determining the performance of the error correction schemes. In conclusion, the merit of achieving higher performances cannot be ascribed to specific properties of a code, but rather to the properties of a code *together* with a family of errors it is designed to correct. This final remark is in excellent agreement with the fact that, for instance, degeneracy must not be regarded as a property of a quantum code alone, but rather a property of a code together with a class of errors it is designed to recover.

In conclusion, we feel we have tried to advance our understanding of approximate QEC of GAD errors for various qubit codes, both additive and nonadditive, from an analytical standpoint. However, in all fairness, it is very likely that quantitative results in QEC will always require the help of numerical investigations. In future efforts, we wish to further sharpen our analytic estimations by using, if possible, both additional analytical and numerical scrutiny.

ACKNOWLEDGMENTS

We thank the ERA-Net CHIST-ERA Project HIPERCOM for financial support. C.C. also thanks Marcel Bergmann for numerically testing Eq. (139) and for helpful conversations.

APPENDIX A: THE KRAUS OPERATOR-SUM DECOMPOSITION OF THE GAD CHANNEL

In this Appendix, we provide an explicit derivation of the (2×2)-matrix representation of the Kraus error operators for the GAD channel in Eq. (8).

Let us consider AD from the scattering of a photon via a beam splitter [3]. Consider a single optical mode that contains the quantum state $|\psi\rangle \stackrel{\text{def}}{=} \alpha|0\rangle + \beta|1\rangle$, where $|0\rangle$ is the vacuum state while $|1\rangle$ denotes the single photon state. The scattering of a photon from this mode can be modeled by inserting a beam splitter in the path of the photon. The beam splitter acts on two modes: It performs the unitary operation $U \stackrel{\text{def}}{=} e^{\chi(a^\dagger b - b^\dagger a)}$ and allows the photon to couple to another single optical mode that represents the environment. The operators a, $a^\dagger$ and b, $b^\dagger$ are the annihilation and creation operators, respectively, for photons in the two modes. Assuming the environment starts out with no photons,

$$\rho_{\text{env.}} \stackrel{\text{def}}{=} |0\rangle\langle 0|, \tag{A1}$$

it can be shown that the quantum operation that describes this process reads

$$\Lambda_{\text{AD}}(\rho) \stackrel{\text{def}}{=} A_0 \rho A_0^\dagger + A_1 \rho A_1^\dagger, \tag{A2}$$

with $A_k \stackrel{\text{def}}{=} \langle k\,|U|\,0\rangle$ and

$$A_0 = \begin{pmatrix} 1 & 0 \\ 0 & \sqrt{1-\gamma} \end{pmatrix}, \quad A_1 = \begin{pmatrix} 0 & \sqrt{\gamma} \\ 0 & 0 \end{pmatrix}, \tag{A3}$$

where $\gamma \stackrel{\text{def}}{=} \sin^2\chi$ denotes the probability of losing a photon. If we assume that the environment starts out in a linear superposition of zero and one photons,

$$\rho_{\text{env.}} \stackrel{\text{def}}{=} \sum_{j=0}^{1} q_j |j\rangle\langle j|, \tag{A4}$$

where $q_0 \stackrel{\text{def}}{=} p$, $q_1 = 1-p$, and $0 \leqslant p \leqslant 1$, it turns out that the quantum operation that describes this process reads

$$\Lambda_{\text{GAD}}(\rho) \stackrel{\text{def}}{=} A_{00}\rho A_{00}^\dagger + A_{01}\rho A_{01}^\dagger + A_{11}\rho A_{11}^\dagger + A_{10}\rho A_{10}^\dagger, \tag{A5}$$

with $A_{jk} \stackrel{\text{def}}{=} \sqrt{q_j}\langle k|U|j\rangle$. Observe that $A_{0k} \stackrel{\text{def}}{=} \sqrt{p}\langle k|U|0\rangle$ and $A_{1k} \stackrel{\text{def}}{=} \sqrt{1-p}\langle k|U|1\rangle$, with $k = 0, 1$. Let us first focus on A_{1k}, which can be written as

$$A_{1k} \stackrel{\text{def}}{=} \sum_{m,n} (A_{1k})_{mn} |m\rangle\langle n|, \tag{A6}$$

where the coefficients $(A_{1k})_{mn}$ are defined as

$$(A_{1k})_{mn} \stackrel{\text{def}}{=} \sqrt{1-p}\langle m,k|U|n,1\rangle = \sqrt{1-p}(\langle m,k|)(U|n,1\rangle). \tag{A7}$$

Before computing an explicit expression for $U|n,1\rangle$ in Eq. (A7), observe that using the Baker-Campbell-Hausdorff formula,

$$e^{\chi A} B e^{-\chi A} = B + \chi[A,B] + \frac{\chi^2}{2!}[A,[A,B]] + \frac{\chi^3}{3!}[A,[A,[A,B]]] + O(3), \tag{A8}$$

we obtain

$$\begin{aligned} UaU^\dagger &\stackrel{\text{def}}{=} e^{\chi(a^\dagger b - b^\dagger a)} a e^{-\chi(a^\dagger b - b^\dagger a)} \\ &= a + \chi[a^\dagger b - b^\dagger a, a] + \frac{\chi^2}{2!}[a^\dagger b - b^\dagger a,[a^\dagger b - b^\dagger a,a]] \\ &\quad + \frac{\chi^3}{3!}[a^\dagger b - b^\dagger a,[a^\dagger b - b^\dagger a,[a^\dagger b - b^\dagger a,a]]] + O(3). \end{aligned} \tag{A9}$$

Notice that the commutator $[a^\dagger b - b^\dagger a, a]$ in Eq. (A9) can be written as

$$\begin{aligned} &[a^\dagger b - b^\dagger a, a] \\ &\quad = -b,[a^\dagger b - b^\dagger a,[a^\dagger b - b^\dagger a,a]] \\ &\quad = a,[a^\dagger b - b^\dagger a,[a^\dagger b - b^\dagger a,[a^\dagger b - b^\dagger a,a]]] = -a; \end{aligned} \tag{A10}$$

therefore, $UaU^\dagger$ becomes

$$\begin{aligned} UaU^\dagger &= a - \chi b - \frac{\chi^2}{2!}a + \frac{\chi^3}{3!}b + \cdots \\ &= a\left(1 - \frac{\chi^2}{2!} + \cdots\right) - b\left(\chi - \frac{\chi^3}{3!} + \cdots\right) \\ &= (\cos\chi)a - (\sin\chi)b. \end{aligned} \tag{A11}$$

Following this line of reasoning, we can also show that $UbU^\dagger$ equals

$$UbU^\dagger = (\cos\chi)b - (\sin\chi)a. \tag{A12}$$

Finally, recalling that $(n+m)^l$ can be written as

$$(n+m)^l = \sum_{p=0}^{l} \binom{l}{p} n^p m^{l-p}, \tag{A13}$$

we have that $U|n,1\rangle$ in Eq. (A7) becomes

$$\begin{aligned}
U|n,1\rangle &= U\frac{(a^\dagger)^n}{\sqrt{n!}}b^\dagger|00\rangle = \left[U\frac{(a^\dagger)^n}{\sqrt{n!}}U^\dagger\right][Ub^\dagger U^\dagger]|00\rangle \\
&= \frac{1}{\sqrt{n!}}[(\cos\chi)a^\dagger - (\sin\chi)b^\dagger]^n[(\cos\chi)b^\dagger - (\sin\chi)a^\dagger]|00\rangle \\
&= \frac{1}{\sqrt{n!}}\left[\sum_{p=0}^{n}\binom{n}{p}(\cos\chi)^p(-\sin\chi)^{n-p}(a^\dagger)^p(b^\dagger)^{n-p}\right][(\cos\chi)|01\rangle - (\sin\chi)|10\rangle] \\
&= \frac{1}{\sqrt{n!}}\sum_{p=0}^{n}\binom{n}{p}[(\cos\chi)^{1+p}(-\sin\chi)^{n-p}(a^\dagger)^p(b^\dagger)^{n-p}|01\rangle + (\cos\chi)^p(-\sin\chi)^{n-p+1}(a^\dagger)^p(b^\dagger)^{n-p}|10\rangle] \\
&= \frac{1}{\sqrt{n!}}\sum_{p=0}^{n}\binom{n}{p}[(\cos\chi)^{1+p}(-\sin\chi)^{n-p}(a^\dagger)^p|0\rangle(b^\dagger)^{n-p}|1\rangle + (\cos\chi)^p(-\sin\chi)^{n-p+1}(a^\dagger)^p|1\rangle(b^\dagger)^{n-p}|0\rangle] \\
&= \frac{1}{\sqrt{n!}}\sum_{p=0}^{n}\binom{n}{p}[(\cos\chi)^{1+p}(-\sin\chi)^{n-p}\sqrt{p!}|p\rangle(b^\dagger)^{n-p+1}|0\rangle + (\cos\chi)^p(-\sin\chi)^{n-p+1}(a^\dagger)^{1+p}|0\rangle\sqrt{(n-p)!}|n-p\rangle];
\end{aligned} \tag{A14}$$

that is, after some more algebra,

$$\begin{aligned}
U|n,1\rangle =& \frac{1}{\sqrt{n!}}\sum_{p=0}^{n}\binom{n}{p}[(\cos\chi)^{1+p}(-\sin\chi)^{n-p}\sqrt{p!}\sqrt{(n-p+1)!}\,|p,n-p+1\rangle \\
&+ (\cos\chi)^p(-\sin\chi)^{n-p+1}\sqrt{(1+p)!}\sqrt{(n-p)!}\,|1+p,n-p\rangle] \\
=& \sum_{p=0}^{n}\left[\frac{1}{\sqrt{n!}}\binom{n}{p}\sqrt{p!}\sqrt{(n-p+1)!}\,(\cos\chi)^{1+p}(-\sin\chi)^{n-p}\,|p,n-p+1\rangle\right. \\
&\left.+ \frac{1}{\sqrt{n!}}\binom{n}{p}\sqrt{(1+p)!}\sqrt{(n-p)!}\,(\cos\chi)^p(-\sin\chi)^{n-p+1}\,|1+p,n-p\rangle\right] \\
=& \sum_{p=0}^{n}\left[\sqrt{\binom{n}{p}}\sqrt{(n-p+1)}\,(\cos\chi)^{1+p}(-\sin\chi)^{n-p}\,|p,n-p+1\rangle\right. \\
&\left.+ \sqrt{\binom{n}{p}}\sqrt{(1+p)}\,(\cos\chi)^p(-\sin\chi)^{n-p+1}\,|1+p,n-p\rangle\right].
\end{aligned} \tag{A15}$$

Therefore, substituting Eq. (A15) into Eq. (A7), we obtain

$$\begin{aligned}
\frac{(A_{1k})_{mn}}{\sqrt{1-p}} \overset{\text{def}}{=} \langle m,k|U|n,1\rangle =& \sum_{p=0}^{n}\left[\sqrt{\binom{n}{p}}\sqrt{(n-p+1)}\,(\cos\chi)^{1+p}(-\sin\chi)^{n-p}\,\langle m,k|p,n-p+1\rangle\right. \\
&\left.+ \sqrt{\binom{n}{p}}\sqrt{(1+p)}\,(\cos\chi)^p(-\sin\chi)^{n-p+1}\,\langle m,k|1+p,n-p\rangle\right]
\end{aligned}$$

$$
\begin{aligned}
&= \sum_{p=0}^{n} \left[\sqrt{\binom{n}{p}} \sqrt{(n-p+1)}\, (\cos\chi)^{1+p}\, (-\sin\chi)^{n-p}\, \delta_{m,p}\delta_{k,n-p+1} \right. \\
&\left. + \sqrt{\binom{n}{p}} \sqrt{(1+p)}\, (\cos\chi)^{p}\, (-\sin\chi)^{n-p+1}\, \delta_{m,1+p}\delta_{k,n-p} \right] \\
&= \left[\sqrt{\binom{n}{n-k+1}} \sqrt{k}\, (\cos\chi)^{n-k+2}\, (-\sin\chi)^{k-1}\, \delta_{m,n-k+1} + \sqrt{\binom{n}{n-k}} \sqrt{n-k+1}\, (\cos\chi)^{n-k}\, (-\sin\chi)^{1+k}\, \delta_{m,n-k+1} \right].
\end{aligned} \tag{A16}
$$

Using Eq. (A16), the Kraus operators A_{1k} in Eq. (A6) become

$$
\begin{aligned}
A_{1k} = \sum_{m,n} (A_{1k})_{mn}\, |m\rangle\langle n| = \sqrt{1-p} \left[\sqrt{\binom{n}{n-k+1}} \sqrt{k}\, (\cos\chi)^{n-k+2}\, (-\sin\chi)^{k-1}\, |n-k+1\rangle\langle n| \right. \\
\left. + \sqrt{\binom{n}{n-k}} \sqrt{n-k+1}\, (\cos\chi)^{n-k}\, (-\sin\chi)^{1+k}\, |n-k+1\rangle\langle n| \right].
\end{aligned} \tag{A17}
$$

Therefore, the error operators A_{11} and A_{10} read

$$
\begin{aligned}
A_{11} &= \sqrt{1-p} \sum_{n=0}^{1} \left[\sqrt{\binom{n}{n}}\, (\cos\chi)^{1+n} + \sqrt{\binom{n}{n}} \sqrt{n}\, (\cos\chi)^{n-1}\, (-\sin\chi)^{2} \right] |n\rangle\langle n| \\
&= \sqrt{1-p} \{ (\cos\chi)|0\rangle\langle 0| + [(\cos\chi)^2 + (-\sin\chi)^2] |1\rangle\langle 1| \} = \sqrt{1-p}\, [|1\rangle\langle 1| + (\cos\chi)\, |0\rangle\langle 0|] = \sqrt{1-p} \begin{pmatrix} \sqrt{1-\gamma} & 0 \\ 0 & 1 \end{pmatrix},
\end{aligned} \tag{A18}
$$

where $\gamma \overset{\text{def}}{=} \sin^2\chi \equiv 1 - \cos^2\chi$ and

$$
A_{10} = \sqrt{1-p}(-\sin\chi)|1\rangle\langle 0| = \sqrt{1-p} \begin{pmatrix} 0 & 0 \\ \sqrt{\gamma} & 0 \end{pmatrix}, \tag{A19}
$$

respectively. Following the same line of reasoning employed for computing A_{11} and A_{10} and noticing that

$$
\begin{aligned}
U|00\rangle &= \left[I + \chi(a^\dagger b - b^\dagger a) + \frac{\chi^2}{2!}(a^\dagger b - b^\dagger a)^2 + \cdots \right] |00\rangle \\
&= |00\rangle,
\end{aligned} \tag{A20}
$$

we can also compute the Kraus errors A_{0k}, where

$$
A_{0k} \overset{\text{def}}{=} \sum_{m,n} (A_{0k})_{mn} |m\rangle\langle n|, \tag{A21}
$$

and the coefficients $(A_{0k})_{mn}$ read

$$
(A_{0k})_{mn} \overset{\text{def}}{=} \sqrt{p}\langle m,k|U|n,0\rangle = \sqrt{p}\, (\langle m,k|)\, (U\,|n,0\rangle). \tag{A22}
$$

It turns out that the errors A_{00} and A_{01} become

$$
A_{00} \overset{\text{def}}{=} \sqrt{p}[|0\rangle\langle 0| + \sqrt{1-\gamma}|1\rangle\langle 1|] = \sqrt{p} \begin{pmatrix} 1 & 0 \\ 0 & \sqrt{1-\gamma} \end{pmatrix} \tag{A23}
$$

and

$$
A_{01} \overset{\text{def}}{=} \sqrt{p}\langle 1|U|0\rangle = \sqrt{p}[\sqrt{\gamma}|0\rangle\langle 1|] = \sqrt{p} \begin{pmatrix} 0 & \sqrt{\gamma} \\ 0 & 0 \end{pmatrix}, \tag{A24}
$$

respectively. In conclusion, the GAD channel Λ_{GAD} is given by

$$
\Lambda_{\text{GAD}}(\rho) \overset{\text{def}}{=} A_{00}\rho A_{00}^\dagger + A_{01}\rho A_{10}^\dagger + A_{10}\rho A_{10}^\dagger + A_{11}\rho A_{11}^\dagger, \tag{A25}
$$

where

$$
\begin{aligned}
A_{00} &\overset{\text{def}}{=} \sqrt{p}\, \langle 0\,|U|\,0\rangle = \sqrt{p}[|0\rangle\langle 0| + \sqrt{1-\gamma}|1\rangle\langle 1|] \\
&= \sqrt{p} \begin{pmatrix} 1 & 0 \\ 0 & \sqrt{1-\gamma} \end{pmatrix}, \\
A_{01} &\overset{\text{def}}{=} \sqrt{p}\langle 1|U|0\rangle = \sqrt{p}[\sqrt{\gamma}|0\rangle\langle 1|] = \sqrt{p} \begin{pmatrix} 0 & \sqrt{\gamma} \\ 0 & 0 \end{pmatrix}, \\
A_{10} &\overset{\text{def}}{=} \sqrt{1-p}\langle 0|U|1\rangle = \sqrt{1-p}[\sqrt{\gamma}|1\rangle\langle 0|] \\
&= \sqrt{1-p} \begin{pmatrix} 0 & 0 \\ \sqrt{\gamma} & 0 \end{pmatrix}, \\
A_{11} &\overset{\text{def}}{=} \sqrt{1-p}\langle 1|U|1\rangle = \sqrt{1-p}[\sqrt{1-\gamma}|0\rangle\langle 0| + |1\rangle\langle 1|] \\
&= \sqrt{1-p} \begin{pmatrix} \sqrt{1-\gamma} & 0 \\ 0 & 1 \end{pmatrix}.
\end{aligned} \tag{A26}
$$

Finally, provided that we relabel $A_0 \overset{\text{def}}{=} A_{00}$, $A_1 \overset{\text{def}}{=} A_{01}$, $A_2 \overset{\text{def}}{=} A_{11}$, $A_3 \overset{\text{def}}{=} A_{10}$, the Kraus operators in Eq. (8) are obtained.

For the sake of completeness, we also observe that the analysis provided for this model is formally equivalent to that for the model employed in the main text. For instance, the Hamiltonian of the beam splitter, $H_{\text{int}}^{(\text{bs})} \overset{\text{def}}{=} i\chi(ab^\dagger - a^\dagger b)$, should be replaced by the interaction Hamiltonian between

the two-level atom and the bath of harmonic oscillators, $H_{\text{int}}^{(\text{atom-HO})} \stackrel{\text{def}}{=} g(a^\dagger\sigma_- + a\sigma_+)$. In the definition of $H_{\text{int}}^{(\text{atom-HO})}$, the Pauli raising ($\sigma_+$) and lowering ($\sigma_-$) operators act on the two-level atom. The creation ($a^\dagger$) and annihilation (a) operators are associated with the harmonic oscillator instead. Finally, g is the coupling constant for the interaction between the atom and the oscillator.

APPENDIX B: QUBIT ENTANGLEMENT BREAKING AND THE GAD CHANNEL

A quantum channel Λ is called entanglement breaking if $(\Lambda \otimes I)(\rho)$ is always separable, i.e., any entangled density matrix ρ is mapped to a separable one [59]. In order to check if a channel is entanglement breaking, it is sufficient to look at the separability of the output state corresponding just to an input maximally entangled state. In other words, Λ is entanglement breaking if and only if $(\Lambda \otimes I)(|\beta\rangle\langle\beta|)$ is separable for $|\beta\rangle$ defined as

$$|\beta\rangle \stackrel{\text{def}}{=} \frac{1}{\sqrt{d}}\sum_{j=0}^{d-1} |j\rangle \otimes |j\rangle\,, \tag{B1}$$

d being the dimension of the Hilbert space. A simple way to check the separability of density matrices is by means of the Peres-Horodecki positive partial transpose (PPT) criterion [60,61], which provides a necessary and sufficient condition for the joint density matrix ρ of two $d = 2$-dimensional systems A and B to be separable. Alternatively, the entanglement of a mixed state ρ described by a probabilistic mixture of an ensemble of pure states of quantum systems of dimension 2×2 can be quantified by means of the so-called concurrence [62]. For systems with this dimensionality, the concurrence $\mathcal{C}(\rho)$ of ρ reads

$$\mathcal{C}(\rho) \stackrel{\text{def}}{=} \max\{0, \sqrt{\lambda_1} - \sqrt{\lambda_2} - \sqrt{\lambda_3} - \sqrt{\lambda_4}\}, \tag{B2}$$

where λ_i are the non-negative *real* eigenvalues of the non-Hermitian matrix $\rho\tilde{\rho} \stackrel{\text{def}}{=} \rho(\sigma_y \otimes \sigma_y)\rho^*(\sigma_y \otimes \sigma_y)$, where $\tilde{\rho}$ is the spin-flipped state, λ_1 is the largest eigenvalue, and the complex conjugation is taken with respect to the product basis of eigenvectors of σ_z given by $\{|\uparrow\uparrow\rangle, |\uparrow\downarrow\rangle, |\downarrow\uparrow\rangle, |\downarrow\downarrow\rangle\}$.

For the GAD channel, it can be shown that the concurrence of $\rho \stackrel{\text{def}}{=} (\Lambda_{\text{GAD}} \otimes I)(|\beta\rangle\langle\beta|)$ with $|\beta\rangle \stackrel{\text{def}}{=} \frac{|00\rangle+|11\rangle}{\sqrt{2}}$ reads

$$\mathcal{C}_{\text{GAD}}(\gamma, p) \stackrel{\text{def}}{=} \frac{1}{2}\begin{bmatrix} \sqrt{\left[(2(1-\gamma) + p\gamma^2(1-p)) + 2\sqrt{(1-\gamma)((1-\gamma) + p\gamma^2(1-p))}\right]} \\ -\sqrt{\left[(2(1-\gamma) + p\gamma^2(1-p)) - 2\sqrt{(1-\gamma)((1-\gamma) + p\gamma^2(1-p))}\right]} \\ -2\sqrt{p(1-p)\gamma^2} \end{bmatrix}. \tag{B3}$$

Furthermore, the eigenvalues of the partial transpose of ρ are given by

$$\lambda_1(\gamma, p) = \frac{1}{2}\gamma p + \frac{1}{2}(1-\gamma), \quad \lambda_2(\gamma, p) = \frac{1}{2}(1 - p\gamma),$$

$$\lambda_3(\gamma, p) = \frac{1}{4}\gamma - \frac{1}{2}\sqrt{\frac{1}{4}\gamma^2 - \gamma - p\gamma^2 + p^2\gamma^2 + 1}, \tag{B4}$$

$$\lambda_4(\gamma, p) = \frac{1}{4}\gamma + \frac{1}{2}\sqrt{\frac{1}{4}\gamma^2 - \gamma - p\gamma^2 + p^2\gamma^2 + 1}.$$

The eigenvalues λ_1, λ_2, and λ_4 are positive. The eigenvalue λ_3 is positive provided that

$$p^2\gamma^2 - p\gamma^2 + 1 - \gamma \leqslant 0. \tag{B5}$$

The inequality in Eq. (B5) is fulfilled in the two-dimensional parametric region $(\gamma, p(\gamma))$, where $p_{\min}(\gamma) \leqslant p(\gamma) \leqslant p_{\max}(\gamma)$, with

$$p_{\min}(\gamma) \stackrel{\text{def}}{=} \frac{1}{\gamma^2}\left(\frac{1}{2}\gamma^2 - \frac{1}{2}\sqrt{\gamma^4 + 4\gamma^3 - 4\gamma^2}\right) \quad \text{and}$$

$$p_{\max}(\gamma) \stackrel{\text{def}}{=} \frac{1}{\gamma^2}\left(\frac{1}{2}\gamma^2 + \frac{1}{2}\sqrt{\gamma^4 + 4\gamma^3 - 4\gamma^2}\right). \tag{B6}$$

It turns out that for pairs $(\gamma, p(\gamma))$ within this two-dimensional parametric region, $\mathcal{C}_{\text{GAD}}(\gamma, p)$ equals zero and the GAD channel becomes entanglement breaking.

APPENDIX C: EXPLICIT CONSTRUCTION OF AN ORTHONORMAL BASIS

In general, we can proceed as follows. The rank-nullity theorem allows us, with an algorithmic procedure for enlarging a set of m linearly independent vectors in $\mathbb{C}^n$ with $m \leqslant n$, to obtain a set of n linearly independent vectors in $\mathbb{C}^n$ [63]. The Gram-Schmidt orthonormalization procedure, instead, can be used to construct an orthonormal basis from this set of n linearly independent vectors.

The rank-nullity theorem states that, given a $(m \times n)$ matrix A, it turns out that $n = \text{rank}(A) + \text{nullity}(A)$. The nullity of a $(m \times n)$ matrix A representing a linear map $\hat{A} : \mathbb{C}^n \to \mathbb{C}^m$ is the dimension of its null space (or *kernel*),

$$\ker A \stackrel{\text{def}}{=} \{\vec{x} \in \mathbb{C}^n : A\vec{x} = \vec{0}\}. \tag{C1}$$

The rank of a matrix is the maximum number of linearly independent columns (or rows).

Let us suppose we wish to construct an orthonormal basis $\{|e_k\rangle\}$ with $k = 1, \ldots, 32$ for the 32-dimensional *complex* Hilbert space $\mathcal{H}_2^5$. The first two orthonormal basis vectors can be constructed from the action of the weight-0 error operators

A_{00000} on the codewords $|0_L\rangle$ and $|1_L\rangle$. They read

$$|e_1\rangle \stackrel{\text{def}}{=} N_1(\gamma)\,[-|00000\rangle + (1-\gamma)^2\,|01111\rangle - (1-\gamma)^{\frac{3}{2}}\,|10011\rangle + (1-\gamma)^{\frac{3}{2}}\,|11100\rangle + (1-\gamma)\,|00110\rangle + (1-\gamma)\,|01001\rangle + (1-\gamma)^{\frac{3}{2}}\,|10101\rangle + (1-\gamma)^{\frac{3}{2}}\,|11010\rangle] \tag{C2}$$

and

$$|e_2\rangle \stackrel{\text{def}}{=} N_2(\gamma)\,[-(1-\gamma)^{\frac{5}{2}}\,|11111\rangle + \sqrt{1-\gamma}\,|10000\rangle + (1-\gamma)\,|01100\rangle - (1-\gamma)\,|00011\rangle + (1-\gamma)^{\frac{3}{2}}\,|11001\rangle + (1-\gamma)^{\frac{3}{2}}\,|10110\rangle - (1-\gamma)\,|01010\rangle - (1-\gamma)\,|00101\rangle], \tag{C3}$$

respectively. The normalization factors $N_1(\gamma)$ and $N_2(\gamma)$ are given by

$$N_1(\gamma) \stackrel{\text{def}}{=} \frac{1}{\sqrt{1+(1-\gamma)^4+4(1-\gamma)^3+2(1-\gamma)^2}} \quad \text{and} \quad N_2(\gamma) \stackrel{\text{def}}{=} \frac{1}{\sqrt{(1-\gamma)^5+2(1-\gamma)^3+4(1-\gamma)^2+(1-\gamma)}}. \tag{C4}$$

The next ten orthonormal vectors can be constructed by taking into consideration the action of the five weight-1 error operators A_{10000}, A_{01000}, A_{00100}, A_{00010}, A_{00001} on the codewords. The action of A_{10000} on the codewords $|0_L\rangle$ and $|1_L\rangle$ leads to

$$|e_3\rangle \stackrel{\text{def}}{=} \frac{-|00011\rangle + |01100\rangle + |00101\rangle + |01010\rangle}{\sqrt{4}} \tag{C5}$$

and

$$|e_4\rangle \stackrel{\text{def}}{=} \frac{-(1-\gamma)^2\,|01111\rangle + |00000\rangle + (1-\gamma)\,|01001\rangle + (1-\gamma)\,|00110\rangle}{\sqrt{1+(1-\gamma)^4+2(1-\gamma)^2}}, \tag{C6}$$

respectively. The action of A_{01000} on the codewords $|0_L\rangle$ and $|1_L\rangle$ yields

$$|e_5\rangle \stackrel{\text{def}}{=} \frac{(1-\gamma)^{\frac{3}{2}}\,|00111\rangle + (1-\gamma)\,|10100\rangle + \sqrt{1-\gamma}\,|00001\rangle + (1-\gamma)\,|10010\rangle}{\sqrt{(1-\gamma)^3+2(1-\gamma)^2+(1-\gamma)}} \tag{C7}$$

and

$$|e_6\rangle \stackrel{\text{def}}{=} \frac{-(1-\gamma)^2\,|10111\rangle + \sqrt{1-\gamma}\,|00100\rangle + (1-\gamma)\,|10001\rangle - \sqrt{1-\gamma}\,|00010\rangle}{\sqrt{(1-\gamma)^4+(1-\gamma)^2+2(1-\gamma)}}, \tag{C8}$$

respectively. The action of A_{00100} on the codewords $|0_L\rangle$ and $|1_L\rangle$ leads to

$$|e_7\rangle \stackrel{\text{def}}{=} \frac{(1-\gamma)^{\frac{3}{2}}\,|01011\rangle + (1-\gamma)\,|11000\rangle + (1-\gamma)\,|10001\rangle + \sqrt{1-\gamma}\,|00010\rangle}{\sqrt{(1-\gamma)^3+2(1-\gamma)^2+(1-\gamma)}} \tag{C9}$$

and

$$|e_8\rangle \stackrel{\text{def}}{=} \frac{-(1-\gamma)^2\,|11011\rangle + \sqrt{1-\gamma}\,|01000\rangle + (1-\gamma)\,|10010\rangle - \sqrt{1-\gamma}\,|00001\rangle}{\sqrt{(1-\gamma)^4+(1-\gamma)^2+2(1-\gamma)}}, \tag{C10}$$

respectively. The action of A_{00010} on the codewords $|0_L\rangle$ and $|1_L\rangle$ yields

$$|e_9\rangle \stackrel{\text{def}}{=} \frac{(1-\gamma)^{\frac{3}{2}}\,|01101\rangle - (1-\gamma)\,|10001\rangle + \sqrt{1-\gamma}\,|00100\rangle + (1-\gamma)\,|11000\rangle}{\sqrt{(1-\gamma)^3+2(1-\gamma)^2+(1-\gamma)}} \tag{C11}$$

and

$$|e_{10}\rangle \stackrel{\text{def}}{=} \frac{-(1-\gamma)^2\,|11101\rangle - \sqrt{1-\gamma}\,|00001\rangle + (1-\gamma)\,|10100\rangle - \sqrt{1-\gamma}\,|01000\rangle}{\sqrt{(1-\gamma)^4+(1-\gamma)^2+2(1-\gamma)}}, \tag{C12}$$

respectively. Finally, the action of A_{00001} on the codewords $|0_L\rangle$ and $|1_L\rangle$ gives

$$|e_{11}\rangle \stackrel{\text{def}}{=} \frac{(1-\gamma)^{\frac{3}{2}}\,|01110\rangle - (1-\gamma)\,|10010\rangle + \sqrt{1-\gamma}\,|01000\rangle + (1-\gamma)\,|10100\rangle}{\sqrt{(1-\gamma)^3+2(1-\gamma)^2+(1-\gamma)}} \tag{C13}$$

and

$$|e_{12}\rangle \stackrel{\text{def}}{=} \frac{-(1-\gamma)^2\,|11110\rangle - \sqrt{1-\gamma}\,|00010\rangle + (1-\gamma)\,|11000\rangle - \sqrt{1-\gamma}\,|00100\rangle}{\sqrt{(1-\gamma)^4+(1-\gamma)^2+2(1-\gamma)}}, \tag{C14}$$

respectively. The next ten orthonormal vectors can be constructed by considering the action of the five weight-1 error operators A_{30000}, A_{03000}, A_{00300}, A_{00030}, A_{00003} on the codewords. The action of A_{30000} on the codewords $|0_L\rangle$ and $|1_L\rangle$ leads to

$$|e_{13}\rangle \stackrel{\text{def}}{=} \frac{-|10000\rangle + (1-\gamma)^2\,|11111\rangle + (1-\gamma)\,|10110\rangle + (1-\gamma)\,|11001\rangle}{\sqrt{1+(1-\gamma)^4+2\,(1-\gamma)^2}} \tag{C15}$$

and

$$|e_{14}\rangle \stackrel{\text{def}}{=} \frac{|11100\rangle - |10011\rangle - |11010\rangle - |10101\rangle}{\sqrt{4}}, \tag{C16}$$

respectively. The action of A_{03000} on the codewords $|0_L\rangle$ and $|1_L\rangle$ yields

$$|e_{15}\rangle \stackrel{\text{def}}{=} \frac{-|01000\rangle - (1-\gamma)^{\frac{3}{2}}\,|11011\rangle + (1-\gamma)\,|01110\rangle + (1-\gamma)^{\frac{3}{2}}\,|11101\rangle}{\sqrt{1+2\,(1-\gamma)^3+(1-\gamma)^2}} \tag{C17}$$

and

$$|e_{16}\rangle \stackrel{\text{def}}{=} \frac{\sqrt{1-\gamma}\,|11000\rangle - (1-\gamma)\,|01011\rangle + (1-\gamma)^{\frac{3}{2}}\,|11110\rangle - (1-\gamma)\,|01101\rangle}{\sqrt{(1-\gamma)^3+2\,(1-\gamma)^2+(1-\gamma)}}, \tag{C18}$$

respectively. The action of A_{00300} on the codewords $|0_L\rangle$ and $|1_L\rangle$ leads to

$$|e_{17}\rangle \stackrel{\text{def}}{=} \frac{-|00100\rangle - (1-\gamma)^{\frac{3}{2}}\,|10111\rangle + (1-\gamma)\,|01101\rangle + (1-\gamma)^{\frac{3}{2}}\,|11110\rangle}{\sqrt{1+2\,(1-\gamma)^3+(1-\gamma)^2}} \tag{C19}$$

and

$$|e_{18}\rangle \stackrel{\text{def}}{=} \frac{\sqrt{1-\gamma}\,|10100\rangle - (1-\gamma)\,|00111\rangle + (1-\gamma)^{\frac{3}{2}}\,|11101\rangle - (1-\gamma)\,|01110\rangle}{\sqrt{(1-\gamma)^3+2\,(1-\gamma)^2+(1-\gamma)}}, \tag{C20}$$

respectively. The action of A_{00030} on the codewords $|0_L\rangle$ and $|1_L\rangle$ yields

$$|e_{19}\rangle \stackrel{\text{def}}{=} \frac{-|00010\rangle + (1-\gamma)^{\frac{3}{2}}\,|11110\rangle + (1-\gamma)\,|01011\rangle + (1-\gamma)^{\frac{3}{2}}\,|10111\rangle}{\sqrt{1+2\,(1-\gamma)^3+(1-\gamma)^2}} \tag{C21}$$

and

$$|e_{20}\rangle \stackrel{\text{def}}{=} \frac{\sqrt{1-\gamma}\,|10010\rangle + (1-\gamma)\,|01110\rangle + (1-\gamma)^{\frac{3}{2}}\,|11011\rangle - (1-\gamma)\,|00111\rangle}{\sqrt{(1-\gamma)^3+2\,(1-\gamma)^2+(1-\gamma)}}, \tag{C22}$$

respectively. Finally, The action of A_{00003} on the codewords $|0_L\rangle$ and $|1_L\rangle$ leads to

$$|e_{21}\rangle \stackrel{\text{def}}{=} \frac{-|00001\rangle + (1-\gamma)^{\frac{3}{2}}\,|11101\rangle + (1-\gamma)\,|00111\rangle + (1-\gamma)^{\frac{3}{2}}\,|11011\rangle}{\sqrt{1+2\,(1-\gamma)^3+(1-\gamma)^2}} \tag{C23}$$

and

$$|e_{22}\rangle \stackrel{\text{def}}{=} \frac{\sqrt{1-\gamma}\,|10001\rangle + (1-\gamma)\,|01101\rangle + (1-\gamma)^{\frac{3}{2}}\,|10111\rangle - (1-\gamma)\,|01011\rangle}{\sqrt{(1-\gamma)^3+2\,(1-\gamma)^2+(1-\gamma)}}, \tag{C24}$$

respectively. We have 22 orthonormal vectors and we need 10 more. From Eqs. (C2) and (C3), it turns out that the following six linearly independent orthonormal vectors are orthogonal to both $|e_1\rangle$ and $|e_2\rangle$:

$$\begin{aligned} |e_{23}\rangle &\stackrel{\text{def}}{=} \frac{|10110\rangle - |11001\rangle}{\sqrt{2}}, \quad |e_{24}\rangle \stackrel{\text{def}}{=} \frac{|11100\rangle + |10011\rangle}{\sqrt{2}}, \quad |e_{25}\rangle \stackrel{\text{def}}{=} \frac{|11010\rangle - |10101\rangle}{\sqrt{2}}, \\ |e_{26}\rangle &\stackrel{\text{def}}{=} \frac{|00011\rangle + |01100\rangle}{\sqrt{2}}, \quad |e_{27}\rangle \stackrel{\text{def}}{=} \frac{|00101\rangle - |01010\rangle}{\sqrt{2}}, \quad |e_{28}\rangle \stackrel{\text{def}}{=} \frac{|01001\rangle - |00110\rangle}{\sqrt{2}}. \end{aligned} \tag{C25}$$

Indeed, it can be explicitly checked that $\langle e_k e_{k'}\rangle = \delta_{kk'}$ for any k and k' in $\{1,\ldots,28\}$. The last four vectors are uncovered as follows. First, we add four linearly independent vectors in such a manner to have a basis for $\mathcal{H}_2^5$ and then we apply the Gram-Schmidt orthonormalization procedure to obtain an orthogonal basis. It finally turns out that the remaining four vectors

needed are given by

$$|e_{29}\rangle \stackrel{\text{def}}{=} \frac{|11000\rangle - (1-\gamma)|e_7\rangle - (1-\gamma)|e_9\rangle - (1-\gamma)|e_{12}\rangle - \sqrt{1-\gamma}\,|e_{16}\rangle}{\sqrt{1-3(1-\gamma)^2-(1-\gamma)}},$$
$$|e_{30}\rangle \stackrel{\text{def}}{=} \frac{|10100\rangle - (1-\gamma)|e_5\rangle - (1-\gamma)|e_{10}\rangle - (1-\gamma)|e_{11}\rangle - \sqrt{1-\gamma}\,|e_{18}\rangle}{\sqrt{1-3(1-\gamma)^2-(1-\gamma)}},$$
$$|e_{31}\rangle \stackrel{\text{def}}{=} \frac{|10010\rangle - (1-\gamma)|e_5\rangle - (1-\gamma)|e_8\rangle + (1-\gamma)|e_{11}\rangle - \sqrt{1-\gamma}\,|e_{20}\rangle}{\sqrt{1-3(1-\gamma)^2-(1-\gamma)}},$$
$$|e_{32}\rangle \stackrel{\text{def}}{=} \frac{|10001\rangle - (1-\gamma)|e_6\rangle - (1-\gamma)|e_7\rangle + (1-\gamma)|e_9\rangle - \sqrt{1-\gamma}\,|e_{22}\rangle}{\sqrt{1-3(1-\gamma)^2-(1-\gamma)}}. \tag{C26}$$

In conclusion, $\{|e_k\rangle\}$ with $k \in \{1,\ldots,32\}$ is a suitable orthonormal basis for $\mathcal{H}_2^5$.

APPENDIX D: ESTIMATING THE ENTANGLEMENT FIDELITY

The entanglement fidelity $\mathcal{F}(\gamma,\varepsilon)$ of a $((n,K,d))$ quantum code $\mathcal{C}$ for enlarged GAD errors A'_a with $a \in \{0,\ldots,2^{2n}-1\}$ and recovery operation $\mathcal{R} \stackrel{\text{def}}{=} \{R_1,\ldots,R_r,\ldots,R_s,R_{s+1} \stackrel{\text{def}}{=} \hat{O}\}$ reads

$$\mathcal{F}(\gamma,\varepsilon) \stackrel{\text{def}}{=} \frac{1}{K^2}\left[\sum_{a=0}^{2^{2n}-1}\sum_{r=1}^{s}|\mathrm{Tr}(R_r A'_a)_{\mathcal{C}}|^2 + \sum_{a=0}^{2^{2n}-1}|\mathrm{Tr}(\hat{O}A'_a)_{\mathcal{C}}|^2\right], \tag{D1}$$

where the recovery operator $\hat{O}$ is defined as

$$\hat{O} \stackrel{\text{def}}{=} \sum_{b=1}^{2^n-2s}|o_b\rangle\langle o_b|. \tag{D2}$$

The $2s$ orthonormal vectors employed to construct the recovery operators R_r in $\mathcal{R}\backslash\{\hat{O}\}$ together with the 2^n-2s orthonormal vectors used to define the recovery operator $\hat{O}$ form a orthonormal basis of the complex Hilbert space $\mathcal{H}_2^{2n}$. We observe that the entanglement fidelity $\mathcal{F}(\gamma,\varepsilon)$ in Eq. (D1) can be regarded as the sum of two contributions,

$$\mathcal{F}(\gamma,\varepsilon) \stackrel{\text{def}}{=} \mathcal{F}_{\mathcal{R}\backslash\{\hat{O}\}}(\gamma,\varepsilon) + \mathcal{F}_{\hat{O}}(\gamma,\varepsilon), \tag{D3}$$

where

$$\mathcal{F}_{\mathcal{R}\backslash\{\hat{O}\}}(\gamma,\varepsilon) \stackrel{\text{def}}{=} \frac{1}{K^2}\sum_{a=0}^{2^{2n}-1}\sum_{r=1}^{s}|\mathrm{Tr}(R_r A'_a)_{\mathcal{C}}|^2 \quad \text{and}$$
$$\mathcal{F}_{\hat{O}}(\gamma,\varepsilon) \stackrel{\text{def}}{=} \frac{1}{K^2}\sum_{a=0}^{2^{2n}-1}|\mathrm{Tr}(\hat{O}A'_a)_{\mathcal{C}}|^2. \tag{D4}$$

In what follows, we describe our reasoning for the analytic estimates of entanglement fidelities.

1. Part A

Let us first consider $\mathcal{F}_{\mathcal{R}\backslash\{\hat{O}\}}(\gamma,\varepsilon)$ in Eq. (D4). Recall that for $r \in \{1,\ldots,s\}$, the recovery operators R_r read

$$R_r \stackrel{\text{def}}{=} \sum_{j=0}^{K-1}\frac{|j_L\rangle\langle j_L|A_r'^{\dagger}}{\sqrt{\langle j_L|A_r'^{\dagger}A'_r|j_L\rangle}}. \tag{D5}$$

Using Eq. (D5), $\mathcal{F}_{\mathcal{R}\backslash\{\hat{O}\}}(\gamma,\varepsilon)$ becomes

$$\mathcal{F}_{\mathcal{R}\backslash\{\hat{O}\}}(\gamma,\varepsilon) \stackrel{\text{def}}{=} \frac{1}{K^2}\sum_{a=0}^{2^{2n}-1}\sum_{r=1}^{s}\left|\sum_{i=0}^{K-1}\frac{\langle i_L|A_r'^{\dagger}A'_a|i_L\rangle}{\sqrt{\langle i_L|A_r'^{\dagger}A'_r|i_L\rangle}}\right|^2. \tag{D6}$$

Let us denote with $\mathcal{K}$ the index set of all the enlarged GAD error operators. This set has cardinality 2^{2n} and can be decomposed in two parts,

$$\mathcal{K} \stackrel{\text{def}}{=} \mathcal{K}_{\mathcal{R}\backslash\{\hat{O}\}} \oplus \mathcal{K}'. \tag{D7}$$

The set $\mathcal{K}_{\mathcal{R}\backslash\{\hat{O}\}}$ is the index set of all the enlarged GAD errors $\{A'_a\}$ recovered by means of the recovery operators $\{R_r\}$ in $\mathcal{R}\backslash\{\hat{O}\}$ and it has cardinality s. The cardinality of the index set $\mathcal{K}'$ is $2^{2n}-s$ and denotes the number of all the remaining potentially contributing enlarged error operators. Since we only aim at finding estimates of $\mathcal{F}(\gamma,\varepsilon)$ with $\mathcal{F}(\gamma,\varepsilon) \gtrsim 1-O(2)$ and assuming as working hypothesis $0 \leqslant \varepsilon \ll \gamma \ll 1$, we only need to consider a subset of $\mathcal{K}'$ for the estimation of $\mathcal{F}_{\mathcal{R}\backslash\{\hat{O}\}}(\gamma,\varepsilon)$. In the worst scenario, we have to consider the subset $\mathcal{K}_{\text{weight-2}} \subset \mathcal{K}'$ of cardinality $3^2\binom{n}{2}$ of all the weight-2 enlarged GAD errors and

$$\mathcal{F}_{\mathcal{R}\backslash\{\hat{O}\}}(\gamma,\varepsilon) \approx \frac{1}{K^2}\sum_{a\in\mathcal{K}''}\sum_{r=1}^{s}\left|\sum_{i=0}^{K-1}\frac{\langle i_L|A_r'^{\dagger}A'_a|i_L\rangle}{\sqrt{\langle i_L|A_r'^{\dagger}A'_r|i_L\rangle}}\right|^2, \tag{D8}$$

with $\mathcal{K}'' \stackrel{\text{def}}{=} \mathcal{K}_{\mathcal{R}\backslash\{\hat{O}\}} \cup \mathcal{K}_{\text{weight-2}}$. In addition, among these $3^2\binom{n}{2}$ errors, some of them are more likely to occur than others. Denote with $[ik]$ the set of cardinality $\binom{n}{2}$ with weight-2 enlarged error operators acting on n-qubit quantum states defined by means of single-qubit errors of type A_i and A_k,

$$[ik] \stackrel{\text{def}}{=} \{A_{ik0\cdots0}, A_{i0k0\cdots0}, \ldots, A_{00\cdots0ik}\}. \tag{D9}$$

It turns out that the probabilities of occurrence $\Pr([ik]) \stackrel{\text{def}}{=} \Pr_{ik}(\gamma,\varepsilon)$ of errors in the set $[ik]$ scale in terms of the perturbation parameters γ and ε as follows:

$$\begin{pmatrix}\Pr_{11} & \Pr_{12} & \Pr_{13}\\ \Pr_{21} & \Pr_{22} & \Pr_{23}\\ \Pr_{31} & \Pr_{32} & \Pr_{33}\end{pmatrix} \approx \begin{pmatrix}\gamma^2 & \varepsilon\gamma & \varepsilon\gamma^2\\ \varepsilon\gamma & \varepsilon^2 & \varepsilon^2\gamma\\ \varepsilon\gamma^2 & \varepsilon^2\gamma & \varepsilon^2\gamma^2\end{pmatrix}. \tag{D10}$$

Therefore, in addition, to limit our attention to these $3^2\binom{n}{2}$ weight-2 errors in $\mathcal{K}_{\text{weight-2}}$, we also rank the relevance of each of these nine possible subsets $[ik]$ of cardinality $\binom{n}{2}$ according to the γ and ε dependencies of the probabilities of occurrence of their errors.

2. Part B

Let us now take into consideration $\mathcal{F}_{\hat{O}}(\gamma,\varepsilon)$ in Eq. (D4). We notice that

$$\begin{aligned}\mathcal{F}_{\hat{O}}(\gamma,\varepsilon) &\stackrel{\text{def}}{=} \frac{1}{K^2}\sum_{a=0}^{2^{2n}-1}|\text{Tr}(\hat{O}A'_a)_{\mathcal{C}}|^2 \\ &= \frac{1}{K^2}\sum_{a=0}^{2^{2n}-1}\left|\sum_{i=0}^{K-1}\langle i_L|\hat{O}A'_a|i_L\rangle\right|^2 \\ &\leqslant \frac{2^{2n}}{K}|\langle\bar{\imath}_L|\hat{O}A'_{\bar{a}}|\bar{\imath}_L\rangle|^2, \end{aligned} \tag{D11}$$

with

$$\langle\bar{\imath}_L|\hat{O}A'_{\bar{a}}|\bar{\imath}_L\rangle \stackrel{\text{def}}{=} \max_{i,a}\{\langle i_L|\hat{O}A'_a|i_L\rangle\}. \tag{D12}$$

If the index $\bar{a}$ labels an enlarged GAD error recovered by a recovery operation R_r in $\mathcal{R}\backslash\{\hat{O}\}$, then $\mathcal{F}_{\hat{O}}(\gamma,\varepsilon)$ is identically zero by construction. Therefore, let us assume that $\bar{a}$ is not such an index. Using Eq. (D2), $\langle\bar{\imath}_L|\hat{O}A'_{\bar{a}}|\bar{\imath}_L\rangle$ becomes

$$\langle\bar{\imath}_L|\hat{O}A'_{\bar{a}}|\bar{\imath}_L\rangle = \sum_{b=1}^{2^n-2s}\langle\bar{\imath}_L|o_b\rangle\langle o_b|A'_{\bar{a}}|\bar{\imath}_L\rangle. \tag{D13}$$

We observe that $\langle\bar{\imath}_L|o_b\rangle$ would be identically zero for any $b\in\{1,\ldots,2^n-2s\}$ if the enlarged identity error operator belonged to the error model. Unfortunately, this is not our case. Nevertheless, it turns out that

$$\langle\bar{\imath}_L|o_b\rangle \approx \gamma\langle\bar{\imath}_L|T'|o_b\rangle, \tag{D14}$$

where the operator T' acting on n-qubit quantum states is defined as

$$\begin{aligned}T' \stackrel{\text{def}}{=}& T^1\otimes I^2\otimes\cdots\otimes I^{n-1}\otimes I^n \\ &+ I^1\otimes T^2\otimes\cdots\otimes I^{n-1}\otimes I^n \\ &+ I^1\otimes I^2\otimes\cdots\otimes I^{n-1}\otimes T^n, \end{aligned} \tag{D15}$$

with

$$T^k \stackrel{\text{def}}{=} \tfrac{1}{4}\left(I^k-\sigma_z^k\right). \tag{D16}$$

Substituting Eq. (D14) into Eq. (D13), we get

$$\langle\bar{\imath}_L|\hat{O}A'_{\bar{a}}|\bar{\imath}_L\rangle \approx \gamma\sum_{b=1}^{2^n-2s}\langle\bar{\imath}_L|T'|o_b\rangle\langle o_b|A'_{\bar{a}}|\bar{\imath}_L\rangle. \tag{D17}$$

We remark that both $|\bar{\imath}_L\rangle$ and T' are γ-independent quantities while the states $|o_b\rangle$ are the sum-decomposition of n-qubit quantum states where γ-dependent expansion coefficients may appear. However, as we have noticed from our explicit construction in the previous Appendix, these coefficients do not exhibit nontrivial γ dependence in the limit of γ approaching zero. Therefore, terms like $\langle\bar{\imath}_L|T'|o_b\rangle$ do not possess relevant scaling laws in the damping probability parameter γ approaching zero. On the contrary, terms like $\langle o_b|A'_{\bar{a}}|\bar{\imath}_L\rangle$ do exhibit important γ-scaling laws,

$$\langle o_b|A'_{\bar{a}}|\bar{\imath}_L\rangle \approx \gamma^{\frac{\text{wt}(A'_{\bar{a}})}{2}}\langle o_b|\tilde{A}'_{\bar{a}}|\bar{\imath}_L\rangle, \tag{D18}$$

where $\text{wt}(A'_{\bar{a}})$ denotes the weight of the operator $A'_{\bar{a}}$ and $\langle o_b|\tilde{A}'_{\bar{a}}|\bar{\imath}_L\rangle$ is redefined in such a manner to have no relevant γ dependence. Substituting Eqs. (D17) and (D18) into Eq. (D11), we finally obtain

$$\mathcal{F}_{\hat{O}}(\gamma,\varepsilon) \lesssim \frac{2^{2n}}{K}\gamma^{2+\text{wt}(A'_{\bar{a}})}\left|\sum_{b=1}^{2^n-2s}\langle\bar{\imath}_L|T'|o_b\rangle\langle o_b|\tilde{A}'_{\bar{a}}|\bar{\imath}_L\rangle\right|^2. \tag{D19}$$

From Eq. (D19), we conclude that while $\mathcal{F}_{\hat{O}}(\gamma,\varepsilon)$ could be, in principle, nonvanishing and contribute to the computation of the entanglement fidelity $\mathcal{F}(\gamma,\varepsilon)$, its contribution is negligible given the order of approximations chosen for our analytic estimates.

In what follows, we report a more explicit example. For the sake of reasoning, consider the CSS seven-qubit code and AD errors. Does any weight-2 enlarged error operator contribute to the computation of the entanglement fidelity? In general, errors A_l for which no corresponding recovery operator R_{A_l} is constructed can contribute to the computation of the entanglement fidelity via the expression given by

$$\begin{aligned}\mathcal{F}_{\hat{O}}^{[[7,1,3]]}(\gamma) \stackrel{\text{def}}{=}& \frac{1}{4}\sum_{l,k}[\langle 0_L|v_k\rangle\langle v_k|A_l|0_L\rangle \\ &+\langle 1_L|v_k\rangle\langle v_k|A_l|1_L\rangle]^2, \end{aligned} \tag{D20}$$

where the operator $\hat{O}$ reads

$$\hat{O} \stackrel{\text{def}}{=} \sum_k |v_k\rangle\langle v_k|. \tag{D21}$$

We notice that state vectors $\{|v_k\rangle\}$ in Eq. (D20) lead to nonvanishing contributions provided that (i) $|v_k\rangle$ has some nonzero component along $|0_L\rangle$ and/or $|1_L\rangle$; (ii) $|v_k\rangle$ has some nonzero component along $A_l|0_L\rangle$ and/or $A_l|1_L\rangle$; (iii) $\{|v_k\rangle, A_l^{\text{correctable}}|i_L\rangle\}$ forms an orthonormal basis of $\mathcal{H}_2^7$.

Before proceeding along this line of reasoning, we would like to emphasize that we could have proceeded along a alternative route. Observe that $D \stackrel{\text{def}}{=} \dim_{\mathbb{C}}\mathcal{H}_2^7 = 2^7 = 128$. Furthermore, the cardinality c' of the set S' of linearly independent and orthogonal vectors in the sum decomposition of the correctable weight-0 and weight-1 enlarged errors is given by

$$c' \stackrel{\text{def}}{=} 2\times\binom{7}{0}\times 8 + 2\times\binom{7}{1}\times 4 = 72. \tag{D22}$$

Therefore, there also exists a new set S'' that consists of $c'' \stackrel{\text{def}}{=} D-c' = 56$ linearly independent and orthogonal vectors such that vectors in S' and S'' form an orthonormal basis of $\mathcal{H}_2^7$. If any of these 56 vectors is in the vector sum-decomposition of any of the $\binom{7}{2}=21$ weight-2 errors, then some weight-2 error could contribute to the entanglement fidelity provided that the selected vector in S'' has some nonzero component along $|0_L\rangle$ and/or $|1_L\rangle$ [see Eq. (D20)]. We checked that all

the $2 \times \binom{7}{2} \times 2 = 84$ state vectors in the sum decomposition of $A_l |i_L\rangle$ with A_l any weight-2 error operator are orthogonal to $|i_L\rangle$ with $i \in \{0,1\}$. Therefore, we cannot take this shortcut and are forced to proceed in a more general manner. As a consequence, constructing these vectors $|v_k\rangle$ is going to be more involved, since we wish to provide a constructive explanation avoiding numerics that could obscure the construction itself.

Let us then return to the more general approach. For the sake of clarity, fucus on the possible partial recovery of the weight-2 error $A_{1100000}$. This error is not correctable because it is incompatible with the weight-1 error $A_{0010000}$. Having observed this and recalling the three conditions for good state vectors $\{|v_k\rangle\}$, it turns out that a suitable vector $|v_{\bar{k}}\rangle$ in the definition of $\hat{O}$ so that $|v_{\bar{k}}\rangle\langle v_{\bar{k}}|$ can partially recover $A_{1100000}$ reads

$$|v_{\bar{k}}\rangle \stackrel{\text{def}}{=} \frac{|0000110\rangle - |1100000\rangle + |0110011\rangle - (1-\gamma)^2 |0000000\rangle}{\sqrt{3+(1-\gamma)^4}}. \tag{D23}$$

This contribution of $A_{1100000}$ to the computation of the entanglement fidelity becomes

$$\mathcal{F}^{[[7,1,3]]}_{|v_{\bar{k}}\rangle\langle v_{\bar{k}}|}(\gamma) \stackrel{\text{def}}{=} \frac{1}{4}\left(\langle 0_L|v_{\bar{k}}\rangle\langle v_{\bar{k}}|A_{1100000}|0_L\rangle\right)^2 = \frac{1}{32}\left[\frac{1-(1-\gamma)^2}{\sqrt{3+(1-\gamma)^4}} \times \frac{\gamma(1-\gamma)}{\sqrt{3+(1-\gamma)^4}}\right]^2 \approx \gamma^4. \tag{D24}$$

From Eq. (D24), we conclude that although $A_{1100000}$ contributes to the computation of the entanglement fidelity, its contribution is negligible given our chosen order of approximation. Analogously, for each weight-2 enlarged error operator, a similar line of reasoning can be carried out.

APPENDIX E: ON THE CSS SEVEN-QUBIT CODE

For $\varepsilon = 0$, the nontruncated expression for the entanglement fidelity reads

$$\begin{aligned}\mathcal{F}^{[[7,1,3]]}_{\text{nontruncated}}(\gamma) &\stackrel{\text{def}}{=} \frac{1}{4}\left[\sqrt{\frac{1+7(1-\gamma)^4}{8}} + \sqrt{\frac{(1-\gamma)^7+7(1-\gamma)^3}{8}}\right]^2 \\ &+ \frac{7}{4}\left[\sqrt{\frac{4\gamma(1-\gamma)^3}{8}} + \sqrt{\frac{\gamma(1-\gamma)^6+3\gamma(1-\gamma)^2}{8}}\right]^2.\end{aligned} \tag{E1}$$

The Taylor expansion of $\mathcal{F}^{[[7,1,3]]}(\gamma)$ up to the tenth order is given by

$$\begin{aligned}\mathcal{F}^{[[7,1,3]]}_{\text{nontruncated}}(\gamma) \approx 1 &- \tfrac{21}{4}\gamma^2 + \tfrac{35}{4}\gamma^3 - \tfrac{63}{8}\gamma^4 + \tfrac{609}{128}\gamma^5 - \tfrac{315}{256}\gamma^6 \\ &- \tfrac{51}{256}\gamma^7 - \tfrac{63}{256}\gamma^8 + \tfrac{1701}{8192}\gamma^9 + O(\gamma^{10}),\end{aligned} \tag{E2}$$

while the 1-qubit baseline performance is given by

$$\mathcal{F}^{\text{1-qubit}}_{\text{baseline}}(\gamma) \stackrel{\text{def}}{=} 2^{-2}(1+\sqrt{1-\gamma})^2. \tag{E3}$$

We checked the good overlap between our results (nontruncated fidelity expressions with and without error correction) and the ones plotted in [12]. See also Fig. 7.

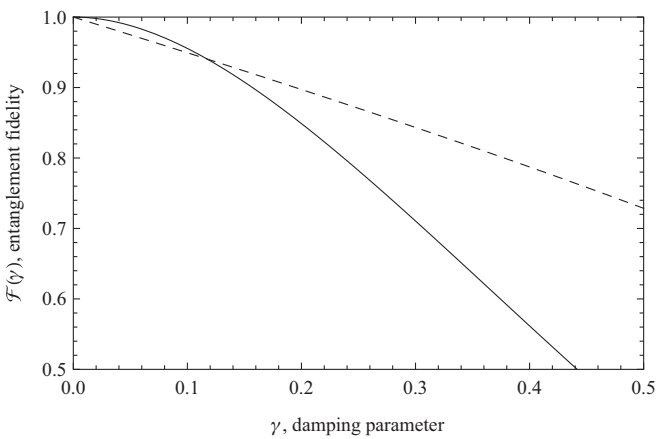

FIG. 7. Performance of the CSS seven-qubit code. The nontruncated expression of the entanglement fidelity $\mathcal{F}(\gamma)$ vs the AD parameter γ in the presence (thin solid line) and absence (dashed line) of QEC.

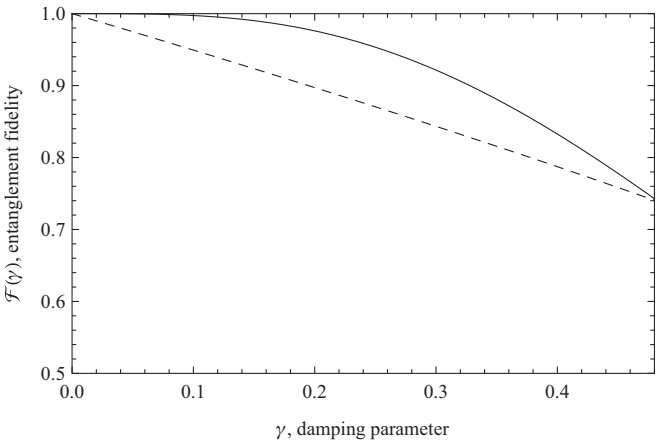

FIG. 8. Performance of the Shor nine-qubit code. The nontruncated expression of the entanglement fidelity $\mathcal{F}(\gamma)$ vs the AD parameter γ in the presence (thin solid line) and absence (dashed line) of QEC.

APPENDIX F: ON THE SHOR NINE-QUBIT CODE

For $\varepsilon = 0$, the nontruncated expression for the entanglement fidelity reads

$$\mathcal{F}^{[[9,1,3]]}_{\text{nontruncated}}(\gamma) \stackrel{\text{def}}{=} 1 - \tfrac{3}{2}\gamma^3 - \tfrac{135}{8}\gamma^4 + \tfrac{513}{8}\gamma^5 - \tfrac{201}{2}\gamma^6 + \tfrac{675}{8}\gamma^7 - \tfrac{297}{8}\gamma^8 + \tfrac{53}{8}\gamma^9, \quad \text{(F1)}$$

while the 1-qubit baseline performance is given by

$$\mathcal{F}^{\text{1-qubit}}_{\text{baseline}}(\gamma) \stackrel{\text{def}}{=} 2^{-2}(1 + \sqrt{1-\gamma})^2. \quad \text{(F2)}$$

We checked the good overlap between our results (nontruncated fidelity expressions with and without error correction) and the ones plotted in [8]. See also Fig. 8.

[1] P. W. Shor, Phys. Rev. A **52**, R2493 (1995).
[2] D. Gottesman, in *Quantum Information Science and Its Contributions to Mathematics*, Proceedings of Symposia in Applied Mathematics Vol. 68 (American Mathematical Society, Providence, RI, 2010), pp. 13–58.
[3] M. A. Nielsen and I. L. Chuang, *Quantum Computation and Information* (Cambridge University Press, Cambridge, UK, 2000).
[4] I. L. Chuang, D. W. Leung, and Y. Yamamoto, Phys. Rev. A **56**, 1114 (1997).
[5] R. Laflamme, C. Miquel, J. P. Paz, and W. H. Zurek, Phys. Rev. Lett. **77**, 198 (1996).
[6] C. H. Bennett, D. P. DiVincenzo, J. A. Smolin, and W. K. Wootters, Phys. Rev. A **54**, 3824 (1996).
[7] D. W. Leung, M. A. Nielsen, I. L. Chuang, and Y. Yamamoto, Phys. Rev. A **56**, 2567 (1997).
[8] A. S. Fletcher, P. W. Shor, and M. Z. Win, IEEE Trans. Inf. Theory **54**, 5705 (2008).
[9] A. S. Fletcher, P. W. Shor, and M. Z. Win, Phys. Rev. A **75**, 012338 (2007).
[10] C. H. Papadimitriou and K. Steiglitz, *Combinatorial Optimization: Algorithms and Complexity* (Dover, New York, 1998).
[11] B. Schumacher, Phys. Rev. A **54**, 2614 (1996).
[12] A. S. Fletcher, P. W. Shor, and M. Z. Win, Phys. Rev. A **77**, 012320 (2008).
[13] H. Barnum and E. Knill, J. Math. Phys. **43**, 2097 (2002).
[14] H. K. Ng and P. Mandayam, Phys. Rev. A **81**, 062342 (2010).
[15] E. Knill and R. Laflamme, Phys. Rev. A **55**, 900 (1997).
[16] P. Mandayam and H. K. Ng, Phys. Rev. A **86**, 012335 (2012).
[17] A. Gilchrist, N. K. Langford, and M. A. Nielsen, Phys. Rev. A **71**, 062310 (2005).
[18] I. Sainz and G. Björk, Phys. Rev. A **77**, 052307 (2008).
[19] C. Cafaro, S. L'Innocente, C. Lupo, and S. Mancini, Open Syst. Inf. Dyn. **18**, 1 (2011).
[20] R. Wickert, N. K. Bernardes, and P. van Loock, Phys. Rev. A **81**, 062344 (2010).
[21] R. Wickert and P. van Loock, arXiv:1303.0273 [quant-ph].
[22] R. Wickert and P. van Loock, arXiv:1303.0279 [quant-ph].
[23] R. Lang and P. W. Shor, arXiv:0712.2586 [quant-ph].
[24] P. W. Shor, G. Smith, J. A. Smolin, and B. Zeng, IEEE Trans. Inf. Theory **57**, 7180 (2011).
[25] A. Cross, G. Smith, J. A. Smolin, and B. Zeng, IEEE Trans. Inf. Theory **55**, 433 (2009).
[26] R. Duan, M. Grassl, Z. Ji, and B. Zeng, arXiv:1001.2356.
[27] C. Cafaro and S. Mancini, Phys. Rev. A **82**, 012306 (2010).
[28] C. Cafaro, F. Maiolini, and S. Mancini, Phys. Rev. A **86**, 022308 (2012).
[29] M. O. Scully and M. S. Zubairy, *Quantum Optics* (Cambridge University Press, Cambridge, UK, 1997).
[30] S. Banerjee and R. Srikanth, Eur. Phys. J. D **46**, 335 (2008).
[31] R. Srikanth and S. Banerjee, Phys. Rev. A **77**, 012318 (2008).
[32] S. Y. Looi, L. Yu, V. Gheorghiu, and R. B. Griffiths, Phys. Rev. A **78**, 042303 (2008).
[33] F. Gaitan, *Quantum Error Correction and Fault Tolerant Quantum Computing* (CRC Press, Boca Raton, FL, 2008).
[34] J. Tyson, J. Math. Phys. **51**, 092204 (2010).
[35] C. Bény and O. Oreshkov, Phys. Rev. Lett. **104**, 120501 (2010).
[36] M. A. Nielsen, arXiv:quant-ph/9606012.
[37] P. Kaye, R. Laflamme, and M. Mosca, *An Introduction to Quantum Computing* (Oxford University Press, Oxford, UK, 2006).
[38] D. Gottesman, Ph.D. thesis, California Institute of Technology, Pasadena, 1997.
[39] A. S. Fletcher, Ph.D. thesis, Massachusetts Institute of Technology, Cambridge, UK, 2007.
[40] A. R. Calderbank and P. W. Shor, Phys. Rev. A **54**, 1098 (1996).
[41] A. M. Steane, Proc. R. Soc. Lond. A **452**, 2551 (1996).
[42] M. Grassl, Th. Beth, and T. Pellizzari, Phys. Rev. A **56**, 33 (1997).
[43] J. Preskill, *Lecture Notes for Physics 229: Quantum Information and Computation* (California Institute of Technology, Pasadena, 1998).
[44] P. Sarvepalli and A. Klappenecker, Phys. Rev. A **81**, 032318 (2010).
[45] D. P. Di Vincenzo, P. W. Shor, and J. A. Smolin, Phys. Rev. A **57**, 830 (1998).
[46] G. Smith and J. A. Smolin, Phys. Rev. Lett. **98**, 030501 (2007).
[47] A. R. Calderbank, E. M. Rains, P. W. Shor, and N. J. A. Sloane, IEEE Trans. Inf. Theory **44**, 1369 (1998).
[48] B. Shaw, M. M. Wilde, O. Oreshkov, I. Kremsky, and D. A. Lidar, Phys. Rev. A **78**, 012337 (2008).
[49] E. M. Rains, R. H. Hardin, P. W. Shor, and N. J. A. Sloane, Phys. Rev. Lett. **79**, 953 (1997).
[50] J. A. Smolin, G. Smith, and S. Wehner, Phys. Rev. Lett. **99**, 130505 (2007).
[51] M. Hein, J. Eisert, and H. J. Briegel, Phys. Rev. A **69**, 062311 (2004).
[52] S. Yu, Q. Chen, and C. H. Oh, arXiv:0901.1935.
[53] V. P. Roychowdhury and F. Vatan, Lect. Notes Comput. Sci. **325**, 1509 (1999).
[54] S. Yu, Q. Chen, C. H. Lai, and C. H. Oh, Phys. Rev. Lett. **101**, 090501 (2008).
[55] D. Schlingemann and R. F. Werner, Phys. Rev. A **65**, 012308 (2001).
[56] D. Gottesman, Phys. Rev. A **54**, 1862 (1996).

[57] E. Dennis, A. Kitaev, A. Landahl, and J. Preskill, J. Math. Phys. **43**, 4452 (2002).
[58] H. Bombin, R. S. Andrist, M. Ohzeki, H. G. Katzgraber, and M. A. Martin-Delgado, Phys. Rev. X **2**, 021004 (2012).
[59] M. B. Ruskai, Rev. Math. Phys. **15**, 643 (2003).
[60] A. Peres, Phys. Rev. Lett. **77**, 1413 (1996).
[61] H. Horodecki, P. Horodecki, and R. Horodecki, Phys. Lett. A **223**, 1 (1996).
[62] W. K. Wootters, Phys. Rev. Lett. **80**, 2245 (1998).
[63] S. Lang, *Linear Algebra* (Springer, Berlin, 1987).